Feasibility Study of a Nuclear-powered Passenger Aircraft

Heat cycle design for the RECREATE cruiser

T.J.H.S. Schuwer

Delft University of Technology

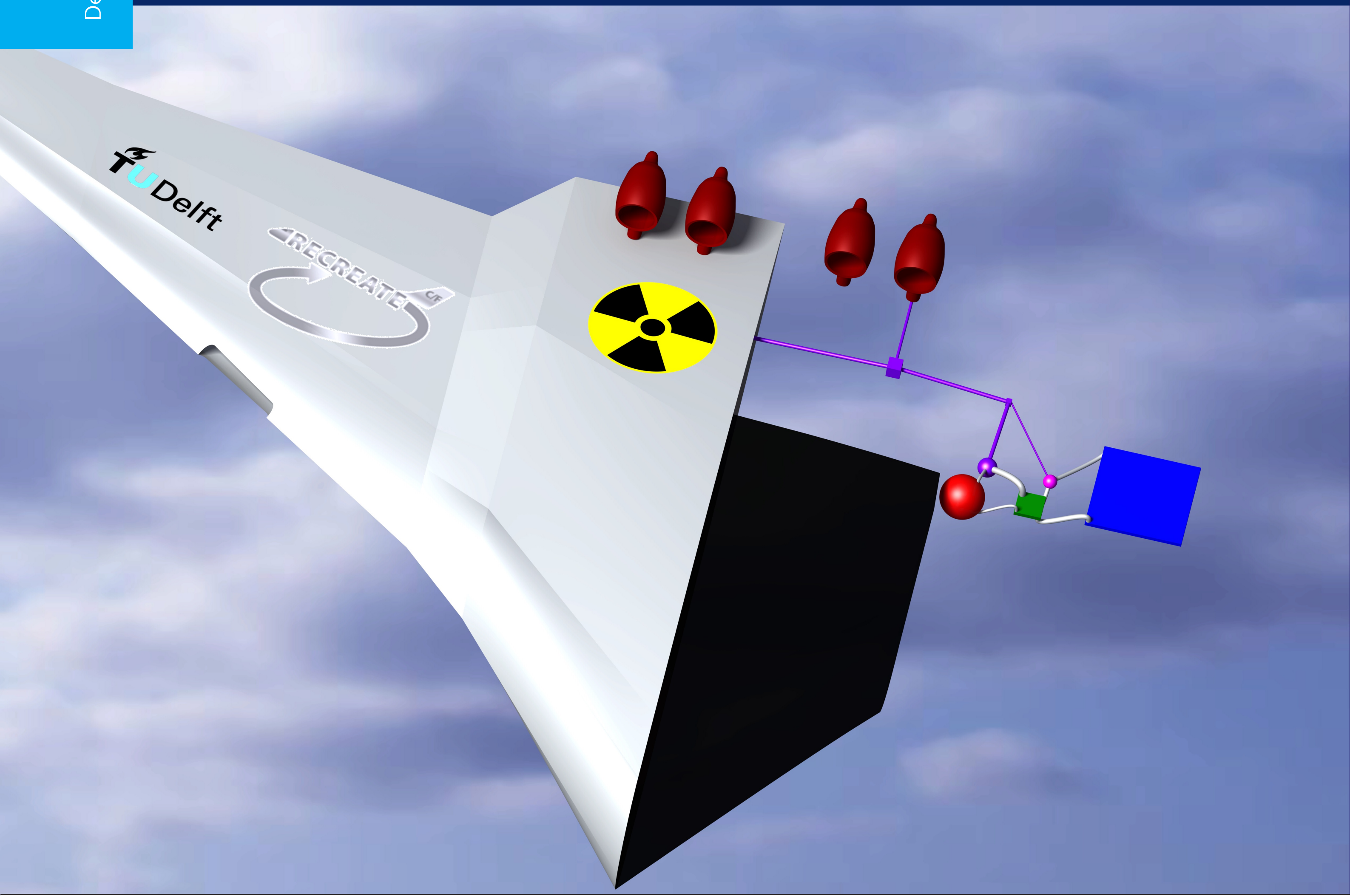

TU Delft Delft University of Technology

Challenge the future

Feasibility Study of a Nuclear-powered Passenger Aircraft

Heat cycle design for the RECREATE cruiser

by

T.J.H.S. Schuwer

in partial fulfilment of the requirements for the degree of

Master of Science
in Aerospace Engineering

at the Delft University of Technology,
to be defended publicly on June 22nd, 2015 at 15:00 PM.

Thesis registration number:	$255\#15\#MT\#SEAD-FPP$	
Supervisor:	Dr. ir. G. La Rocca	
Thesis committee:	Dr. A. G. Rao,	TU Delft
	Dr. ir. H. G. Visser,	TU Delft
	Dr. ir. J. C. Kuijper,	Independent Consultant Nuclear Technology and Reactor Physics Expert

Delft University of Technology

Dedicated to 'oma' Anneke Schuwer-Tergau

The single most gratifying feeling is fulfilling your duty of using your talents

Abstract

In view of stricter environmental regulations, diminishing fossil fuel reserves, and the resulting increase in fuel prices the aviation industry is required to make severe changes to ensure its continued existence. Even though more fuel efficient variations on current designs can help for now, long term solutions will only be found in a thorough redesign of the entire industry, including operation, aircraft design and propulsion systems. Whereas current aircraft have to be designed for cruise as well as take-off and landing, the European Commission sponsors the RECREATE research project to investigate the cruiser-feeder set up, in which cruise-optimised aircraft stay aloft for extended periods while feeder aircraft provide the link to the ground delivering payload and/or fuel to the cruiser. This study focusses on the design of a cruiser aircraft that uses nuclear power to transport up to 1000 passengers so that its endurance is only limited by maintenance intervals.

A nuclear-powered passenger aircraft requires extensive safety considerations to be operated with minimal danger to its passengers as well as the environment. Even though the Cold War produced some design options for nuclear aircraft, new research is needed to assess this concept's feasibility in the near future aircraft industry. RECREATE has provided a preliminary layout for the cruiser aircraft, however weight estimation of the propulsion system that converts reactor power into propulsion proves to be a major hurdle in assessing the feasibility of the cruiser design. Within the 1 million kg weight budget that has been set, 100,000 kg is reserved for each heat cycle. Therefore, this study sets out to design a weight optimised propulsion system, for which various heat cycles are being considered and thoroughly analysed.

The heat cycle design process starts by determining the reactor coolant, which is selected to be LBE because of its inherent radiation shielding and heat transfer properties. The heat from this primary fluid is transferred to a secondary cycle, outside of the shielding vessel to generate propulsive power. Three options are investigated for this secondary cycle: an open cycle using FLiBe as a working fluid, and two variants of closed cycle using s-CO_2, one with a regenerative and one with a recompression set-up. Because LBE limits the output temperature, the open cycle proves to be inapplicable for the cruiser so this study focusses on the closed cycle options. To come up with preliminary sizing results, the optimisation process is initiated by a grid search, in which the heat cycle components' weights are minimised for a distinct set of cycle input parameters. This provides the starting point for the overall optimisation that comes up with the final minimum weight heat cycle. In this process, cycle and component efficiencies are linked to the output weight by means of a reactor power weight penalty. The weight optimisation includes the sizing of heat exchangers and piping of the system, whilst leaving turbomachinery and driveshafts to be optimised in other studies.

In the grid search, the regenerative cycle's reduced number of components and lower mass flow causes it to come out as the lightest of the two remaining options. After the optimisation the minimum weight cycle has an overall thermodynamic efficiency of 45.4% using a maximum pressure of 60.5 MPa. The CO_2 cooler, using air as the cooling fluid, proves to be the biggest weight contribution, which is to be expected given the poor heat transfer properties of air, and the total cycle weight is 65,600 kg. This leaves a budget of 34,400 kg for the systems that have not been sized such as the compressors and turbines. This is considered more than sufficient, thereby allowing the overall heat cycle weight to remain within the required 100,000 kg. The design of a nuclear cruiser requires comprehensive additional research and validation before it can actually be flown. Besides the detailed design of the reactor and safety features, the results of this thesis have to be corroborated by further calculations, simulations, and experiments. Nevertheless, this research has provided an important initial assessment of nuclear-powered propulsion for civil aviation.

Preface

Graduating as an aerospace engineer is the culmination of a quarter century of learning. With the defending of this thesis comes an end to the most educational period of my life so far. This thesis, along with the courses, practicals, projects, and especially the internship has provided me with the tools to confidently start the next phase of my life. A phase in which the theory can finally be brought into practice, but where the education will never stop. Also outside of the faculty life I have grown a lot, for which I would like to take this opportunity to thank the people that made all this possible.

First of all I would like to thank Gianfranco La Rocca for guiding me through the final thesis process. In the same period Jim Kuijper has taught me many interesting things about nuclear reactors and their working, for which I am very grateful. I am also indebted to Sebastian Bahamonde Noriega, who allowed me to use his design code and helped me develop insight into the underlying mechanisms of heat exchange. I also owe thanks to Mo Li, who was prepared to discuss the tasks at hand and provide useful input. Finally, I thank all the people in the thesis room for always being ready to answer questions or just have a good laugh.

Outside the university I thank all my friends and family for sticking with me over the past years and motivating me to do my best. Your encouragement has been invaluable to me and it really helped me complete my studies and helped me to grow tremendously in personality! In the end, the biggest appreciation has to go out to my parents, who have always supported me in everything I have done and continuously try to help me make the most of every aspect of life. Thank you all for everything you have done!

T.J.H.S. Schuwer
Delft, June 2015

Contents

Nomenclature

Latin Symbols

A	Area	[m^2]
Af	Coefficient for LBE Nusselt number	[-]
BPR	Bypass ratio	[-]
C_p	Specific heat capacity at constant pressure	[$J/kg \cdot K$]
D	Drag	[N]
H	Enthalpy	[J/kg]
HV	Heating Value	[MJ/kg]
J	Optimisation objective	[kg]
L	Lift	[N]
M	Mach number	[-]
N	Number of channels	[-]
Nu	Nusselt number	[-]
P	Pressure	[N/m^2 or Pa]
PP	Reactor power-to-weight penalty	[kg/MW]
PR	Pressure ratio	[-]
Pe	Peclet number	[-]
Pr	Prandtl number	[-]
Q	Power	[W]
Re	Reynolds number	[-]
T	Temperature	[K]
Th	Thrust	[N]
U	Overall heat transfer coefficient	[$W/m^2 \cdot K$]
V	Velocity	[m/s]
Vol	Volume	[m^3]
W	Weight	[N]
a	Speed of sound	[m/s]
d	Diameter	[m]
g	Gravitational acceleration	[m/s^2]
h	Altitude, PCHE frontal dimension	[m]
l	Length	[m]
m	Mass	[kg]
mmol	Molar mass	[g/mol]
$\dot{m}$	Mass flow	[kg/s]
p	Perimeter, circumference	[m]
r	Radius	[m]
s	Entropy	[$kJ/kg \cdot K$]
t	Thickness	[m]

GREEK SYMBOLS

Δ	Change in variable	[-]
Ψ	Weighted heat capacity	[$J/m^3 \cdot K$]
α	Heat transfer coefficient	[$W/m^2 \cdot K$]
α	Recompression cycle bypass ratio	[-]
γ	Ratio of specific heats	[-]
δ	Containment vessel deformation	[m]
γ	Ratio of specific heats	[-]
η	Efficiency	[-]
λ	Thermal conductivity	[$W/m \cdot K$]
μ	Dynamic viscosity	[$kg/m \cdot s$]
ρ	Density	[kg/m^3]
σ	Stress	[N/m^2 or Pa]

SUBSCRIPTS

C	Cold
CE	Cold entering
CH	Channel
CL	Cold leaving
CV	Containment vessel
H	Hot
HE	Hot entering
HEX	Heat exchanger
HL	Hot leaving
cm	Compressor
co	Cooler
coms	Components
cru	Cruiser
des	Design
eng	Engine
eq	Equivalent
h	Hoop or circumferential
hc	Heat cycle
he	Heater
i	Internal
in	Inlet conditions
max	Maximum
melt	Melting conditions
mem	Membrane
min	Minimum
net	Netto value
o	External
out	Outlet conditions
p	Piping
pl	Plate
pp	Power penalty
reac	Reactor
reg	Regenerator
req	Required
sw	Side wall
tot	Total
tr	Turbine
w	Wall

List of Figures

List of Tables

Part 1

Thesis Report

1

INTRODUCTION

In view of stricter environmental regulations[1], diminishing fossil fuel reserves[2], and the resulting increase in fuel prices[3] the aviation industry is required to make severe changes to ensure its continued existence. Even though more fuel efficient variations on current designs can help for now, long term solutions will only be found in a thorough redesign of the entire industry, including operation, aircraft design and propulsion systems.

The European Commission initiated a research group to think out of the box and come up with concepts that cater flight operations into the 22^{nd} century. After exploratory research performed by this research group[4], the cruiser-feeder concept appeared as one of the most feasible options out of the 100 ideas for achieving this goal. The *RECREATE* (REsearch on a CRuiser Enabled Air Transport Environment) project has been sponsored by the European Commission to investigate this concept in particular.

1.1. THE CRUISER-FEEDER CONCEPT AND THE NUCLEAR CRUISER

Several options in design and operations exist within the cruiser-feeder concept[5]. Each of these include a cruiser aircraft that stays aloft for extended periods of time, while feeder aircraft fly shorter legs between their bases and the cruiser to exchange resources in flight. One aspect that all options have in common is that the cruiser-feeder set-up requires two distinct aircraft, each optimised for its specific mission. This is a contrast with the current operation of aircraft, which have to be designed for efficient cruise as well as frequent landing and takeoff operations with adequate performance. The cruiser-feeder concept entails a cruiser aircraft, which is almost completely catered towards maximal flight efficiency, and a feeder aircraft that is designed specifically for takeoff and landing performance.

Several categories can be distinguished within the cruiser-feeder operational approach: concepts without any transfer of aircraft contents, concepts in which the aircraft exchange fuel, and concepts where payload is exchanged in flight. The RECREATE project investigated two solutions from the last two categories. In the first, fuel is exchanged[6]. The second concept, which is the subject of this thesis, falls in the last category. Feeder aircraft transfer passengers from airports to cruise altitude. There the feeder aircraft transfer their fuselage to the cruiser via a transport mechanism aboard the cruiser. A picture of the concept proposed by the project can be seen in figure 1.1, with a detail of the passenger transfer process being depicted in figure 1.2.

Once contained in the cruiser, passengers can exit the feeder fuselage and are seated in the large cruiser fuselage for the duration of their flight. The cruiser functions as a “hub in the sky” so that passengers with different destinations can depart from the same location in the same feeder. Once the feeder to a specific destination is nearing the cruiser for docking, passengers for that destination transfer back to a feeder fuselage and are flown to their destination by the feeder. The overall mission profile of this concept can be seen in figure 1.3

This set-up is most effective if the cruiser can stay airborne for as long as possible without having to be refuelled. Therefore, the option is presented to power the cruiser using an on-board nuclear reactor instead of conventional jet fuel. A nuclear fission process uses a negligible fuel weight if compared to the thousands of kilograms of jet fuel that are burned during cruise by current aircraft. Moreover, nuclear propulsion has no production of greenhouse gases. In principle, a nuclear-powered aircraft only has to land in order to perform maintenance.

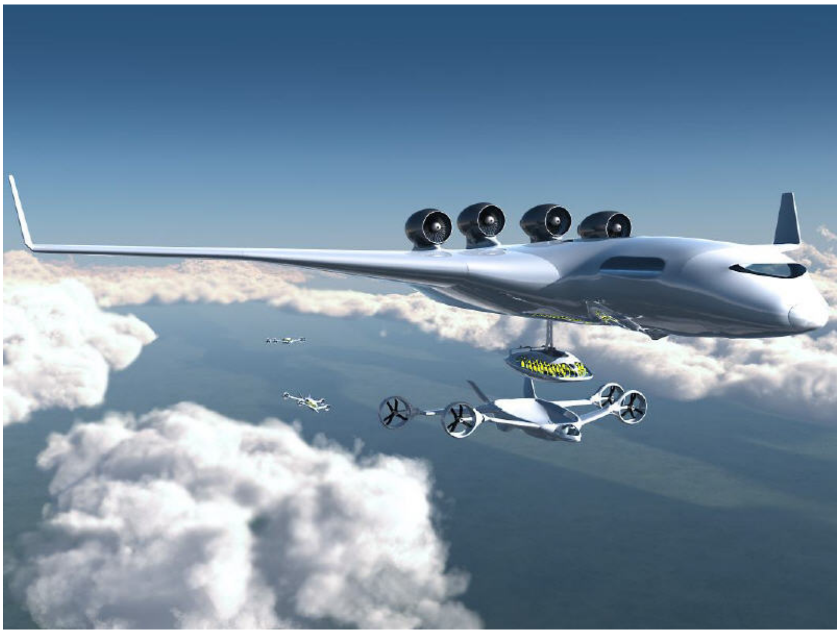

Figure 1.1: Artist's impression of the cruiser and feeder aircraft, from [7]

Figure 1.2: Detail of the process of transferring passenger fuselages from the feeder structure, from [7]

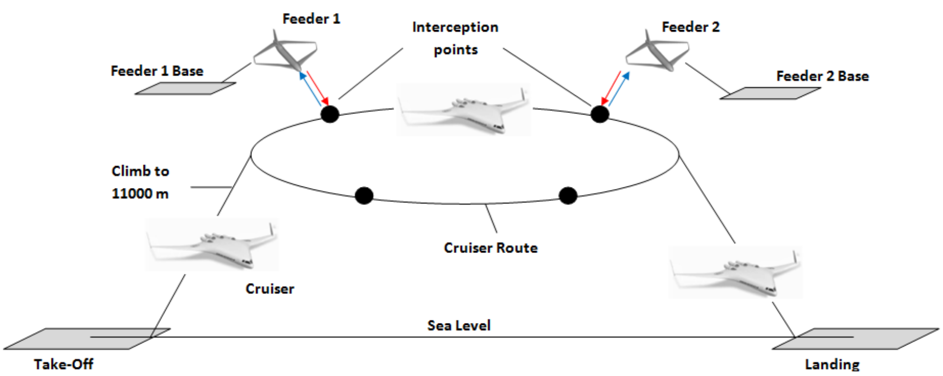

Figure 1.3: Schematic mission profile of the cruiser-feeder concept, from [8]

Flying a powerful nuclear reactor at high speeds across the globe does present an extensive set of unique operational problems to be dealt with, the most important of which are treated in the following sections.

A more detailed investigation into reactor safety and how to deal with nuclear problems on the cruiser is presented in chapter 6.

1.1.1. NUCLEAR FLIGHT

To decrease the risk that the nuclear cruiser presents to its passengers and the public, a number of measures have to be taken with regards to flight plans and operations.

As long as the reactor is set to run at minimum power, which should be considered to be equal to switching it off but requires less drastic measures than an emergency shutdown, it does not pose a significant risk provided the cooling system works correctly. In that situation the latent heat produced is lead away from the reactor and any dangers like meltdown are prevented. To protect the people on the ground, the reactor is put into this state when flying over land. The cruiser travels in circles over the Atlantic Ocean to replace the flights between Europe and North America[5]. The result is that nuclear flight can be sustained for the vast majority of its flight hours, switching to alternative non-nuclear fuel only during takeoff and landing operations.

The necessity of switching off nuclear power during landing and takeoff has two causes. The first, safety, has been discussed in the previous paragraph. Switching to fuel-powered propulsion nullifies the need for constructing airports at sea and allows them to be built on land (albeit at the coast to minimise the duration of over-land flight). Another safety aspect is that the vast majority of accidents happen during the takeoff and landing flight phases. A study published by Boeing[9] states that around 90% of fatal accidents and around 80% fatalities occurred during takeoff, climb, descent, and landing between 2002 and 2011. If the reactor is inactive during these phases, the risk of nuclear incidents happening on or near land and population as a result of a crash is lowered significantly. Secondly there is the purely technical aspect of the inability of nuclear heat cycles to cope with sudden changes in power demand. As is further explained in section 3.4 the reactor and heat cycle are not able to provide adequate power during all flight phases and are in need of a fuel-powered additional cycle to perform takeoff and landing operations.

1.1.2. AIRFIELD

When the cruiser has to land for maintenance or during an emergency, it needs to do so at an airport that is able to deal with the risks of a landing nuclear aircraft. This sets a number of requirements for the airfields needed for nuclear cruiser operation.

As mentioned in section 1.1.1, the cruiser will not fly over land on nuclear power. So cruiser airfields are ideally located at the coast, but away from populated areas. In this way, the danger to the public is lowered and the amount of fuel needed for flight over land is minimised as well. Also, because of the extreme dimensions and weight of the nuclear cruiser, its required runway length will exceed that of most conventional airports. On top of that preliminary designs such as those performed by Chiozzi[8] predict a wingspan that greatly exceeds the conventional 80x80m box that is reserved for each aircraft on airfields. Constructing dedicated airports for handling nuclear cruisers also has the advantage that the teams that are stationed at the airports can be trained specifically for the challenging task. The team members should have knowledge about aircraft, as well as nuclear matters and the absence of other aircraft means that they can focus completely on the task at hand.

Compliance with health and safety regulations for the personnel on the aircraft and the airfield requires them to be shielded from radioactive fission products and radiation during normal operation of the cruiser. The reactor and containment vessel should therefore be designed such that the radiation dose on their perimeter is below the bound set by the International Atomic Energy Agency at $1 \cdot 10^{-3}$ sievert per year[10]. Therefore any maintenance on systems and structure of the nuclear cruiser outside of these vessels can be performed without any special precautions. For reactor maintenance and nuclear refuelling operations the airfield should include a separate building where the containment vessel can be removed from the aircraft and opened for performing these operations.

Revolutionary as a nuclear-powered aircraft may sound, it has been designed and even tested before. A short overview of these efforts is given in the following section.

1.1.3. HISTORY OF NUCLEAR-POWERED FLIGHT

The attention for nuclear propulsion for aircraft started directly after the first successful man-made nuclear reactor was operated in the USA. If such power could be controlled, can it be used to overcome the need for fossil fuels? Designs were made for nuclear-powered houses, ships, and even cars. Also the US Air Force set out to harness nuclear energy when it initiated the *Nuclear Energy for the Propulsion of Aircraft* or NEPA project in 1946. This was renamed to the *Aircraft Nuclear Propulsion* (ANP) venture in 1951. Also in Russia a program was set up to try to achieve nuclear-powered flight before the Americans did. The invention of intercontinental ballistic missiles provided both countries with a cheaper and easier alternative to the large bomber that was envisioned by the programs and therefore both programs were cancelled before their target of nuclear flight was met.

In exploring the possibilities for nuclear propulsion, both sides came up with possible thermodynamic cycles that could be used to transform the reactor heat into useful thrust. This process resulted in two distinct cycles: an open cycle in which the airflow in the engine is directly led through the reactor core[11][12] and a closed cycle that uses heat exchangers to prevent contact of radioactive material with the environment[11–13]. These concepts will be dealt with in more detail in section 3.1. Another concept that resulted from this Arms Race is that of distributed shielding. To decrease the weight budget that has to be dedicated to reactor shielding, choices were made to shield only what was absolutely necessary: the pilots. In distributed or divided shielding[14], only some rudimentary shielding material is present around the reactor, most of it facing the direction of the crew compartment. Additionally, the cockpit is surrounded by its own shielding layer. This ensures a safe flight for the pilots but does result in increased levels of nuclear radiation in other directions. An example of what a cockpit from a divided shield aircraft looks like is shown in figure 1.4, where the cockpit is lined in layers of lead and rubber to protect the crew from radiation.

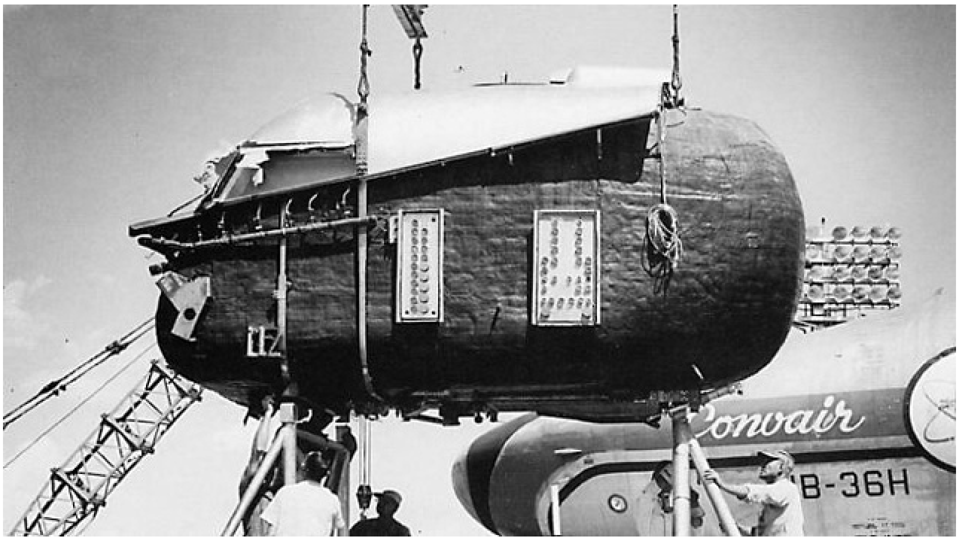

Figure 1.4: A cockpit assembly from a divided shield aircraft, from
http://www.aviation-history.com/articles/nuke-american.htm

Despite all the research, the results of the *ANP* program were meager: no aircraft was flown on nuclear power. The reactor was only present and powered up on board of existing bombers to test various variables but it never powered the engines. The results of the Russian program are not very clear. Officially, they did not achieve nuclear-powered flight and like the Americans only flew an aircraft with an active reactor on board. However, after the collapse of the Iron Curtain rumours started of documents indicating Russian nuclear-powered flight was achieved by simply disregarding the existing problems of shielding and safety at the cost of the operating crew. One fact is certain: no organisation has ever been able to safely and successfully operate a feasible design of a nuclear-powered aircraft.

Today nuclear-powered submarines and ships are an accepted and standard of transport, but with the exception of a few merchant ships and icebreakers only for military applications. In the civil sector nuclear power plants continue to be operated and constructed to cope with the world's increasing power needs. New designs are being researched to increase their efficiency and level of safety.

1.2. NUCLEAR AIRCRAFT DESIGN PROCESS

When designing the nuclear cruiser some steps in the process of aircraft design cannot simply be applied. Due to the unconventional power system, general empirical design rules such as those used in the aircraft design books by Roskam[15] and Raymer[16] have to be reformulated before application to nuclear aircraft is possible.

Preliminary design methods mostly use empirically derived weight distributions to estimate the characteristics of parts of the aircraft from its total weight and other general information. The envisioned weight of a nuclear aircraft is far beyond that of the current heaviest aircraft, which is the Antonov-225 with a maximum takeoff weight of $640 \cdot 10^3$ kg. Moreover, the design proposed by *RECREATE* is a BWB configuration[8]. Combining the excessive weight with the unusual configuration, it is questionable whether the known relations are still valid. The main reason for the required reformulation is the fact that the cruiser only uses fuel during takeoff and landing, and emergency operation. This means that the usual fuel fractions are not valid for a nuclear aircraft and dismisses the possibility of using, for example, the Breguet range equation. Moreover, the weight of the fuel makes up a much smaller portion of the total weight. Then there is the weight fraction of the nuclear reactors and heat cycle components, which is not present for fossil fuel-powered aircraft at all. For preliminary design of a nuclear aircraft some rules have been provided in [11–13] but considering the age of these sources, the validity of these rules has to be confirmed. In an aircraft design study in the RECREATE project an iterative approach of weight estimations is performed to converge to a total weight for the cruiser using semi-empirical relations[8]. However, the unknown weight fractions of the nuclear system and heat cycle makes this approach unreliable until the outcome of this thesis provides an accurate description of the heat cycle.

The complete design loop within the RECREATE project is presented in figure 1.5, in which the contribution of this thesis is highlighted in red. This figure also shows the most important pieces of information that the individual parts of the design process share with the other parts, to come up with an overall design that fits all the components inside the aircraft within the requirements described in section 1.3. Depending on the outcome of the research in this thesis and the outcome of the reactor design, the cruiser design can have a positive or negative margin with respect to the weight budget. In this case, the weight budget can be shifted appropriately or the weight fractions can be updated. For example, if the total weight remains under the weight budget, the weight fraction of additional fuel can be raised, which increases the cruiser's diversion range. If the weight budget is changed, the calculation scheme developed in this thesis can be used to design an updated version of the optimal heat cycle.

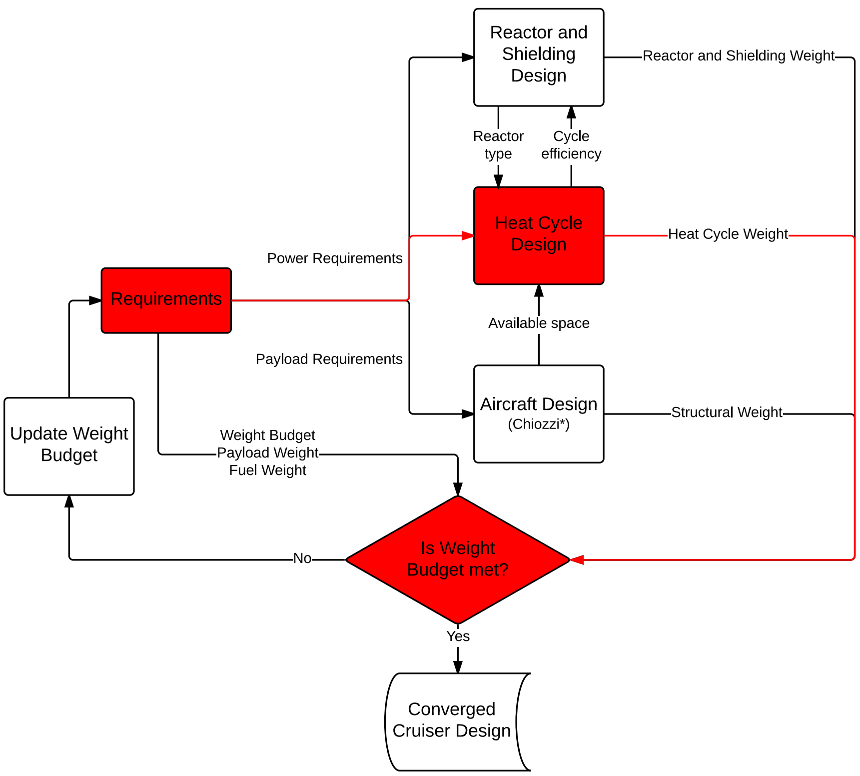

Figure 1.5: Schematic of the RECREATE cruiser design loop. *: for the initial outcome of this study, see [8]

From the initial aircraft design by Chiozzi[8], the basic lay-out of the cruiser shown in figure 1.6 is transferred to this thesis. The design chooses a blended wing-body configuration with the nuclear reactors in the wing roots. Chiozzi assumes a water/steam cycle to generate thrust, which requires a large cooling surface for condensing the steam. This system fills a large portion of the wing structure. Another design input to this thesis is the preliminary engine design as presented in [6], which is a geared turbofan engine.

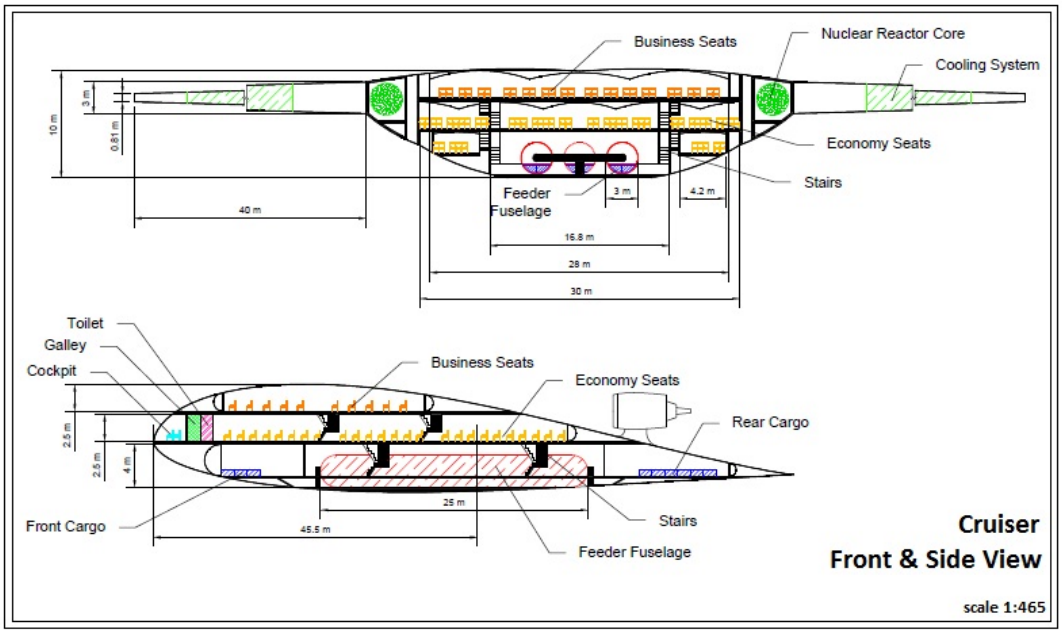

Figure 1.6: Initial design of the nuclear cruiser, from [8]

1.3. TOP LEVEL DESIGN REQUIREMENTS FOR THE RECREATE NUCLEAR CRUISER

At the start of its research, the *RECREATE* group formulated some requirements for the nuclear cruiser. These will be used to guide this research and are listed in table 1.1.

Parameter	**Value**	**Note**
Capacity	1000 passengers	Assuming 100 kg each
Range	> 60,000 nm	1 week endurance
Maximum Take Off Mass	2,000,000 lb	≈ 1000 tons
Cruise Speed	M = 0.8	
L/D	> 20	
Maximum radiation levels	$1 \cdot 10^{-3}$ Sievert per year	Enforced by regulations[10]
Entry into service	Before 2100	
Propulsion	Hybrid nuclear/chemical fuel	For back-up operation, take-off, and landing

Table 1.1: Driving requirements as set by the *RECREATE* consortium[5]

The requirement for maximum radiation level in table 1.1 means that reactor shielding must be such that nobody involved with the aircraft (passengers, flight crew, and maintenance personnel alike) is exposed to excessive amounts of radiation. Also, the cruiser must include adequate safety provision that are designed to prevent the release of radioactive material in the worst possible aircraft accident scenario. These additional requirements are largely equal to those set for an American nuclear aircraft program back in 1967, as described in [17]. The date of entry into service is included in the requirements to ensure that the technologies and materials that are used in the research have to be available currently or can reasonably be expected in the near future.

These top level requirements can be condensed into the following driving requirements that are relevant for the heat cycle design and subsequent feasibility study in this thesis:

- **Weight:** To stay within the weight budget of 1000 tons, every aspect of the design will have to be as light as possible. The options and design methods for minimising the weight of other components of aircraft have been studied extensively since the time of the *ANP* program. However, the design of a nuclear reactor and heat cycle for use on an aircraft has received no attention since the Cold War. This report deals with the question whether technological advances can do the same for a nuclear heat cycle and reduce the component weights enough to meet the weight budget. In [6] a breakdown of the cruiser weight is given. In this breakdown it is assumed that the propulsion system of the cruiser weighs 462,200 kg. Excluding the four engines (112,200 kg) and assumed reactor weight budget (150,000 kg) this leaves 200,000 kg as the weight budget for the heat cycle components. The entire weight breakdown of the nuclear cruiser is shown schematically in figure 1.7.

- **Safety:** Overcoming the overwhelming fear of the general public regarding nuclear energy, let alone flying a nuclear reactor around, is a hard enough challenge as it is. To make it somewhat easier it is vital for each aspect of its design to be as safe as possible. Every incident scenario has to be dealt with to try to prevent the release of radioactive material as well as radiation.

- **Mission:** The heat cycle must be designed to provide enough thrust to fly an aircraft with specifications matching the requirements in table 1.1 at the set speed and conditions.

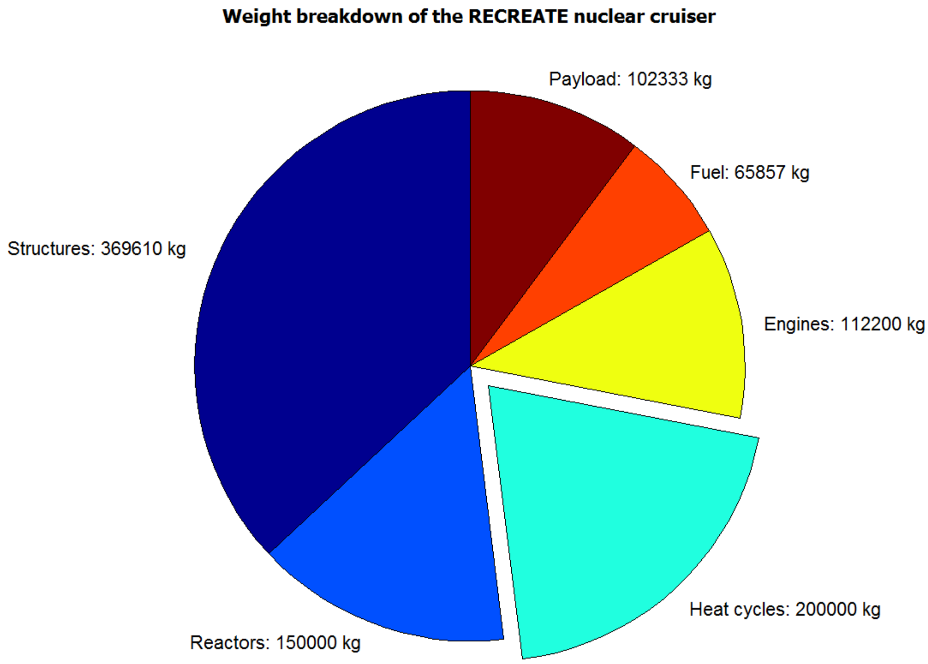

Figure 1.7: Weight distribution of the nuclear cruiser highlighting the focus of this research, from [6]

If a design can be found that meets these requirements, a reasonable conclusion is to state that the nuclear cruiser is a technically feasible option. It is important to note that this research only discusses the *technical* feasibility of the nuclear cruiser aircraft. Another vital discussion will be necessary to explore the feasibility in the spotlights of ethics, economy, social acceptance, and politics before the cruiser can actually be constructed and operated.

1.4. RESEARCH QUESTION AND SUB-QUESTIONS OF THIS THESIS

The main research question is formulated as follows: *Is it possible, using current or near-future technology, to come up with a feasible design of a heat cycle for a nuclear cruiser aircraft, as proposed in the* RECREATE *research project?* This question can be answered by answering the following sub-questions:

- Can the heat transfer system be designed to be light enough to remain inside the weight budget of the RECREATE cruiser?

- What provisions are needed in design and operations to ensure the safety of the aircraft, its passengers and crew, as well as the general public and environment during all phases of cruiser operation?

To answer the sub-question concerning the propulsion and heat transfer system, the following questions are deemed relevant:

- *What are the design options and constraints for the heat cycle and the propulsion system?* Systems considered in the past, as well as possible novel configurations are considered in this. An investigation has to be performed to determine the combination of heat cycle layout, heat cycle fluid, and propulsion system that yields a design that is feasible in weight as well as safety considerations

- *What is the weight of the heat cycle?* The weight of the heat cycle should be as low as possible. The total weight of the aircraft is set by the weight budget of the *RECREATE* consortium, where the heat cycle has to be designed within the 200,000 kg requirement for the weight budget to be met and the overall cruiser design to be feasible

To determine the relevant safety considerations that have to be made in the design and operations the cruiser the following questions need to be answered:

- *Can the reactor be designed such that the cruiser can be operated safely in every situation throughout its lifetime?* Do systems exist that can ensure that the reactor stays intact (meaning at least leak tight and recoverable) under all crash conditions? If not, is it reasonable to assume that additional research can make these systems available by the envisioned date into entry?

- *What are the options to continue flight after reactor failure?* Options have to be explored in the domain of backup propulsion systems as well as how to handle the faulty reactor

- *Which additional safety considerations result from including a nuclear reactor in an aircraft design?* The answer to this question is especially important for further research into the nuclear cruiser concept and gives the future decision makers a more complete picture of all the safety aspects that are involved in nuclear flight

1.5. THESIS RESEARCH GOAL AND SUB-GOALS

This research strives to determine the feasibility of designing a nuclear-powered cruiser aircraft by designing a minimum weight heat cycle, as well as identifying and suggesting solutions for specific safety issues of a nuclear aircraft. This primary goal is divided into sub-goals, which need to be achieved in order to successfully complete the research.

The first goal, dealing with the design of the heat cycle, contains the following sub-goals:

- Develop a list of suitable heat cycle options, heat cycle fluids, and available variables within the heat cycle design

- Set up a calculation scheme to compute and design the heat cycle components and determine their sizes and weights

- Find an optimum in the available design variables, which minimises the overall weight of the heat cycle system

- Check whether the minimum weight satisfies the required weight budget

The second part of the research goal consists of:

- List specific safety concerns in both design and operation of the nuclear cruiser, which are unique to an aircraft with an on-board reactor

- Attempt to find suggested solutions in literature from previous researches into the concept

- If these are not present, suggest a solution and assess its feasibility

1.6. THESIS STRUCTURE

After this introductory chapter, the thesis report will continue by listing the available reactor options in chapter 2, which also contains a trade-off to determine the most feasible reactor type and coolant for the nuclear cruiser. Then chapter 3 deals with the description of different heat cycle layout options and the selection of the layouts that are considered in detail during the design phase. This chapter also contains the design options for including hybrid propulsion into the cruiser design. The heat cycle design process, along with the theory of the underlying calculations is presented in chapter 4, after which its results are treated in chapter 5. In chapter 6, some additional safety considerations are explained, before the report is concluded in chapter 7. After this, part 2 of the report briefly describes the calculations codes that have been developed and how to use and/or change them for future research.

2

Reactor Type and Primary Cycle Fluid Selection

The essential power source of the nuclear cruiser is its reactor. The underlying principle of atomic energy production is as follows: a fissionable large atom (most commonly Uranium) encounters a free neutron, which causes it to split into two smaller atoms. During this split exothermic energy is produced, along with additional free neutrons and other byproducts. These produced neutrons are then free to collide with another large atom, causing a nuclear chain reaction. Careful moderation and adequate cooling makes the chain reaction stable and provides a constant large amount of energy to the coolant. This heat can then be used to generate electricity or, in the case of a nuclear engine, propulsion. Even though the principle of nuclear energy generation is the same for every current reactor, the configuration of a nuclear reactor has many design options.

In this research the reactor is treated as a black box that provides a certain amount of power. The exact design of the reactor is left to the nuclear technology experts within the *RECREATE* consortium. This study assumes a set-up as shown in figure 2.1, in which the reactor vessel is the aforementioned black box. However, the type of reactor employed in the cruiser can be important to the design of the heat cycle that transforms the reactor heat into propulsion . The most important parameter for a reactor suitable for aeronautic applications is the power density: the reactor has to be as (small and) light as possible for a certain power output.

The influence of reactor type on the design of the heat cycle is mainly determined by the coolant that is chosen to divert the heat away from the reactor core. Therefore, the coolant selection will be the focus of this chapter. Established reactor concepts are treated, as well as some experimental ideas for novel types of nuclear reactions that have been under investigation or are being investigated at the moment, which are briefly discussed in section 2.1. In the final section of this chapter, all options are compared to find the most feasible combination of reactor type and coolant for use in the nuclear cruiser. The framework of this comparison, consisting of the applicable criteria and manner of comparing the options, is treated in section 2.3.

2.1. Available reactor type options

There are two main types of fission reactors: thermal reactors and fast neutron reactors. The main difference between the two, as suggested by the denomination, lies in the velocity at which the neutrons are released during the reaction. Almost all operational nuclear reactors worldwide are thermal reactors because they are cheaper to construct and operate. However, the increased thermal energy of fast reactors are beneficial for operation on the nuclear cruiser because the increase in energy leads to a higher achievable power density. Moreover, fast reactors are more sustainable because they produce less nuclear waste that requires long-term storage than thermal reactors.

The choice between fast and thermal reactors has an influence on the coolants that can be employed by the reactor. Thermal reactors generally use lighter coolants such as water because of their moderating effect due to slowing the fast neutrons that result from the nuclear reaction. In fast reactors, this slowing down is unwanted so heavier coolants such as liquid metals are used.

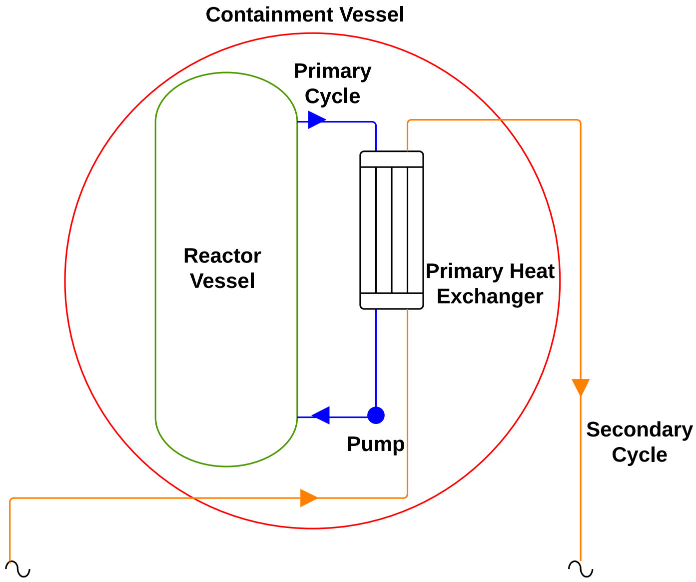

Figure 2.1: Schematic drawing showing the assumed internal lay-out of the containment vessel

2.1.1. EXPERIMENTAL IDEAS

Besides the currently available fission process, there are other methods for generating energy from nuclear processes. Especially the nuclear fusion reactor concept has generated a lot of excitement when Lockheed Martin's Skunk Works research team announced a design study into a nuclear fusion-powered aircraft.[1] Fusion promises a large amount of heat generated with minimal production of radiation, which would be very beneficial for aircraft operation. However, it does require a stable plasma environment, which can only be supplied using immensely large magnets. Including all this into the aircraft design results in a vastly different design process than the current configuration of the RECREATE project. Weight fractions of shielding should be changed and the surrounding structure and exact layout of the fusion reactor has to be known in order to design the cruiser as a fusion-powered aircraft. These changes, along with the fact that large-scale fusion has not been proven experimentally causes a fusion reactor to not be considered in this study.

During the literature research of nuclear propulsion options, a radical concept was found. In 1999, a research was published that reported about a new way of generating energy called Triggered Isomer Heat Exchanger (TIHE)[18]. Using simple X-ray radiation on an isomer of Hafnium, energy is generated while only producing low energy gamma rays. This kind of radiation is easier to shield than the radiation from a regular neutron-induced nuclear reaction because of the lower energy of the radiation and the fact that no neutrons are emitted. Therefore, the shielding around the reactor can be made much lighter. The possible efficiency gains triggered some master theses to be performed on designing aircraft powered by TIHE reactions, like [19] for a military drone similar to the current Global Hawk. However, the excitement proved to be immature because other researchers trying to corroborate the findings of [18] found that the release of energy was not present to the extent that it had been claimed[20].

Another, more well-known, concept for alternative nuclear energy is that of Low Energy Nuclear Reactions (LENR). This is a general term that encompasses different processes that claim to achieve nuclear fusion at temperatures far below the plasma environment that is normally required for nuclear fusion to take place. The most well-known claim started in 1989 by Fleischmann and Pons with the publication of an article reporting excessive heat production during an experiment that involved electrolysis of heavy water on the surface of a palladium electrode[21]. Reporting net energy productions of 300% the energy input, this sparked a lot of enthusiasm throughout the (scientific) community. From the publication date onwards, nu-

[1] http://aviationweek.com/technology/skunk-works-reveals-compact-fusion-reactor-details

merous researchers have tried to replicate the aforementioned results. Some have found energy gains but most were futile. A summary is given in [22] with the following sentence. "So far all microscopic investigations have shown that the low-temperature fusion reaction is taking place only on tiny, isolated areas of the surface of Pd and also other metals." This explains why some experiments have measured favourable results from identical experiments where others measured nothing useful. Due to the amount of information that is still unknown about particle physics, many effects cannot be fully explained. The beneficial effect might be present for some of the claims but actually harnessing the process for large scale energy production has not been achieved for any of the experimental options, nor is it likely to happen in the near future.

2.1.2. REACTOR TYPE PRELIMINARY SELECTION

Experimental reactor options treated in section 2.1.1 are not involved in the selection of feasible reactor types in this study because of their disputed working. The technology readiness level of both TIHE and LENR options can be called uncertain at best. Added to that is the fact that the design of an aircraft around a different reactor type is completely different from a design around a regular fission reactor. To be able to compare different heat cycle options and maintain the applicability of the initial design work, only fission reactors (thermal as well as fast) are selected in the *RECREATE* design for now.

One important remark that has to be made and that is valid for every reactor design is the shielding distribution. In section 1.1.3 the concept of divided shielding is introduced as being a lightweight alternative to the conventional unit (or 4π) shielding. However, for a civilian cruiser aircraft with the strict safety requirements set earlier such a concept is infeasible. In order to protect the passengers, maintenance personnel, environment, as well as the general public in case of a crash emission of radioactive byproducts and radiation has to be prevented in all directions and during every phase of the cruiser's operation. This is why 4π shielding, in which 4π stands for the number of steradians over which the shielding is dispersed around the reactor core, is essential for the nuclear cruiser.

2.2. REACTOR COOLANT OPTIONS

Regardless of the reactor type, a primary cycle fluid or coolant is needed to transport the reaction heat away from the reactor core and transfer it to the heat exchanger in order to be processed further. The range of possible reactor coolants is large. Different types of reactor coolants that are being operated, tested or planned for the near future are presented in [23]. Most literature, such as [24], differentiates between six main classes of so-called generation IV reactors that are relevant for this thesis, each with its own designated coolant. The six different cooling methods that are compared further in this chapter are cooling by water, gas, molten uranium salts that double as reactor fuel, molten salt, heavy metal, and alkali metal. The options within the classes, as well as some general characteristics are treated in the list below. From each class, the most promising option is chosen for comparison against the other options in section 2.4, which treats the selection of the overall most optimum coolant of the nuclear cruiser's reactor.

- **Water-cooled reactors** are the most common reactor type and can be divided into three main groups; pressurised water reactors, boiling water reactors, and supercritical water reactors. The difference between them lies in the phase of the coolant. In pressurised water reactors, as the name indicates, the water is pressurised to ensure that it remains liquid throughout the primary cooling cycle. In boiling water reactors the heat from the reactor causes the liquid water to boil only to become liquid again after the coolant has transferred its energy to the turbine in the cycle and is ran through a condenser. Supercritical water coolant indicates that the water is in a superheated steam phase in the complete cycle. General characteristics of water-cooled reactors include reasonable heat transfer capabilities, some degree of required pressurisation, a non-toxic and abundant coolant, and chemical attack on structural materials at high temperatures. <u>The most applicable option within this class seems the supercritical water option</u> due to its single phase coolant, which enhances safety, and the superior heat transfer properties at the critical point compared to the other two options. The downside to this option is that supercritical water reactors have not been constructed yet, whereas pressurised and boiling water reactors are very common and are well-documented in their operations and characteristics

- **Gaseous coolants** that are used in reactors include helium and carbon dioxide. Due to its nuclear and chemical inertness, even at elevated reactor temperatures, <u>helium is deemed the most optimal gaseous reactor coolant</u>. In general, gas coolants have low heat transfer capabilities, require a pressurised system but are light and stable at reactor conditions. Helium has been the coolant of choice for many reactor concepts treated in the nuclear aircraft designs of the Cold War era. It is also selected as the baseline for gas coolants in the comparison at the end of this chapter. Only some current reactors actually employ helium cooling, other gas-cooled reactors mainly use CO_2

- **Molten fuel** reactor types abandon the classical division of fuel in rods or elements with coolant flowing past to remove the fission heat. Instead, the uranium is dissolved in a salt with another element like fluoride. When molten, the resulting fluid is capable of sustaining a nuclear reaction in what is called a liquid core reactor. The resulting characteristics for this kind of reactor include a large design effort in order to decrease the risk of nuclear radiation escaping. This is a result of the large volume of active material and the fact that it is nuclearly active throughout the entire cycle

- There are a number of **molten salts** that can be used to cool a reactor core. Three main groups can be identified by classifying the salts into those containing beryllium, those with zirconium tetrafluoride, and salts that contain lithium fluoride. All three groups have in common that they do not require any pressurisation, they corrode structural material at high temperatures and they are solid at room temperature, which requires an additional heating system in the nuclear cruiser to facilitate reactor start-up. The most useful salt for the nuclear cruiser's design seems to be Fluorine-Lithium-Beryllium (or FLiBe), which has superior qualities in neutron activation when compared to other salts, as well as a lower melting point

- Different **heavy metals** can be used in molten form to transfer heat away from the reactor. The most common options mentioned in literature are liquid tin, mercury, lead, and Lead-Bismuth Eutectic (LBE). General characteristics of heavy metal coolants are their high density, excellent heat transfer properties, and high boiling point. This last item is not applicable to mercury but that coolant is not a feasible option due to its extreme toxicity. The most feasible option in the heavy metal class of coolants is LBE. Because lead is present in its composition, the LBE coolant provides some inherent shielding to the reactor. The combination with bismuth decreases the LBE melting point by 200°, which is favourable for starting up the reactor

- **Alkali metals** are the final class of coolants that is treated in this thesis. Options include lithium, sodium, and potassium. Its higher boiling point and lower nuclear reactivity make sodium the most interesting option. However, despite their good heat transfer properties, alkali metals do pose serious safety hazards in the form of their explosive reaction with water, spontaneous combustion in air, and toxicity. A large number of current nuclear plants are operated with sodium cooling, so this is used as a benchmark for further research

2.3. SELECTION PROCESS FOR THE REACTOR COOLANT

To find the most beneficial reactor coolant for a nuclear aircraft, the presented options have to be compared and ranked against each other. To structure this comparison, seven criteria have been selected on which the concepts are graded. The criteria are briefly explained below.

- **Weight:** This is a measure of how the choice for a certain coolant influences the total weight of the aircraft. This includes not just the weight of the coolant but also piping, which is heavier for a pressurised system, heat cycle components like compressors, and shielding, which may differ in composition or size for different coolants.

- **Nuclear activation:** The highest scores in this category are assigned to the coolant that is most immune to absorption of radiation and byproducts and thereby becoming radioactive. Coolants that form large amounts of radioactive reaction products in the presence of a radiation source present a higher danger to the passengers in case of leakage and to personnel assigned to maintenance of the heat cycle.

- **Health effects:** If a coolant is toxic, its score in this criterion will be low. Coolants that do not present any health hazards are deemed safer in case of a leak and during maintenance.

- **Design effort:** A pressurised coolant requires more attention during the design of the heat cycle and reactor vessel to ensure that the required pressure is maintained. This extra effort stems from additional calculations needed to ensure that the piping and cycle components are able to contain the pressure, even at the extremely high temperatures at which the primary cycle operates. High pressures combined with elevated temperatures are risk factors for phenomena like material creep, which have to be avoided by design making adequate design choices.

- **Leak safety:** Despite careful design of the piping carrying the coolant, a leak can always occur. The consequences of a small leak determine the score that a certain coolant achieves in this field. If a small leak causes an explosion or total drainage of the system, the reactor is in danger of overheating and this poses a serious safety hazard. Therefore, such a coolant receives a low score.
- **Maintenance operations:** The fuel of the nuclear reactor has to be replaced occasionally, or other maintenance has to be performed which involves gaining access to the reactor core. This requires the reactor to be shut down and the coolant to be removed from the surroundings of the fuel elements. The effort needed for this is determined by the ease of blocking the coolant flow and removing the heat source without the coolant undergoing phase changes. Liquid coolants with a high melting point receive a lower score whereas single phase coolant cycles have the upper hand in this field.
- **Cooling properties:** Heat transfer properties and the maximum operating temperature of a coolant are important for efficient heat removal from the core. A large heat transfer coefficient and heat capacity of the coolant reduces the size of the heat exchangers in the cycle and stable properties at high temperature provide an added degree of safety, resulting in a higher score. Liquid coolants with low boiling points or high vapour pressures do not score high in this criterion. High temperature operation is not only required to transport a large amount of heat to the propulsion system, but it also has a safety aspect. If the reactor experiences supercriticality or meltdown, the temperature in the reactor can rise above its maximum operating temperature. The coolant has to be stable in these conditions so that there is no additional danger next to the already faulty reactor.

Not all criteria are equally important for the final decision. Referring to the top-level requirements mentioned in section 1.3, the selection categories are weighted as shown in table 2.1. The explanation of these assigned values lies in the fact that the highest scores are assigned to the criteria that stem directly from the most important requirements that the resulting design should be as light and safe as possible. Both nuclear activation and cooling properties do influence the weight of the cycle due to additional shielding that needs to be added or a higher mass flow being needed to compensate for the lower efficiency. Therefore, despite the indirect influence on the system weight, these criteria are still assigned a high weight. Design effort and maintenance operations are deemed least important in this decision because those can be compensated for in other parts of the design process. Moreover, they do not directly influence the safety or weight of the aircraft.

Criterion	Importance
Weight	2
Nuclear activation	2
Health effects	2
Design effort	1
Leak safety	2
Maintenance operations	1
Coolant properties	2

Table 2.1: Table of weights for reactor coolant trade-off criteria

The detailed reactor design is outside the scope of this thesis, and therefore the exact effects of the choice of coolant on some categories like weight and design effort cannot be expressed in numbers. Other criteria like safety can only be graded since there is no unit in which they can be expressed. Therefore, the comparison in section 2.4 is done only on a qualitative base. Each of the options is ranked against the other options to establish an idea of which is the most favourable in each category. Additionally a short explanation is given to substantiate the ranking.

2.4. REACTOR COOLANT SELECTION PROCESS

Now that the reactor options have been mentioned and explained, this section ranks them in the categories mentioned in section 2.3. To come up with a preferred reactor coolant, the options mentioned in section 2.2

are graded in each of the predetermined categories. A list of the categories is now presented, in which the score of each option in each category is shortly explained. The resulting scores and indication of the final choice is presented in table 2.2.

- **Weight:** In this important category the lowest scores are assigned to the water- and gas-cooled reactor options, despite their low density. Heat cycles using these fluids have to be pressurised, which increases the weight of both piping and compressors. Even when pressurised, the heat transfer properties of especially gasses are worse than for the other options. Because of this, gas-cooled reactors need bigger heat exchangers and also water cycles need a bigger weight budget for these components. Another downside to the system weight of choosing water or gas cooling is that the reactor can only be a thermal reactor, which has inherently lower power density than a fast reactor. This results in a higher reactor weight for the same power output. Alkali metal-, molten salt-, and fuel-cooled reactors have a lower system weight than the gas- and water-cooled options because these cycles operate at atmospheric pressures and the higher heat transfer coefficients reduce the weight of heat exchangers in this cycle. The weight savings due to heat exchangers results not only from the reduction in size of the heat exchanger, but also the resulting opportunity of reducing the size of the reactor vessel. This reduces the weight needed for shielding and impact protection drastically because the weight of the reactor vessel material is proportional to the cube of its radius:

$$W_{vessel} \propto r_{CV}^3 \tag{2.1}$$

  The lightest system is gained by selecting LBE as reactor coolant. Despite the high density of the coolant itself weight can be saved in every other aspect of this criterion. There is no need for pressurisation of the cycle, although the high density of the coolant does require a higher pumping power. Finally, the presence of lead in LBE provides an inherent shielding capability. This means that the shielding around the vessel has to block a smaller dose of radiation and can be decreased in thickness and thus weight.

- **Nuclear activation:** In this category, the scores are very far apart. Whereas molten fuel reactors have very high nuclear reactivity (the entire coolant cycle is designed to be highly radioactive), helium has a negligible activation level in the presence of radiation sources. All other options are scored as average, although there is still a clear distinction between them. Each of the remaining options, being salt, LBE, sodium, and water, have some degree of nuclear activation. Especially LBE is worth mentioning since the bismuth contained in it captures neutrons to eventually produce polonium 210. This is a potent emitter of hazardous α-radiation so extra precautions need to be taken in case the reactor or primary cycle require maintenance. Normally, α-radiation is not a large hazard because it can be shielded by as little as a sheet of paper. However, when inhaled or in direct contact with the skin it presents a high danger, which is why the precautions are especially necessary during maintenance and other instances when the cycle is opened.

- **Health effects:** The danger of liquid fuel reactors to human health and safety is obvious and punishing in this category. FLiBe, LBE, and sodium all contain toxic elements that are harmful to people that come into contact with the coolant. Water and helium present no significant health concerns and are therefore awarded the highest score in this row of table 2.2.

- **Design effort:** Because of the need for pressurisation the water-cooled reactor option has the highest design effort. Even though the helium-cooled option also has to be pressurised, it is indicated as a smaller design effort than water. This is because gas-cooled reactors do not have the danger of phase changes in case of a loss of pressurisation that water-cooled reactor do. Because of the reactivity of the coolant, fuel-cooled reactors also require a higher design effort. The cycle has to be designed such that criticality is only achieved in the reactor core and has to be prevented in the remaining points of the cycle. FLiBe, LBE, and sodium present the smallest design effort because the operate in near-atmospheric conditions.

- **Leak safety:** If a leak occurs, the pressurisation of the water and helium cycles can cause the leaking pipe to burst catastrophically. Even if this does not happen the coolant does not seal the leak and the entire cycle will drain out, depriving the reactor of coolant and putting it at risk of melting down. Sodium ignites spontaneously in air and reacts explosively with water so a small leak in a sodium coolant cycle will also pose a serious threat to the nuclear cruiser. If a liquid fuel reactor experiences a leak, the leaked material is highly radioactive and will form a pool at the bottom of the shielding vessel.

If this pool is large enough it can sustain a nuclear reaction of its own, as explained in section 6.1. The safest options in case of leakage are FLiBe and LBE. If a small leak occurs in a pipe containing these fluids they will solidify upon exit, thereby closing the leak. Even though it is a temporary solution and the reactor still has to be shut down for maintenance, the solidification does prevent a complete drainage of the cooling cycle.

- **Maintenance operations:** During reactor shut-down and fuel operations, the heat source to the coolant is removed. For gas-cooled reactors, this has the lowest effect since the coolant will not undergo phase changes and can easily be contained in the piping during maintenance. FLiBe has a high melting point at 730 K (457 °C), which requires an external heater to be active in order to prevent solidification of the coolant during maintenance operations. LBE has a lower melting point at around 400 K (125 °C), so except for during extensive time-consuming maintenance the coolant should be able to remain liquid with only minimal heating. However, the aforementioned release of Po-210 poses a serious hazard during open-cycle maintenance or leaks and requires extra precautionary measures. The latter is naturally also valid for liquid fuel reactors. In addition to that the entire system has to be drained to replace the reactor fuel, which has a negative effect on maintenance time and cost. Sodium and water are also graded as average in this category because they also run the risk of phase changes (solidification and condensation, respectively) during periods of prolonged absence of a heat source. For sodium, there is the added danger of accidental releases of highly reactive coolant that has to be prevented at any cost.

- **Cooling properties:** Helium has by far the worst heat transfer properties of all the selected coolants, but its prospective of operating at high temperatures without chemical damage to structural materials is a positive point that needs to be mentioned. Water has good heat transfer properties but its high vapour pressure and extreme corrosion properties cause it to only achieve an average rating in this category. Sodium, LBE, FLiBe and fuel all have excellent heat transfer properties. However, sodium has a boiling point of 1154 K (881 °C) so it presents a risk at high temperature operation. All of the coolants, except for helium, induce some form of chemical attack on structural steels that limits their maximum design temperature. That is the reason that, despite its poor heat transfer properties, helium is rated average in this category.

Criterion	**Fuel**	**FLiBe**	***LBE***	**Sodium**	**Water**	**Helium**	**Weight**
Weight	O	O	+	O	-	-	2
Nuclear activation	-	O	**O**	O	O	+	2
Health effects	-	O	**O**	O	+	+	2
Design effort	O	+	+	+	-	O	1
Leak safety	O	+	+	-	-	-	2
Maintenance operations	O	-	-	O	O	+	1
Cooling properties	+	+	+	O	O	O	2

Table 2.2: Decision table for reactor coolant

2.4.1. FINAL CHOICE AND ADDITIONAL INFORMATION

From the data presented in table 2.2 and the accompanying text of this chapter it becomes apparent that LBE is the most optimal coolant choice for operation of the nuclear cruiser. It allows for the cruiser to have a fast reactor, which has many benefits as mentioned in section 2.1. Due to its outstanding heat transfer properties and high boiling point, it can transfer large amounts of heat safely to the propulsive cycle. Its inherent shielding properties for nuclear radiation are essential for saving weight and increasing the safety of the nuclear cruiser. The only negative score in the table is in the category of maintenance operations but, as mentioned before and indicated by its low category-weight, this is not a decisive negative aspect because it does not directly influence the weight or safety of the cruiser itself and the maintenance facilities can be designed to cope with the problems it is faced with, even though this will require a lot of effort.

The maximum operating temperature for LBE depends on the type of steel used in the construction of the heat cycle[25]. Various constituents of structural steels can be absorbed by the molten lead, leading to corrosion and change of structural properties of the piping. Ferritic steels with increased chromium content can be used up to 923 K (650 °C), whereas especially austenitic nickel-containing steels stop being effective above 773 K (500 °C). Due to extensive research performed in Russia it is known that an increased level of safety can be achieved by active oxygen control in the LBE loop. This generates a protective oxide layer on the surface of the pipes, which prevents solution of structural material into the liquid metal[26]. This oxide layer is shown to be self-healing in the paper by Li[27]. The dynamic stability of the protective oxide layer is unknown. Studies do suggest that the flow speed for LBE is limited to around 3 m/s because of this[28]. Other studies suggest advanced materials called *functionally graded composites* that do not undergo degradation in an environment of LBE at temperatures up to 973 K[29]. A final favorable safety aspect of LBE is the fact that it can sustain natural circulation. In case of failure in the coolant pumping system, the reactor core still needs to be cooled to prevent meltdown. Other coolants require a backup pump to achieve this but the large density and low heat capacity of LBE cause it to be able to sustain convective flow due to density differences induced by the heating of the fluid on the side of the loop where the fluid travels upwards and placing the intermediate heat exchanger on the downward side.

3

Heat Cycle Layout and Secondary Cycle Fluid Selection

In this design and feasibility study the most pressing unknown, apart from the reactor, is the system that converts the reactor heat into useful work, in the form of propulsive power. Besides being efficient and safe, which is required for every heat cycle, regardless of its application, the cycle used in a nuclear-powered cruiser also has to be as light as possible. This leaves more of the weight budget available for passengers and cargo. This chapter discusses the design options for the heat cycle, as well as the fluid that is used. After that, a selection is made in section 3.3 of the configurations that are put up for further research in this thesis. The chapter is concluded by a section that discusses several safety features that are included in the heat cycle to ensure adequate power generation throughout the flight.

3.1. Heat cycle layout options

This section introduces the various cycle set-ups that have been introduced in the past and that may be useful for using the heat from the nuclear reactor and generating propulsive force. For each of the options a short description of the cycle layout is given, along with the advantages and disadvantages of the design with respect to efficiency, weight, and safety.

Two different types of cycles are introduced in this section: *open* or *direct drive* cycles and *closed* or *indirect drive* cycles. Open cycles are similar to current jet engines with air acting as the final working fluid. Using the preliminary engine design mentioned in section 1.2, this means that the combustion chamber of the turbofan is replaced by a heat exchanger to allow the secondary cycle fluid to heat the airflow in the engine. Indirect drive cycles are mainly used in power generation and employ a working fluid that is led through a closed system of pipes and components designed to perform thermodynamical work on the fluid. Eventually the heated working fluid passes through a turbine, which is used on the nuclear cruiser to directly drive the fan of the engine through a series of driveshafts and gearboxes. Because the heat cycle is sized for cruise power only and the fan of a turbofan engine delivers the vast majority of propulsive power during cruise, this set-up does not have significant consequences for the engine design.

3.1.1. Through and through direct cycle

During the Cold War research performed in the United States, a very simple concept for nuclear aircraft propulsion was conceived. With examples being treated in [30, 31] and shown in figure 3.1, this direct drive cycle leads the air directly through the reactor core to cool the reactor and power a jet engine as usual. The only difference is that the air is not heated by fuel combustion but by the heat from the nuclear reactor. The process is schematically represented in figure 3.2.

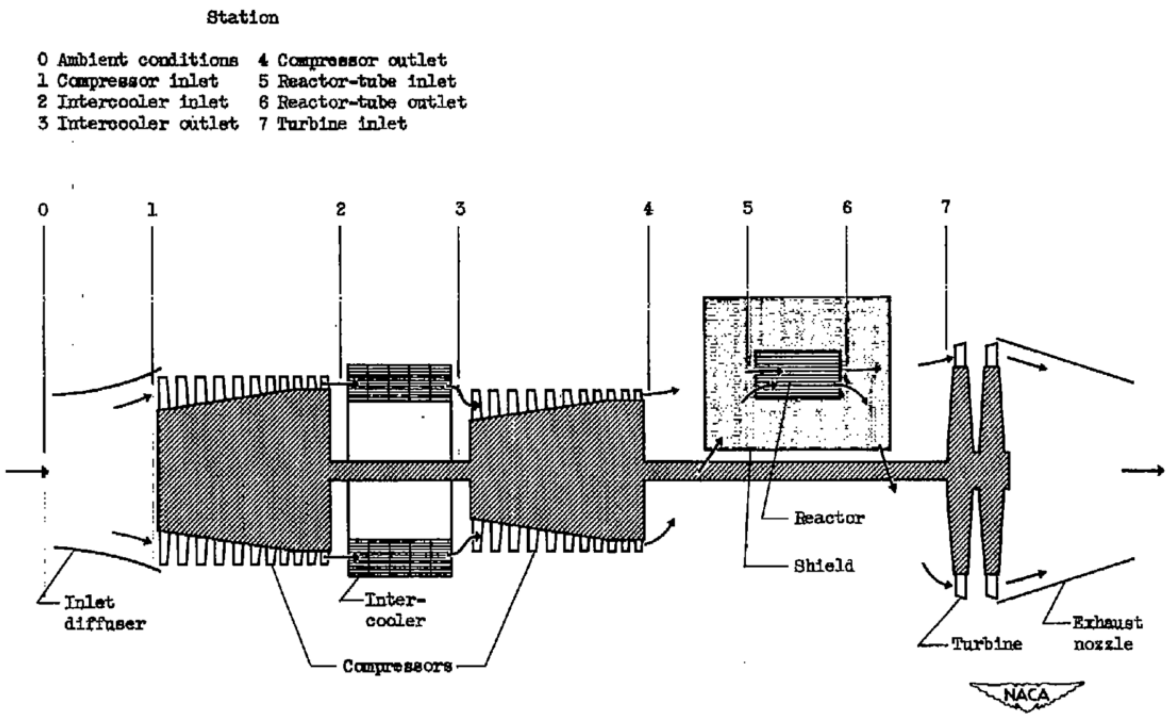

Figure 3.1: Example of a through and through direct cycle, as presented in [30]

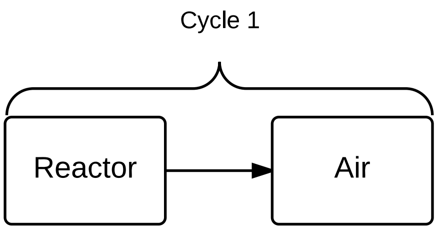

Figure 3.2: Schematic representation of the through and through set-up

Even though such a design would impose the least amount of changes on the aircraft and engine designs, as well as save the addition of a heat cycle, its safety issues are unacceptable. The air will pick up fission products as it travels through the reactor core, which results in radioactive exhaust streams. Additionally there is the problem that any leak in the piping can transport nuclear material outside of the shielding and into the jet exhaust. Moreover, the heat transfer properties of air are very poor so the airflow has to be very large and stable to prevent the reactor from melting down. For all these reasons, this concept is not considered a viable option for the nuclear cruiser.

3.1.2. SINGLE DIRECT CYCLE

To overcome the issues of the through and through direct cycle, another option is proposed that uses an additional fluid to transport the heat from the reactor to a heat exchanger in the engine pod. This heat exchanger then heats the air in the jet engine, thereby replacing the usual fuel combustor. A design for such a cycle is shown in figure 3.3, with the schematics being portrayed in figure 3.4. The fluid can be chosen using a process similar to the process explained in chapter 2, for example [32] proposes liquid metal and [31] chooses helium.

Despite the safety of the system being raised by the addition of the fluid cycle, the risk of nuclear spillage is still too high to consider this option for the nuclear cruiser. It has to be assumed that the material in the so-called primary cycle (which is the heat cycle that runs through the reactor) becomes radioactive to some degree. This means that all the piping shown in figure 3.3 should also be shielded. Another risk is added by the possibility of the heat exchanger in the engine developing a leak. This would directly result in radioactive

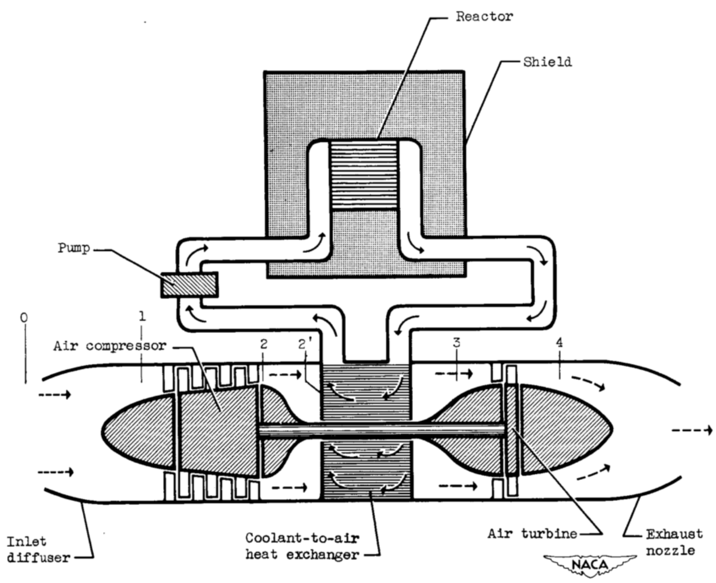

Figure 3.3: Example of a single direct cycle, as presented in [32]

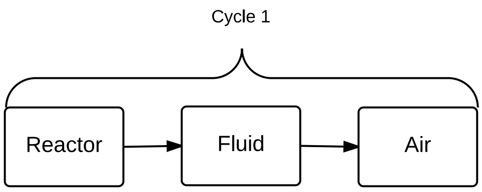

Figure 3.4: Schematic representation of the single direct cycle

contamination of the air and the environment. The conclusion is that a double cycle is needed to ensure safe operation of the cruiser. The primary cycle has to lie completely within the reactor shielding vessel, as mentioned in chapter 2, and a heat exchanger is used to transfer the heat to the secondary cycle, which is outside of the shielding and provides the aircraft with thrust. The options for such a double cycle set-up are treated in the following sections. Note that the primary cycle is a closed cycle filled with the reactor coolant selected in chapter 2 in each case. The distinctions are made in the specifics of the secondary cycle.

3.1.3. DOUBLE INDIRECT DRIVE DUAL-PHASE CYCLE

The phase change in the secondary cycle can be beneficial because compressing the working fluid in liquid form requires less work than compressing its vapour. However, there is a loss of enthalpy involved in each phase change. This decreases the efficiency of such a Rankine cycle. For most fluids this decrease is compensated for by the decreased energy needed for the compressor to compress the liquid. The main problem with the Rankine cycle for use on the nuclear cruiser is that the condensing process requires a strict temperature regime in the condenser. If the cooling side is too warm, the condensing will not take place and the subsequent compressor is unable to compress the fluid enough for the power output of the cycle to be anywhere near the designed levels. In regular power stations, where Rankine cycles are often used, a steady supply of constant-temperature cooling fluid (usually water) can be guaranteed but in aircraft operation it cannot. Even on a hot day, the cruiser still has to be able to fly. For that reason, the Rankine cycle is not considered for further calculations. A schematic lay-out of a double indirect drive cycle is shown in figure 3.5.

3.1.4. DOUBLE INDIRECT DRIVE SINGLE-PHASE CYCLE

This option is equal in general lay-out to the dual-phase option treated in section 3.1.3. In addition to varying the fluid in this cycle, the effects of which are treated in section 3.2, the closed indirect drive cycle can also be varied in layout. Employing various stages of intercooling and recompression of the working fluid, the efficiency of the thermodynamic cycle can be enhanced. Examples of this for cycles using supercritical car-

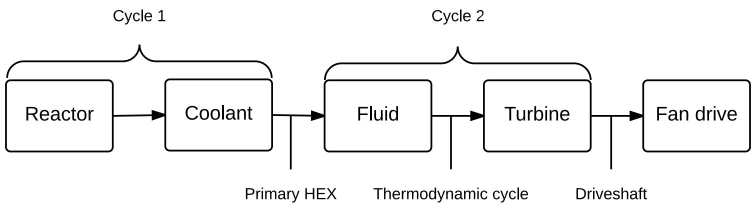

Figure 3.5: Schematic representation of the double indirect cycle

bondioxide (s-CO_2) are treated by Angelino[33] and Dostal[34]. The weight and efficiency of the cycle and its components depends on which of the layouts is selected. This is treated in more detail in section 3.3. As with the Rankine cycle mentioned in the previous section, this cycle is also sensitive to cooling conditions. However, because there is no phase change involved, the effect of an increase in coolant temperature on the power output of the cycle is less severe than it is in a dual-phase cycle. Therefore, this cycle option is considered for further research.

3.1.5. DOUBLE DIRECT DRIVE CYCLE

This open cycle is an extension of the open cycles mentioned before in sections 3.1.1 and 3.1.2. The difference lies in the addition of the primary loop to separate the reactor from the propulsion unit. The working is similar: a heat exchanger in the secondary loop acts as the cooler of that cycle and heats the air in the engine pod, which can then be used to generate thrust. A schematic representation of a double indirect drive cycle is shown in figure 3.6. The absence of regenerators and other components that are present in the closed cycle presents an opportunity for weight savings in case the direct drive cycle is selected. However, the poor heat transfer properties of air can prove to require a very large heat exchanger in the engine pod in order to provide enough energy to the air. This weight addition may nullify the weight savings mentioned earlier but because the exact weight distributions of the various cycles are unknown it does merit the choice to further investigate this cycle option.

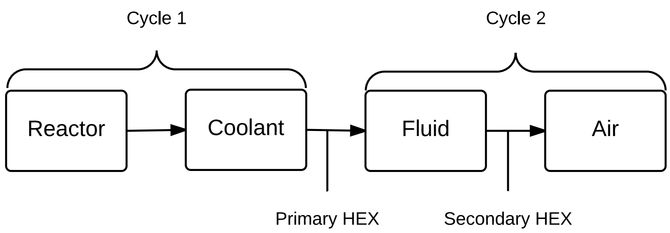

Figure 3.6: Schematic representation of the double direct cycle

3.2. HEAT CYCLE FLUID

With only dual cycle set-ups chosen, two decisions have to be made regarding the fluid to fill each of the cycles. The primary cycle fluid depends on the reactor type and has been treated in detail in chapter 2. A similar decision process can be applied to the secondary cycle, but only after the options have been listed and the updated fluid requirements are introduced. In choosing the appropriate fluid, it is important to realise which set-up is under investigation because the needs for an open cycle fluid will differ from those of a closed cycle. Therefore, two sets of options are treated in this section. In each of the two following sections the requirements for the cycle fluid are set out, followed by the fluid options and the explanation of the final decision. A large part of this discussion is equal to that treated in the selection of the primary fluid cycle. In order to avoid repeating information, only the differing aspects are discussed for the secondary cycle, while the other decision criteria are only mentioned shortly.

3.2.1. OPEN CYCLE FLUID SELECTION

Initial examination of the criteria used in the selection of the primary cycle fluid and how they influenced the final choice is the first step in determining the secondary cycle fluid. The analogy between the primary cycle and the secondary cycle in a direct drive set-up is obvious, because both cycles are designed to perform the same task: transport the largest possible amount of energy efficiently to the subsequent working fluid. The main decisive difference is that the secondary cycle lies outside of the shielding vessel. This diminishes the snowball effect that the size of the cycle has on the total weight of the system but also increases the relative importance of the nuclear activation because there is no shielding to absorb any accidentally-formed byproducts. Therefore, there are four decisive criteria that remain for the selection of the secondary cycle fluid.

- Weight
- Reactivity (combining of nuclear activation and chemical reactivity with the environment)
- Health effects
- Thermal properties

Taking into consideration the statements made during the primary fluid selection, along with the updated requirements, only four of the options considered for the first cycle remain feasible in this selection. Especially the importance of the coolant's heat transporting properties eliminates the gas coolants as an option. So the remaining options for further assessment are *LBE, FLiBe, sodium*, and *water*. These options are now compared in each of the categories listed above to come up with the most realistic fluid for further designs.

This paragraph recalls the criteria that were selected earlier and discusses the properties of each of the fluid options for those criteria.

- **Weight:** In order to achieve the highest possible heat transfer the water should be kept liquid. At the temperatures involved this means pressurising the water, which adds weight compared to the other non-pressurised cycle options. Because of the thermal properties of the fluids, the size of the heat exchanger will vary slightly. The same goes for the compressor weight and power needed to ensure the coolant flow rate. However, apart from the pressurisation of water these differences will not prove to be decisive.
- **Reactivity:** The points made in section 2.4 during the primary cycle fluid selection are still valid here, with some extra remarks that need to be made. The production of ^{210}Po by the bismuth in LBE is a larger hazard in the secondary cycle because there is no shielding or containment present to prevent spreading of this isotope in case of a leak. For sodium, the risk of violent reactions is an even bigger issue due to the higher probability of coming into contact with air or moisture in the secondary cycle.
- **Health effects:** As mentioned in the primary fluid selection, this criterion favours water because it is the only non-toxic fluid of the four options.
- **Thermal properties:** While all of the selected fluids have highly beneficial heat transfer properties, the thermal conductivity of sodium is better than the others', whereas the specific heat capacity (measured in the unit J/m^3K) of LBE and FLiBe is higher.

Because of the pressurisation of the cycle, water will not be considered in further research. The same goes for sodium due to the reactivity with air and water. LBE and FLiBe are then left to be analysed further. Between those two fluids, the polonium production is decisive to make the final decision for the secondary direct drive cycle. In the primary heat exchanger there is always the possibility of nuclear activation of the secondary coolant. The results of even small amounts of leaked neutrons on LBE are detrimental to the safety of the cycle so that FLiBe becomes the fluid of choice for the secondary cycle of the open cycle set-up.

3.2.2. CLOSED CYCLE FLUID SELECTION

The function of the fluid in a closed cycle is different from that in a direct drive cycle. In stead of only having to transport heat between two heat exchangers, the fluid in an indirect cycle has to facilitate an efficient thermodynamic process in which as much of the energy gathered from the intermediate heat exchanger is converted to useful work to the shaft that is connected to the turbine in the closed cycle. This also changes the requirements for the cycle's content. The decisive factors in this selection are *weight, health effects*, and *coolant properties*.

The selected fluid options for the secondary cycle are taken from the selection of primary fluids presented in chapter 2, augmented by suggestions from literature. The selected fluids are listed below, after which a comparison of the fluids in the selected criteria is presented.

- Sodium vapor, as presented in a compression cycle as an option during the ANP programme[35]
- Supercritical CO_2, suggested by several researches[33, 34] and even investigated for aircraft propulsion in [36]
- Water in various possible cycles differing in the state of the water throughout the cycle. This can be pressurised liquid, combined liquid/steam cycle with condensation, superheated steam cycle without condensation. Water has been investigated for the *RECREATE* cruiser's propulsion system in [37]
- Helium, which was an often-chosen fluid in the ANP period research[11–13]
- Mercury, which has also been used in nuclear aircraft propulsion system designs during the ANP era[38]

The properties of each of these fluid options in the decisive criteria is listed below.

- **Weight:** The weight of the secondary cycles consists of the weight of the fluid itself, the weight of the components such as compressors and coolers, and the weight of the piping, which is influenced by the operating pressure of the cycle. In fluid density, the liquid metals are the obvious heaviest system, followed by water, s-CO_2, and helium. The pressurisation of the systems shows an opposite trend. The mercury system proposed in [38] is pressurised to 2 bar (= 0.2 MPa), and [35] pressurises the sodium vapor to about 2 MPa. The various helium cycles that are proposed use pressures up to 14 MPa, and [37] uses a maximum steam pressure of 21 MPa. The highest pressures are necessary in s-CO_2 cycles, which stay above the critical pressure of 7.4 MPa throughout the cycle and can reach as high as 70 MPa in [36]. The increase in piping weight that this induces for the CO_2 cycle is compensated by the component weight. Due to the favourable conditions at the compressor and turbine, s-CO_2 only needs turbomachinery that measures a fraction of the of the size of other cycles'. The big difference in component weight between water, helium and s-CO_2 is illustrated by figure 3.7. Moreover, the single-phase cycle in CO_2 and helium dismisses the need for a large condenser, which proves to be too big to fit in the cruiser in Hsia's research[37].
- **Health effects:** There is a clear distinction in this category between the toxic sodium and mercury on one hand and harmless water, helium and CO_2 on the other.
- **Thermal properties:** The metals mercury and sodium have the most favourable thermodynamic properties but their high densities and viscosities also make that a lot of work is required to pump them around. Water has the potential of reaching high efficiencies, just like helium, which is why they are often used in current power stations. However, utilising the optimal conditions around the critical point, these high efficiencies can be surpassed by s-CO_2.

The adverse health effects of mercury and sodium are again prohibitive for using these materials in the nuclear cruiser. Considering the possible gains in weight and efficiency that s-CO_2 promises over water and helium, it seems that s-CO_2 is the most optimal fluid for operating the dual closed system. But then why do so many power stations still use water? s-CO_2 has not been used much in power generation up to now due to the high pressures and temperatures involved in the system. Additionally, in making the design choices for stationary power generation weight does not play a major role because there is no loss in efficiency of the system that results from a higher cycle weight. For the nuclear cruiser on the other hand, weight is obviously a critical factor. Also, scientific attention for this fluid has increased over the past decades and advances in structural materials as well as the fact that the temperature is limited to around 923 K by the choice of LBE in the primary cycle makes s-CO_2 an optimal candidate for the secondary closed cycle.

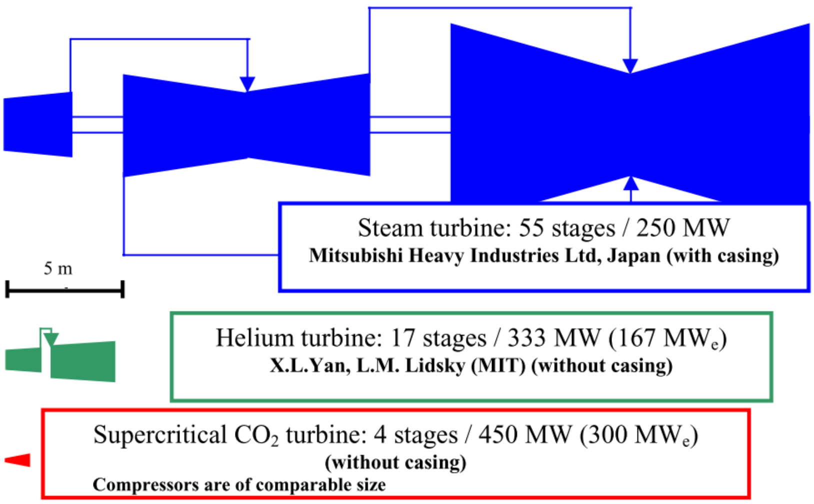

Figure 3.7: Comparison of turbine sizes for several fluids, from [34]

3.3. HEAT CYCLE SELECTION PROCESS

Now that the optimal fluids for each of the cycle options have been established, the cycle design options can be introduced. These designs are then analysed further in chapter 4, where the components are sized and their weight calculated to generate a final optimal design for the heat cycle of the *RECREATE* nuclear cruiser.

For the direct drive cycle, the chosen design is straightforward. The design option for further consideration is the cycle shown in figure 3.8, filled with FLiBe. The necessity for a back-up fuel burner is explained in detail in section 3.4.

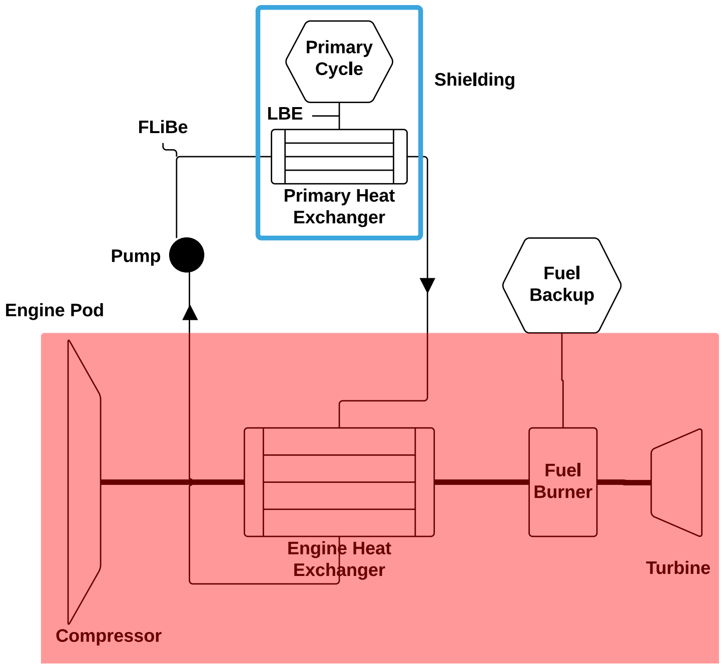

Figure 3.8: Direct drive heat cycle lay-out

For the closed cycle, some more analyses are needed before a design option can be proposed for further analysis. When the indirect cycle was introduced in section 3.1.4 it was already mentioned that the efficiency of the cycle can be increased by including extra intercoolers, generators, and compressors. This is done at the cost of additional weight to be added to the aircraft due to the extra components in the cycle. In literature mainly the cost and efficiency of heat cycles is treated because the weight of the heat cycle has no influence on its design for ground power stations. Contrary to that, the amount of power required from the heat cycle aboard the cruiser is a function of the aircraft weight, of which the propulsion system is a part. The result is that at some point the increased number and size of components will add so much extra weight to the heat cycle that the gain in efficiency is nullified. The lack of literature treating the weight optimisation of heat cycles makes that it is very hard to determine in advance which of the cycles is most optimal for the nuclear cruiser. It is assumed that it will either be the simple regenerative cycle or the single recompressive. Schematics of these cycles are shown in figures 3.9 and 3.10 for regenerative and recompression, respectively. The addition of the extra compression in the recompressive cycle increases the efficiency of the cycle, which means that the reactor has to generate less power to achieve the same propulsive power. This results in a weight saving of the reactor and primary cycle. Also the working pressure needed in a recompressive cycle is lower, which means that the piping can be made thinner and lighter than for a regenerative cycle. On the other hand, the regenerative cycle does save weight because of the fact that it needs only one regenerator and compressor, in stead of two. It also has a lower mass flow than the recompressive cycle. All these considerations make that a straightforward choice cannot be made between both cycles. That is the reason why both the regenerative s-CO_2 cycle, as well as the recompressive version of the same cycle, are selected for further analysis and comparison in weight to the open cycle selected earlier. This brings the total number of cycles to be studied further to three: one open cycle set-up using FLiBe, and two closed cycle set-ups using s-CO_2 namely a regenerative and a recompression cycle.

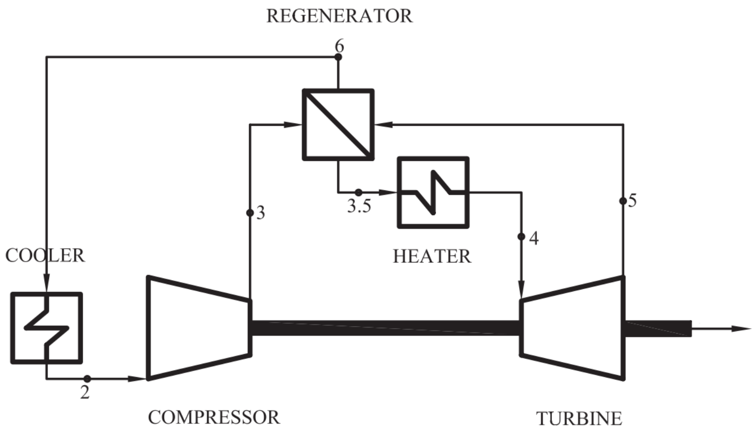

Figure 3.9: Regenerative heat cycle option for s-CO_2, from [36]

3.4. HYBRID AND BACK-UP PROPULSION

In case of a failure in the propulsion system, it is important for the cruiser to have alternative sources of propulsion to ensure a safe flight and emergency landing. Another reason for the inclusion of additional power sources lies in the inability of almost all types of nuclear reactor to cope with sudden changes in power demand. This type of power delivery is called load-following power generation and a clear example of such generation is a hydroelectric plant. In such a power plant the flow of water can be varied to regulate the output of electricity so that it matches the demand as closely as possible. A nuclear reactor on the other hand is strong in generating a large amount of power continuously but is generally slow in changing its power output. This is due to the underlying dynamics of nuclear reactions as well as the time it takes for control rods to move and influence the amount of neutron reactions taking place. However, the main reason for the inability of nuclear power cycles to quickly change between power settings is the thermal inertia of the coolant. Even though the nuclear reaction rate can be controlled relatively quickly, it takes longer for the coolant to actually cool down remove the remaining heat from the reactor core. Lokhov[39] states that most nuclear power plants are therefore used for constant power generation. Some types of reactors may be able to deal with changes in demand between 50% and 100% of rated power with rates of change of 3-5% per minute, which is not fast enough for aircraft operation during take-off and landing. Other types can handle changes of "several percent points per second but only within a narrow band around the rated power level", where the narrowness of the band is not enough to accommodate the changes in power needed in case of a touch and

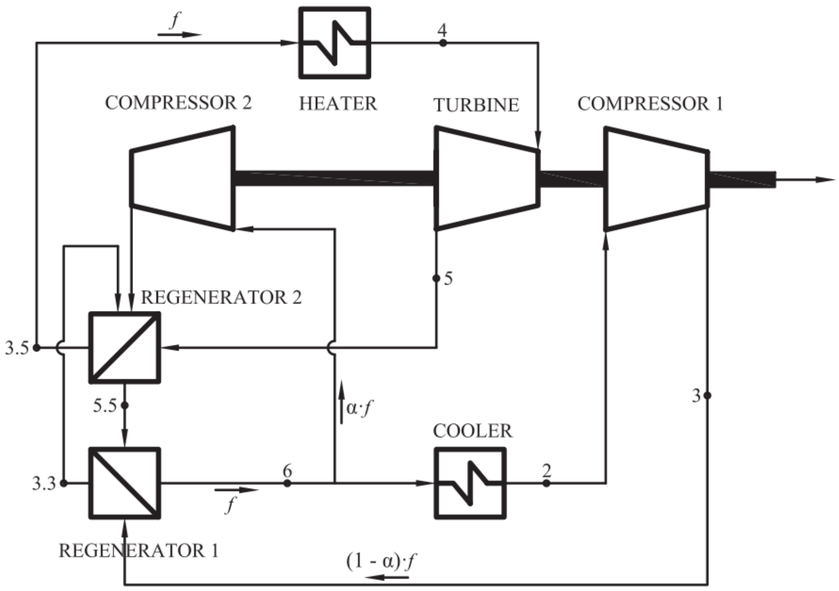

Figure 3.10: Recompressive heat cycle option for s-CO_2, from [36]

go or aborted landing when the power need changes from near 0% to 100% in a few seconds. The necessary back-up capability is achieved in the following ways:

- Two reactors and heat cycles
- Hybrid powered heat cycles, able to switch between nuclear heating and chemical fuel burning
- Hybrid engines, able to augment nuclear heating by chemical fuel burning, or run solely on chemical fuel

Each of the options is shortly described in the following sections. It must be noted that the first option, being two reactors and two heat cycles, does not address the problem of load-following capabilities because both of the heat cycles will still experience the same problem with thermal inertia mentioned before.

3.4.1. DUAL REACTORS

The heat cycle options that have been discussed in previous sections receive heat from a nuclear reactor and use it to generate propulsive power. They can be designed such that one cycle provides all the required power, however Chiozzi[8] already recognizes the opportunity of dividing the power generation over two reactors. In that case, if one reactor fails, the other still provides power to the aircraft and less reserve fuel is needed for emergency operations. In the current research it is assumed that each reactor drives its own heat cycle, which powers half of the number of engines. The other reactor then powers the remaining engines using its heat cycle. Unfortunately there is a weight penalty that has to be taken into account for the dual reactor option. Due to the scaling laws of reactor size and shielding material presented in equation 2.1, the reactor that provides 100% of the power on its own will be significantly lighter than the combined weight of both reactors and cycles in the dual reactor set-up. But if the reactor fails in the case of a single reactor configuration, the cruiser depends solely on reserve kerosene or biofuel to fly to a dedicated airfield and perform an emergency landing. This increases the chemical fuel weight that needs to be carried. The choice of configuration depends on the route that is chosen for cruiser operations and the separation between suitable airfields along that route. If the aircraft has to cover large distances before landing in case of system failure, the dual reactor option is more favourable because 50% of the power needed to cover this distance is provided by the remaining nuclear cycle. With decreasing distance between the airfields, the reserve fuel weight needed for the single reactor configuration also decreases and at some point the total weight of the propulsion system and reserve fuel falls below that of the dual system set-up.

In case a two-reactor set-up is selected, attention must be given to the controlability of the cruiser if one of the heat cycles fails to deliver power. If this happens, power in half of the engines is reduced to the power generated by the combustor in the engine pod, designed to provide power during take-off and landing (the specifics of this are treated in section 3.4.3). If the failing engines would all be on the same side of the aircraft, this generates a large yawing moment. Therefore, it is proposed to cross-link the driveshafts so that one cycle powers the inner engines and the other serves the outer engines. An example of such a set-up for a four-engined cruiser is schematically drawn in figure 3.11.

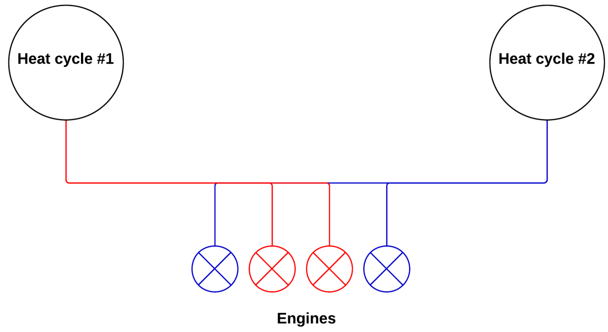

Figure 3.11: Schematic drawing of crossed driveshafts for a two-reactor aircraft

3.4.2. HYBRID HEAT CYCLES

During cruise the heat cycle fluid is heated through a heat exchanger linked to the nuclear primary cycle. However, if this source has to be eliminated the heat cycle can still be used to generate the cruise power by means of heating the fluid in another way. In this concept, the heat cycle operates in a similar fashion regardless of its heat source: all temperatures and pressures throughout the cycle are the same. Careful determination of the required fuel flow is necessary to ensure adequate heat generation.

The introduction of hybrid power for the heat cycle is done through the use of an alternative heater. During take-off and landing, a valve can be switched so that the fluid is no longer led through the heat exchanger that is linked to the primary nuclear system. Instead, the heat cycle fluid is routed through another heating system, in which it takes in the heat from a fuel burner. The addition of the extra route can be seen in the red highlighted area of figure 3.12. The rest of the cycle is identical to the recompression cycle as shown in figure 3.10 and can also be applied in the same manner to a regenerative cycle and the open cycle. This system only powers the heat cycle, which is designed for generating exactly enough power during cruise flight. During take-off and landing additional power is needed, which can be provided by incorporating a hybrid drive engine. This is explained in section 3.4.3.

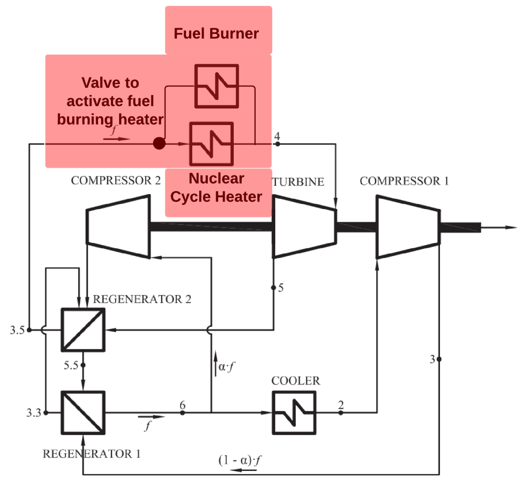

Figure 3.12: Example of a hybrid recompressive heat cycle, with the hybrid part highlighted in red

3.4.3. HYBRID ENGINES

This thesis focusses on the design of the heat cycle for a power output equal to the cruise power. However, as determined in [8], the cruiser requires more power during other stages of the flight such as take-off and manoeuvring. Assuming a hybrid cycle set-up, as explained in section 3.4.2, the heat cycle is able to provide a power equal to the cruise power during all flight phases by means of switching between nuclear heating and fuel burning. To augment the power generated by the heat cycle, the engine design includes an additional fuel burner to increase the power to the fan and provide additional thrust by means of a jet nozzle. For the jet cycle, the additional fuel burner is already visible in figure 3.8, just left of the turbine. For the engine in the direct drive cycles, the resulting design is shown in figure 3.13. During cruise, the additional system is completely shut off by means of a valve blocking the airflow to the fuel burner and turbine. The fan is then fully powered by the heat cycle. If needed, the valve is opened and the engine becomes a regular high bypass turbofan engine like the engines seen regularly on current aircraft. The difference is that the hybrid engine receives additional drive to the fan provided by the heat cycle through the gearbox that links the driveshafts from the turbine inside the engine pod and the turbine from the heat cycle to the fan.

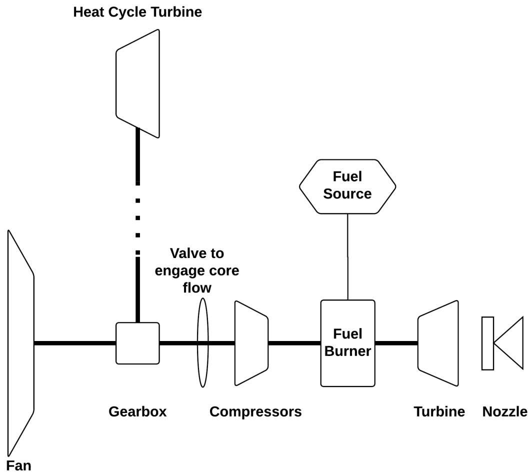

Figure 3.13: Schematic drawing of the hybrid fan engine for a closed cycle. Note the fact that the fan can be driven by the heat cycle turbine as well as the engine turbine

4
Heat Cycle Design Method

After the initial design choices regarding cycle lay-outs and fluids have been made it is time to implement the chosen heat cycles into the cruiser structure and optimise their design. The process starts with deciding where each component of the heat cycle is placed, and from that determining the optimal size and configuration of each component in a series of optimisation steps. This entire procedure is outlined in this chapter.

4.1. Heat cycle placement inside the cruiser

When deciding on the layout of the heat cycle inside the cruiser, the placement of the reactors is the most important design choice to be made. For reasons of safety and stability outlined in more detail in section 6.2, the reactors are placed in the wing roots, as was already suggested in figure 1.6. From this it is most convenient to locate the heat cycle components as close as possible to the reactor to decrease the weight and pressure losses resulting from the pipes between the components. The additional advantage is that the wing root offers the largest volume for placing the components and eases the design of the airflow needed for the cooler, which is explained in section 4.2.5. With the reactor placed, the following sections detail the location of the heat cycle components for the open cycle and the closed cycle, respectively.

4.1.1. Open cycle component placement

With the engine location fixed at the trailing edge of the fuselage and the reactors in the wing root, the placement of the heat exchangers and compressors can be determined. The primary heat exchanger has to be located inside the nuclear containment vessel and from there piping transfers the heated FLiBe to the secondary heat exchanger to heat up the air used for thrust generation. The placement of these secondary heat exchangers can be in any location on the cruiser apart from the front part of the fuselage where the passengers and crew are located. For the open cycle the optimal location for the heat exchangers is inside the engine pod to prevent the need for piping that transports air from the engine to the heat exchanger and back to the engine. However, as detailed in section 4.3, this may not always prove possible due to the size of the heat exchanger. If this is the case the secondary heat exchanger is placed in the aft fuselage.

4.1.2. Closed cycle component placement

For the closed cycle options there are more components and more pipes that have to be placed. The regenerative and recompression cycles both include a relatively large cooler that needs a large mass flow of air to cool the CO_2 and is therefore placed in the wing of the cruiser. To reduce the total length of the pipes the other components are also fitted in the wing instead of the aft fuselage. Figure 4.1 shows the approximate size and position of the heat cycle components. Note that the wing on the left side of the picture contains the set-up for a recompression cycle, whereas the other wing depicts the regenerative cycle components. The difference can be seen from the dual regenerators (depicted in green in the figure) and compressors (the little pink spheres in the picture) used in a recompression cycle. In reality of course the cruiser contains only the most optimal of these cycles, which is present equally in both wings to accommodate the dual reactor set-up introduced in section 3.4.

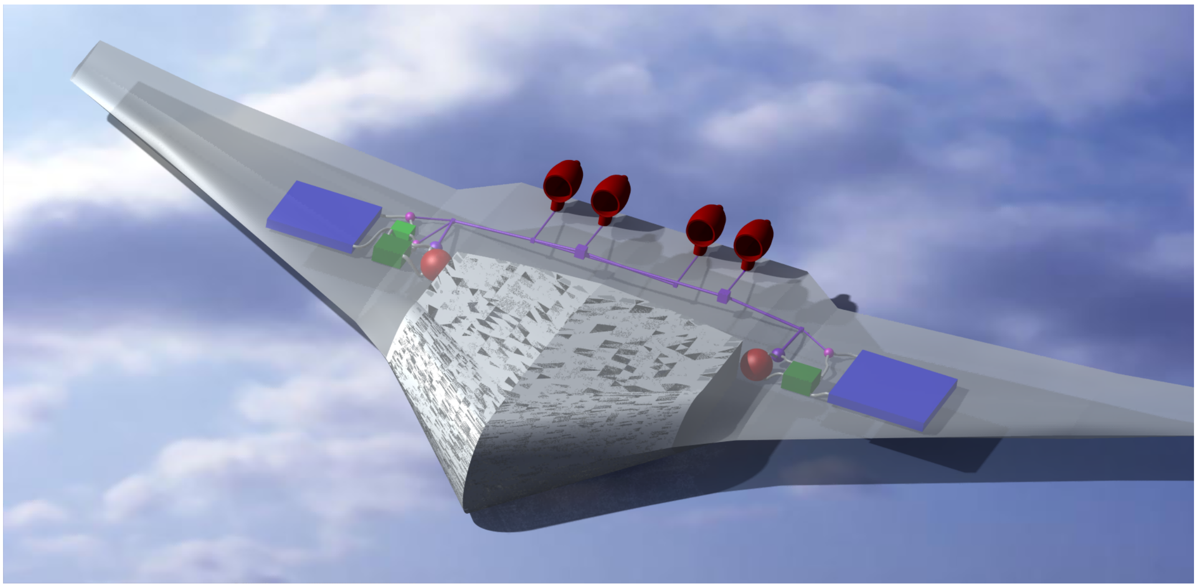

Figure 4.1: Sketch of approximate component placement in cruiser wing

4.1.3. THERMODYNAMIC CYCLE MODELLING

The heat cycles selected in chapter 3 are modelled as a series of heat exchangers and rotating equipment (compressors and turbines), linked up by piping. This study focusses on the design of the heat exchangers and the piping, because these are specific to the research at hand. Weight estimations for CO_2 compressors and turbines are not performed in this research because there is no applicable literature listing the weight of these components, let alone the relation between component weight and fluid pressure ratio and mass flow. As seen in figure 3.7 the compressors and turbines used will be relatively small, which is backed by the study described in [40] in which a mass flow of CO_2 of 5730 kg/s requires a compressor of only two stages with a diameter less than 1 m to compress the CO_2 from its critical point up to 20 MPa. Even though the maximum pressure in this research is higher than that, the general point of small turbomachinery will remain valid. Therefore it can be stated that, as long as the final cycle weight is significantly under the weight budget, the turbomachinery will not require extensive attention or optimisation at this stage. Another consideration has to be made for the driveshafts that link the turbines to the propulsion units. Those are also left out of consideration in this study because they are not specific for the cruiser; other fields of engineering are already researching lightweight options for driveshaft construction[41]. What is certain is that significant driveshaft weight savings can be achieved when compared to the research by Hsia[37], which uses steel bars for their construction.

Heat exchangers exist in many shapes and sizes, each differing in setup and characteristics. Because of the need for reducing heat exchanger weight while retaining high efficiencies, all heat exchangers in the cruiser design are chosen to be *Printed Circuit Heat Exchanger (PCHE)*. These heat exchangers consist of a stack of diffusion bonded plates, which bear chemically etched fluid channels in them. This is shown schematically in figure 4.2 and a cut-away of a PCHE stack is shown in figure 4.3. These heat exchangers ensure a high surface-to-volume ratio, which minimises heat exchanger volume and weight for a certain task, as well as safe operations even at high temperatures and pressures[42]. The calculation methods used to extract answers from the modelled heat cycles are described in the following sections.

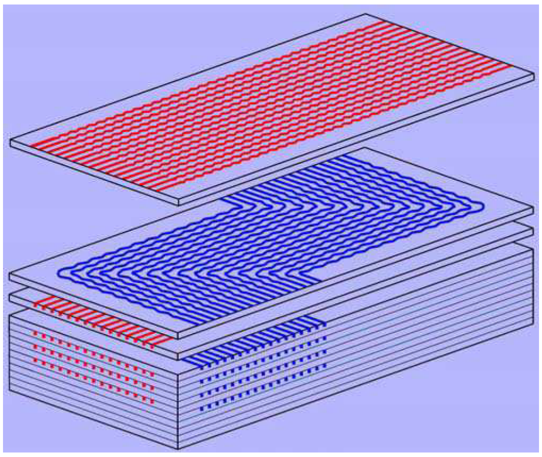

Figure 4.2: Schematic of PCHE buildup, from [36]

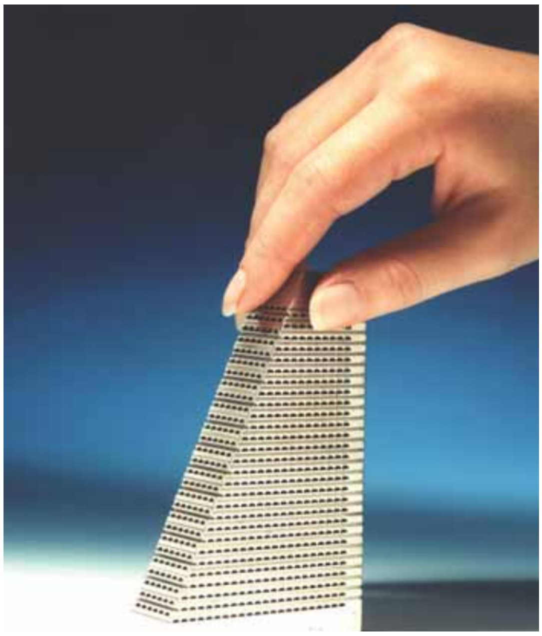

Figure 4.3: Cut-away of a PCHE, showing the fluid channels (from [36])

4.2. CALCULATION METHOD FOR THE CLOSED CYCLE SET-UPS

The obvious procedure for finding a minimum weight heat cycle would be to start a large optimisation, in which all components and variables are optimised simultaneously. However, too little is known about a location for the starting point, interdependencies of variables, and feasible bounds to start such an optimisation straightforwardly. In order to get a better feeling for all these aspects, as well as gaining understanding of the underlying thermodynamic and structural principles a different approach is taken. A UML flowchart of the major steps of the process is presented in figure 4.4. Each of the steps is performed by a separate set of *Matlab* calculation codes, which exchange inputs and outputs to reach a final optimised heat cycle set-up. The steps and their interactions are briefly explained below and detailed explanations of their working is given in subsequent sections.

1. **Input:** At the start of the process, the input data of the cruiser is entered into a code that calculates the required propulsion power

2. **Heat cycle calculation:** Together with inputs of cycle pressure and efficiency, this power is then loaded into the code that simulates the heat cycle and results in lists of temperatures, pressures, and mass flows of the CO_2 at different points of the cycle, as well as component powers. In preparation of the final optimisation it is important to determine a feasible starting point, the search for which is started in this step by varying the pressure and efficiency inputs to create a grid of cycle data to pass on to the following step, this is called the *cycle grid*

3. **Component calculation:** For each of the points on the cycle grid of feasible cycles the output of the heat cycle calculations is part of the input for the design code of each of the heat exchangers in the cycle. The rest of the required input for the heat exchanger codes consists of assumptions concerning the heat exchanger's dimensions, channel diameters, and secondary fluids for the cooler and heater of the cycle. For the piping the input consists of the length and initial guess for the radius per pipe. To come up with the lightest option for each of the heat exchangers at every cycle grid point, the heat exchanger design code is looped over a grid different inputs in what is called the *component grid search*. Because the components are independent of each other the combination of the lightest options for each component results in a minimum weight design for each cycle grid point. From the resulting surface of minimum weight cycle grid points the overall minimum presents a feasible starting point for the final optimisation. Additionally, the inputs per component that resulted in this minimum weight serve as the remaining input values for the optimisation step. A more detailed explanation of this step is given in figure 4.7 in section 4.2.4

4. **Optimisation:** Starting from the input vector of variables that results from the grid search, the optimisation is performed using the *fmincon* function that is standard to Matlab. Up to this point, all calculations are performed for a grid of input values on cycle as well as component level to provide an initial estimate of the minimum weight set-up. The optimisation allows the design code to abandon this discrete input structure and searches for an absolute minimum using continuous variations in input values. This is expected to result in a significant total weight reduction by increasing cycle efficiency and further optimising of the heat exchangers' geometry. Because the component calculations are performed in a multi-dimensional grid of input variables, the bounds of the variables in the optimisation can be taken directly from the grid of variables. A more detailed explanation of this step is given in figure 4.15 in section 4.2.7

The final outcome then consists of the minimum weight cycle set-up, containing the overall pressure and efficiency input as well as all the inputs for the individual components, resulting in an overall minimum weight for the propulsion cycle.

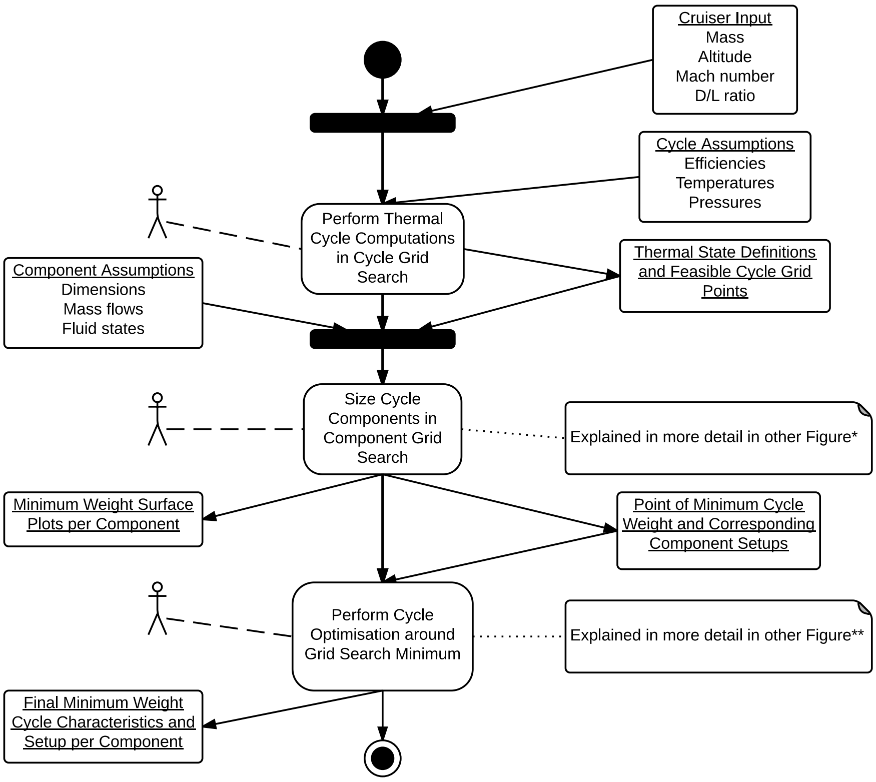

Figure 4.4: UML diagram of the overall Matlab code structure. *: see figure 4.7, **: see figure 4.15

4.2.1. THERMODYNAMIC CYCLE CALCULATIONS

The calculation process starts with a general input file that dictates the overall calculations. The input file contains some general aircraft characteristics which are used to determine the power needed from the heat cycle during cruise. Calculating the required power during cruise starts at the general power equation $Q = Th \cdot V_{cru}$, which puts the required power equal to the product of thrust and velocity, the terms can be rewritten using the assumptions that are valid during cruise. When putting thrust equal to drag, and weight equal to lift, Th can be written as $\frac{D}{L} \cdot m \cdot g$. Rewriting V as $M \cdot a$ yields equation 4.1. In this equation Q_{req} is the required power for propelling the aircraft, $\frac{D}{L}$ is the drag-to-lift ratio of the cruiser, m is the cruiser total mass, g is the gravitational acceleration of 9.81 $\mathrm{m/s^2}$, M is the cruise Mach number, and a is the sound speed at cruise altitude h.

$$Q_{req} = \frac{D}{L} \cdot m \cdot g \cdot M \cdot a(h) \tag{4.1}$$

The values of some these variables are given in the requirements set in table 1.1. The inputs further include the factor that relates power losses to added reactor weight PP. This is used in further calculations of the heat cycle to ensure cycle efficiency and minimise pressure losses. Pressure losses induce power losses because they have to be compensated for by increasing compressor power, which diminishes the effective power output of the cycle. All power losses have to be redeemed by increasing reactor power. This in turn increases the reactor weight, which is used in the final weight estimation and cycle optimisation to couple cycle component weight and cycle efficiency. The rationale that led up to determining the value listed below is given in more detail in section 4.2.7. The engine propulsive efficiency η_{eng} is set at a typical value for modern-day turbofan engines. The input values used in this thesis are listed in table 4.1.

Parameter	**Explanation**	**Value**
m	Cruiser mass, from table 1.1	1,000,000 kg
M	Cruise Mach number, from table 1.1	0.8
h	Cruise altitude, from table 1.1	11 km
D/L	Aerodynamic efficiency, from [6]	1/22.14
PP	Power penalty, explained further in section 4.2.7	1000 kg/MW
η_{eng}	Engine efficiency	0.88

Table 4.1: Top level input values for the heat cycle calculations

Filling in the values from table 4.1 into equation 4.1 yields a cruise power requirement of 104.6 MW. Dividing this power by the engine propulsive efficiency and keeping in mind that there are two heat cycles over which the power requirement is divided, the power requirement from each heat cycle is set at 59.4 MW.

Using this input, the thermodynamic heat cycle calculations are executed using the code by Noriega[36]. Using assumptions about component efficiencies, overall cycle pressure loss, and fluid properties, the calculation is set up such that the fluid properties throughout the cycle and component heat exchanging powers can be dictated by two variables: the pressure of the fluid after the compressor and the desired cycle efficiency. The code then finds the most suitable cycle that adheres to these inputs, while minimising the turbine inlet temperature (TIT). This set-up is convenient for this study because, as mentioned in section 2.4.1, the use of an LBE primary cycle limits the maximum achievable TIT, so maximising efficiency for a certain TIT is vital for increasing the feasibility of the cycle. The determination of CO_2 properties is done using a computational fluid library called *FluidProp*[43], which is capable op accurately calculating properties even around the critical point. Once the cycle operating characteristics have been set, each component is independent of the other components and can be sized separately. The methods used for each of the components are detailed in the following subsections.

4.2.2. HEAT EXCHANGER AND PIPING STRESS CALCULATIONS

Heatric[1], the main supplier of PCHE's, advises PCHE stress calculations to be based on a certain design pressure in stead of a pressure differential between the hot and cold plates. In the calculations, the design pressure is taken as the highest of the cold and hot stream pressures. In [42] Heatric proposes formulas for stress analysis in PCHE's that are based on the ASME design code for non-circular pressure vessels. From the analogy shown in figure 4.5 the side wall thickness t_{sw} (t1 in the picture), the plate thickness t_{pl} (t2 in the picture), and the wall thickness t_w can be calculated using d_{CH} where h is used in the picture and $\frac{d_{CH}}{2}$ for H.

For safe operation of the PCHE, two stress conditions must be met: one regarding the membrane stress and one regarding the total stress. From the design stress, σ_{des}, which is the material yield stress at the operating temperature divided by a safety factor and a bonding factor given as 0.7 for diffusion bonded PCHE's, limits for the so-called membrane stress σ_{mem} and total stress σ_{tot} are set. The total stress is the membrane stress augmented by the principal bending stress. The design limits are given as $\sigma_{des,mem} = \sigma_{des}$ and $\sigma_{des,tot} = 1.5\sigma_{des}$. Rewriting the stress equations to solve for the minimum required thickness yields the following equations. Note in these that, even though the design pressure P_{des} and stress remain equal throughout the PCHE, the possible variation in channel diameter between hot and cold plates causes differences in their construction. Equation 4.2 gives the thickness requirements for the side wall, equation 4.3 gives the thickness requirements for the plate, and equation 4.4 for the walls between the channels on each plate. Note that due to the equality in pressure between channels on the same plate, bending stress does not occur in

[1] http://www.heatric.com

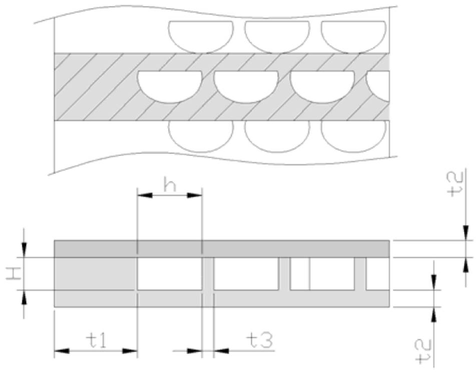

Figure 4.5: Schematic showing structural analogy used in PCHE stress calculations, from [42]

the walls and so the membrane stress is the only relevant factor in calculating its thickness. The value of the plate thickness is given by the maximum of the two thicknesses of equation 4.3. Note that these calculations are done separately for the hot and cold plates, as their thickness might differ as a result of differing internal pressures and channel diameters. For the PCHE side walls, the maximum is selected from all four values (membrane and total for cold plates as well as membrane and total for hot plates) to end up with a PCHE block that can withstand all internal forces.

Stress analysis for PCHE side walls:

$$\sigma_{mem} = \frac{d_{CH}P}{2t_{sw}} \tag{4.2a}$$

$$\sigma_{tot} = \sigma_{mem} + \frac{d_{CH}^2 P \frac{t_{sw}}{2}}{12\frac{t_{sw}^3}{12}} \tag{4.2b}$$

$$\text{Solving for } t_{sw} \text{ yields: } t_{sw,mem} = \frac{d_{CH}P_{des}}{2\sigma_{des,mem}} \tag{4.2c}$$

$$t_{sw,tot} = \frac{d_{CH}\sqrt{P_{des}^2 + 8\sigma_{des,tot}P_{des}} + d_{CH}P_{des}}{4\sigma_{des,tot}} \tag{4.2d}$$

Stress analysis for PCHE plates:

$$\sigma_{mem} = \frac{\frac{d_{CH}}{2}P}{2t_{pl}} \tag{4.3a}$$

$$\sigma_{tot} = \sigma_{mem} + \frac{\left(\frac{d_{CH}}{2}\right)^2 P \frac{t_{pl}}{2}}{12\frac{t_{pl}^3}{12}} \tag{4.3b}$$

$$\text{Solving for } t_{pl} \text{ yields: } t_{pl,mem} = \frac{d_{CH}P_{des}}{4\sigma_{des,mem}} \tag{4.3c}$$

$$t_{pl,tot} = \frac{d_{CH}\sqrt{P_{des}^2 + 32\sigma_{des,tot}P_{des}} + d_{CH}P_{des}}{8\sigma_{des,tot}} \tag{4.3d}$$

Stress analysis for PCHE channel walls:

$$\sigma_{mem} = \frac{d_{CH} P}{t_w} \tag{4.4a}$$

$$\sigma_{tot} = \sigma_{mem} + 0 \tag{4.4b}$$

$$\text{Solving for } t_w \text{ yields: } t_{w,mem} = \frac{d_{CH} P_{des}}{\sigma_{des,mem}} \tag{4.4c}$$

$$t_{w,tot} = \frac{d_{CH} P_{des}}{\sigma_{tot,mem}} \tag{4.4d}$$

For the piping the assumption is made that there is no significant pressure buildup at the heat cycle components. This means that there are no axial stresses in the pipe walls. The stresses that remain are the hoop stress and radial stress. The high pressure in the pipes and low atmospheric pressure warrant the assumption that P_i » P_o, which results in the hoop stress being the limiting factor in piping stress calculations. Assuming P_o=0 reduces the hoop stress equation to the form shown in equation 4.5, which is presented at the point of maximum stress on the inside of the pipe wall ($r=r_i$). Note that the assumption of thin-walled pipes is not made in this research because of the high pressures involved and the desired accuracy of the calculations.

$$\sigma_{h,max} = P_i \frac{r_i^2 + r_o^2}{r_o^2 - r_i^2} \tag{4.5}$$

Replacing r_o with r_i+t and solving for t yields equation 4.6 for the minimum value for the wall thickness, of which the answer on the right provides the only positive outcome. This is used in the calculations introduced in section 4.2.3.

$$t = \frac{\sqrt{\sigma_{h,max}^2 - P_i^2} \cdot r_i + (\sigma_{h,max} - P_i) \cdot r_i}{P_i - \sigma_{h,max}} \vee t = -\frac{\sqrt{\sigma_{h,max}^2 - P_i^2} \cdot r_i + (P_i - \sigma_{h,max}) \cdot r_i}{P_i - \sigma_{h,max}} \tag{4.6}$$

The principal material for the piping is Inconel 718, however its strength drops off dramatically at temperatures above 950 K. Above approximately 990 K, the structural properties of Inconel are surpassed by Waspaloy, which retains its strength better at higher temperatures[44]. This can be seen in figure 4.6 in which the yield stress of the two materials is compared at elevated temperatures. Depending on the temperature of the fluid, the most suitable of the two materials is selected.

Other materials could be considered in future research such as titanium and ceramic composites to save weight and extend high temperature operation if higher temperature reactor options are chosen. This thesis only considers steels because the cost of using titanium or ceramic composites for the large amounts of material that are used in the heat cycle would be very high. Because of the temperatures involved in the current cycle the use of high-temperature materials is not crucial, although the weight savings could be significant. Future research should make a trade-off between the potential weight savings and increasing costs resulting in an economical material choice.

4.2.3. PIPING COMPUTATION

From the thermodynamic cycle calculations each pipe has a predetermined set of relevant input characteristics: mass flow, temperature, and pressure of the fluid inside. From the layout shown in figure 4.1, the initial length of each of the pipes is also known. Using these inputs the piping computations should result in a set of radii and thicknesses of each pipe that results in the lowest weight pipes. The pipe thickness is determined from the internal pressure as described in section 4.2.2. The pipe radius is determined using an optimisation that includes weight and pressure loss. Increasing a pipe's radius increases the material volume needed for its construction and hence its weight, however it decreases the flow speed of the fluid inside. This in turn decreases the pressure drop experienced by the fluid. As is treated in section 4.2.7, all pressure losses have to be compensated for by increasing compressor power, which is converted to a weight penalty using the resulting difference in enthalpy, as explained further in section 4.2.7. The resulting weight penalty is then added to the physical pipe weight to end up with the optimisation parameter.

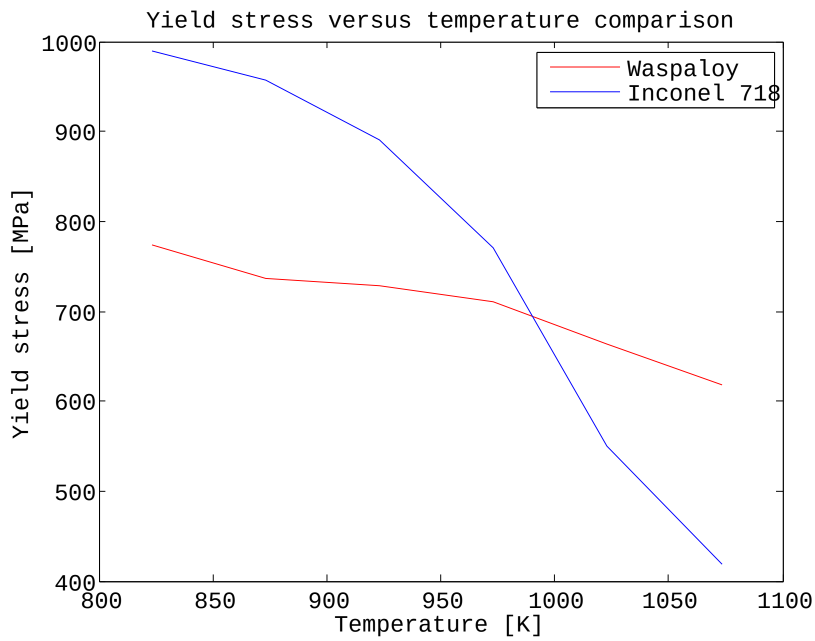

Figure 4.6: Comparison of yield stress at elevated temperatures for Inconel 718 and Waspaloy, adapted from [44]

4.2.4. HEAT EXCHANGERS COMPUTATION

Because there are no off-the-shelf PCHE calculation codes available, the calculation code that is developed in this study is adapted from the code used by Noriega in his thesis[36]. The calculation method used in this code is based on discretising the PCHE into a number of control volumes that each transfer a small portion of the total heat. This is outlined in detail in Noriega's thesis[36] and summarised in figure 4.7. An important fact to keep in mind is that all PCHE's in this study are modelled as counterflow heat exchangers. This entails that the inflow of the cold fluid coincides with the outflow of the hot fluid, which increases efficiency of the heat exchanging process.

This section discusses only the significant alterations made to the code and the reason why these are deemed necessary. This procedure ensures validity of the results as much as possible because the results of Noriega have been verified. The calculations for each heat exchanger are dictated by a set of parameters, which are introduced in table 4.2 along with their source. The source of some variables is different depending on the heat exchangers under consideration. For example, in a regenerator both mass flow inputs are dictated by the outcome of the heat cycle calculations explained in section 4.2.1, whereas for a heater or cooler the mass flow of the fluid other than CO_2 is provided as input. In this thesis the assumption is made that the cross sections of the PCHE perpendicular to the flow are square, so that they can be sized using single input of h_{HEX}. The length of the PCHE (parallel to the flow) is calculated by summing the lengths of the control volumes used to size the PCHE. A schematic representation of a PCHE including the terminology as described above is presented in figure 4.8.

Most of the alterations made stem from the need of the PCHE's in the cycle to cope with different fluids. This is in contrast with Noriega's work, where the PCHE was only used as a regenerator which has similar states and fluids on both sides. One such alteration is found in the computation of the temperature of the plate between two channels, which Noriega simply calculates as the average of the two fluid temperatures. However, Hesselgreaves[45] suggests a general equation when the two fluids have different properties, which is slightly altered to produce the equation shown in equation 4.7. When both fluids' α's are (approximately) equal, the simplification used by Noriega is valid, however especially the heater and cooler call for the use of the full equation in their calculations. Because of the semicircular nature of the channels, the perimeter facing one side is different from that facing the other side. This is reflected in the use of two equations (one for the wall between the circular arc of the cold channel and the straight wall of the hot channel and one vice versa), of which the results are averaged to reach an average wall temperature experienced by the fluid.

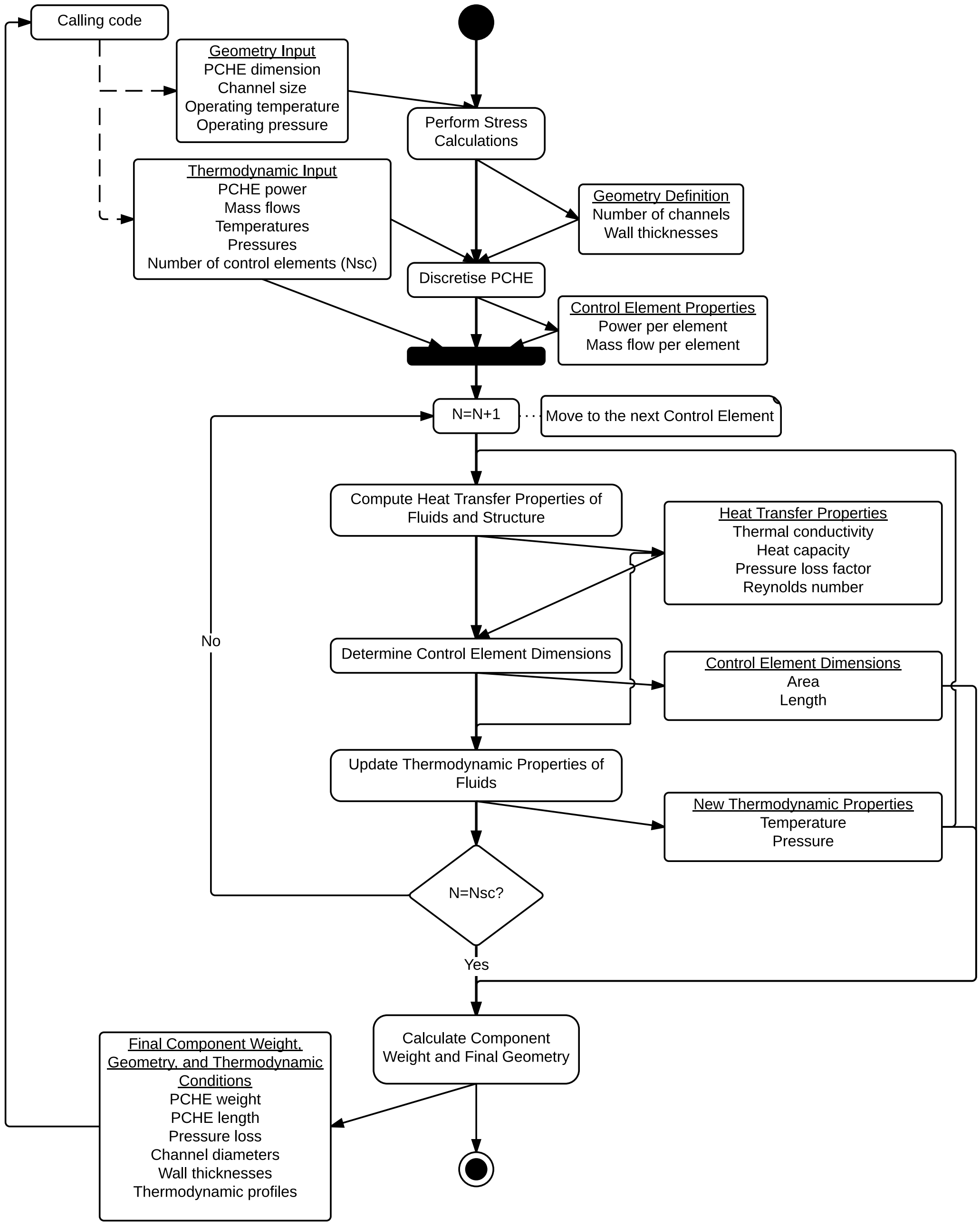

Figure 4.7: UML diagram of the PCHE calculation Matlab code

Variable	Source
PCHE power: Q	heat cycle calculations
Cold side mass flow: $\dot{m}_C$	heat cycle calculations or input
Hot side mass flow: $\dot{m}_H$	heat cycle calculations or input
Pressure of the hot flow leaving the PCHE: P_{HL}	heat cycle calculations or input
Temperature of the hot flow leaving the PCHE: T_{HL}	heat cycle calculations or input
Pressure of the cold flow entering the PCHE: P_{CE}	heat cycle calculations or input
Temperature of the cold flow entering the PCHE: T_{CE}	heat cycle calculations or input
PCHE frontal dimension: h_{HEX}	input
Hot channel diameter: $d_{CH,H}$	input
Cold channel diameter: $d_{CH,C}$	input

Table 4.2: Variables used as input for PCHE calculations

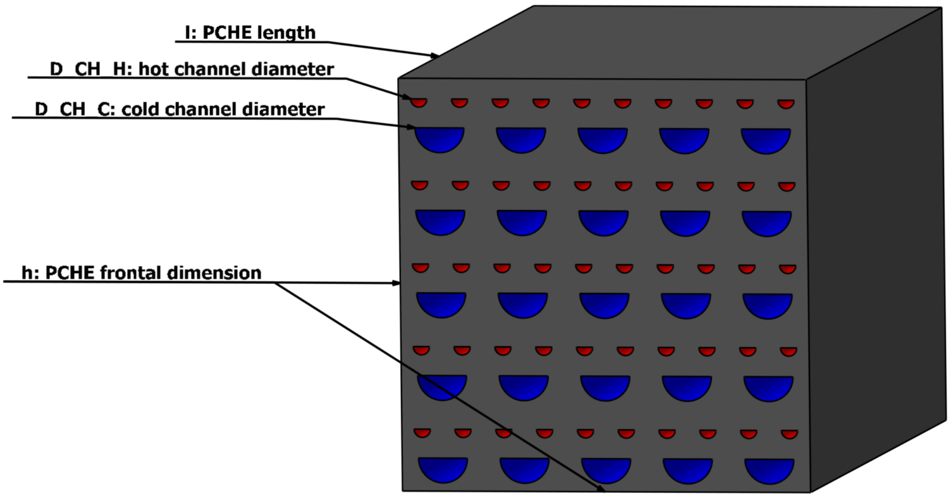

Figure 4.8: Schematic set-up PCHE introducing the terminology used in this thesis

Equations for determining the average wall temperature in a PCHE:

$$T_{w,1} = \frac{\left(T_C \alpha_C \frac{\pi d_{eq,C}}{2}\right) + (T_H \alpha_H d_{CH,H})}{\left(\alpha_C \frac{\pi d_{eq,C}}{2}\right) + (\alpha_H d_{CH,H})} \tag{4.7a}$$

$$T_{w,2} = \frac{\left(T_H \alpha_H \frac{\pi d_{CH,H}}{2}\right) + (T_C \alpha_C d_{eq,C})}{\left(\alpha_H \frac{\pi d_{CH,H}}{2}\right) + (\alpha_C d_{eq,C})} \tag{4.7b}$$

$$T_w = \frac{T_{w,1} + T_{w,2}}{2} \tag{4.7c}$$

Because of the discretisation, the length of the control volume is unknown at this stage of the calculation. Therefore the areas used in the general equation are all divided by the unknown length so that the perimeters of the channels is used to scale their contributions. Because the channels differ in size, each unit of channel perimeter on the hot channel ($p_{CH,H}$) is not necessarily bounded by an equal length of cold perimeter. Therefore, an equivalent cold perimeter is used. This is calculated using equation 4.8. For a semi-circular channel, this equivalent perimeter yields an equivalent diameter from equation 4.9.

$$p_{eq,C} = \frac{p_{CH,C} \cdot N_C}{N_H} \tag{4.8}$$

$$d_{eq,C} = \frac{p_{eq,C}}{1 + \frac{\pi}{2}} \tag{4.9}$$

Even though the PCHE is designed at a single working pressure and temperature, the difference in channel diameter can cause significant differences in plate geometry. This is in contrast with Noriega's thesis where plate thickness and channel diameters were assumed to be constants throughout the heat exchanger. Varying these inputs causes a difference in the formula used to calculate the overall heat transfer coefficient, where a derivation of the more general form from Hesselgreaves[45] is used as detailed in equation 4.10.

$$U_H = \frac{1}{\left(\frac{p_{CH,H}}{\alpha_H \cdot p_{CH,H}} + \frac{p_{CH,H} \cdot \left(\frac{t_{pl,H}+t_{pl,C}}{2}\right)}{\lambda \cdot \left(\frac{p_{CH,H}+p_{eq,C}}{2}\right)} + \frac{p_{CH,H}}{\alpha_C \cdot p_{eq,C}}\right)} \tag{4.10}$$

The overall heat transfer coefficient U is always calculated with respect to a certain area. Since the code is set up to use U to calculate the area needed on the hot side of the heat exchanger, and from that the length of the control volume, it is calculated as U_H. Again, areas are replaced by perimeters in this stage of the calculation.

Another update in the PCHE calculations is the inclusion of airfoil fins in the channels, which replace the wavy channels used in Noriega's code. From[46] it is gathered that the use of airfoil fins decreases the pressure loss of the PCHE by as much as 95%. The heat exchanging capabilities of the PCHE are virtually unaffected. An example of some wavy channels is shown in figure 4.9, and a plate of a PCHE using airfoil fins is depicted in figure 4.10. Including this into the calculations is done by using the same procedure as in Noriega's thesis to simulate the heat exchange and compute the pressure loss, with the friction factor determining the pressure loss being multiplied by 0.1 at the end to include a conservative gain from the airfoil fins. To do this, the angle of the wavy channels is increased from approximately 26° in Noriega's code to 40°, to match the angle used in the comparison in [46].

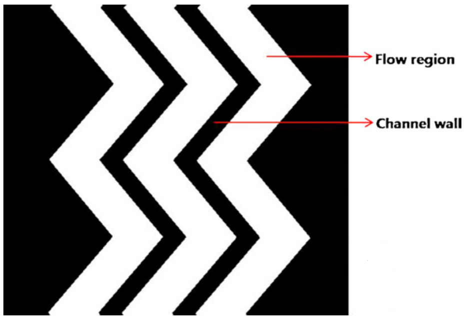

Figure 4.9: Several channels of a zigzag PCHE, from [46]

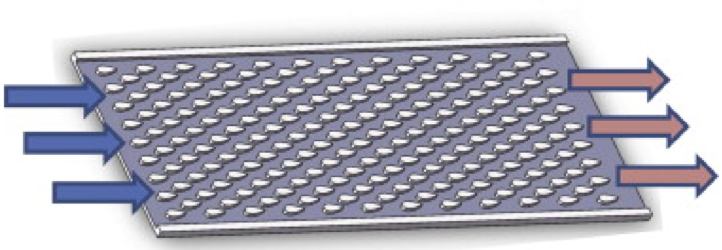

Figure 4.10: A plate of an airfoil-finned PCHE, from [47]

The PCHE codes are generally structured to output the following main parameters for further calculations:

- PCHE structural weight
- Pressure losses of the fluids
- Weight of the fluids inside the channels

The thermodynamic calculations for different fluids in a PCHE are similar to those used for S-CO_2, the difference laying in the procedure used to compute the thermodynamic variables like density, heat transfer coefficient, and C_p. For s-CO_2 and air these can be extracted from FluidProp, but there are no libraries available for LBE and FLiBe. Therefore, the variables for these fluids are calculated using formulas gathered from several sources. These formulas are listed in equation 4.11 for LBE and equation 4.12 for FLiBe.

Equations for thermodynamic variables of LBE:

$$\mu = 4.94 \cdot 10^{-4} \cdot e^{\frac{754.1}{T}} [36] \tag{4.11a}$$

$$\rho = 11065 - (1.293 \cdot T) [36] \tag{4.11b}$$

$$\lambda = 3.284 + 1.617 \cdot 10^{-2} \cdot T - 2.305 \cdot 10^{-6} \cdot T^2 [36] \tag{4.11c}$$

$$C_p = 164.8 - 3.94 \cdot 10^{-2} \cdot T + 1.25 \cdot 10^{-5} \cdot T^2 - 4.56 \cdot 10^5 \cdot T^{-2} [36] \tag{4.11d}$$

$$\begin{aligned} H = {} & 7.627 \cdot 10^4 + 164.8 \cdot (T - T_{melt}) - 1.97 \cdot 10^{-2} \cdot (T^2 - T^2_{melt}) \\ & + 4.167 \cdot 10^{-6} \cdot (T^3 - T^3_{melt}) + 4.56 \cdot 10^5 \cdot (T^{-1} - T^{-1}_{melt}) [36] \end{aligned} \tag{4.11e}$$

$$Nu = Af + 0.018 \cdot Pe^{0.80} [36] \tag{4.11f}$$

$$\text{With: } Pe = Re \cdot Pr \tag{4.11g}$$

$$Af = \begin{cases} 4.5 & \text{if } Pe \leq 1000 \\ 5.4 & \text{if } 1000 > Pe \leq 2000 \\ 3.6 & \text{if } Pe \geq 2000 \end{cases} \tag{4.11h}$$

In these equations Re, Pr, and Pe represent the fluids' Reynolds, Prandtl, and Peclet numbers, respectively. Af represents an empirical coefficient used for the determination of the Nusselt number.

Equations for thermodynamic variables of FLiBe:

$$\mu = 1.16 \cdot 10^{-4} \cdot e^{\frac{3755}{T}} [36] \tag{4.12a}$$

$$\rho = 2280 - (0.488 \cdot (T - 273.15)) [36] \tag{4.12b}$$

$$\lambda = 0.629697 + 0.0005 \cdot T [36] \tag{4.12c}$$

$$C_p = 2347 [36] \tag{4.12d}$$

$$H = (140 \cdot 10^3 + 225 \cdot (T - 800)) \cdot \frac{10^3}{mmol} [36] \tag{4.12e}$$

$$Nu = 0.024 \cdot Re^{0.807} \cdot Pr^{0.301} [36] \tag{4.12f}$$

With $mmol$ being the molar mass of FLiBe, which is equal to 33.1 g/mol. Note that there are no equations listed for the friction factor of LBE or FLiBe. This is due to the insufficient knowledge of behaviour of these fluids in narrow channels such as in PCHE's. Moreover, the compressors of these fluids are not critical in the determination of the final setup and are left out in this research.

All channels in the PCHE regenerators contain s-CO_2, albeit at slightly different temperatures. The properties of the fluid are equal on both sides of the heat exchanger in that case. However, in the cooler and heater of the cruiser heat cycle, the properties in the hot channels differ greatly from those in the cold channels. The resulting difference in heat transfer properties results in an inefficient heat transfer process. To overcome this issue, the PCHE's of the cooler and heater are set up in a so-called double banked configuration. In contrast to the single banked configuration shown in figure 4.2, in which hot and cold plates alternate, a double banked set-up as shown in figure 4.11 has a recurring pattern of three plates. Two hot plates can bound each cold plate, or vice versa. The important parameter in determining the use for double banking is the weighted heat capacity calculated as $\Psi = \frac{C_p}{\rho}$. To check whether double banking of the PCHE is useful the weighted heat capacities of the fluids in the PCHE are divided $\frac{\Psi_C}{\Psi_H}$. If the resulting value is approximately 1, single banking yields the most efficient heat exchanger. If the value is larger than 8 the number of cold plates has to be doubled (double cold banking), if it is smaller than 0.1 double hot banking can be applied. The exact values of these bounds may depend on other variables as well, but these numbers should give a decent initial indication. The plates carrying the fluid with the lowest weighted heat capacity should be the ones to double in number. Carefully designed double banking increases the amount of heat transferred per unit volume of

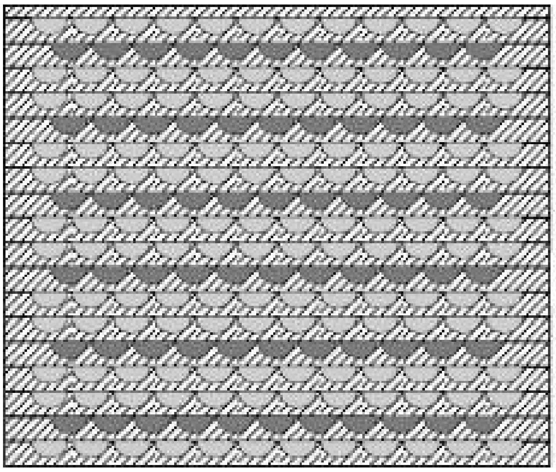

Figure 4.11: Schematic set-up of a double banked PCHE with double hot banking, from [48]

PCHE and reduces the length needed to transfer the required heat enough to compensate for the increased number of plates needed.

An example of the influence of the banking parameter on PCHE design for a typical heater with large differences in heat capacity between the two fluids is given in table 4.3.

Heater: $\Psi_C/\Psi_H \approx 300$			
Variable	**Double cold**	**Single**	**Double hot**
PCHE frontal dimension: h [m]	4	4	5
PCHE mass: m_{HEX} [10^3 kg]	18.6	27.7	32.1

Table 4.3: Table showing the influence of double banking on the results of a grid search for a typical heater

As shown in table 4.3, selecting the right banking parameter for this heater makes a difference around 73% in the mass of the PCHE. Besides selecting the correct banking parameter the cooler design requires additional considerations. These are outlined in the following section.

4.2.5. COOLER

The cooler is the only component of the heat cycle that has an external factor. Whereas all the other components use fluids inside closed circuits, the cooler employs atmospheric air flow to cool the CO_2 down to its critical point. This brings along a unique set of challenges that have to be dealt with. Because of the poor heat transfer properties of air a large mass flow is needed, which results in a large heat exchanger. Therefore, careful design can save a lot of weight in this component.

Because the cooler of the heat cycle is a heat source for the air that is located inside the cruiser wing, lessons can be taken from research performed into the jet wing configuration shown in figure 4.12. This was introduced by Kuchemann[49, 50] and presents opportunities for early-age jet engines to be put in the wing of the aircraft and provide thrust through the trailing edge, filling the wake of the wing. This is a variation on the in-wing engine configuration as used on the well-known De Havilland Comet aircraft, in which both inlet and outlet of the engine are distinct features that extend beyond the leading and trailing edge.

Despite those advantages, the disadvantages of engines in wings in maintenance, safety, and design caused it to become a rare sight on aircraft. Especially the inlet design is a cause of additional design effort because it has to ensure a clean flow of air into the engine to prevent compressor stall, while leaving the flow around the wing as undisturbed as possible to retain its function as an efficient lifting surface. As engines have been growing bigger, putting the engine in the wing is not even an option for most modern passenger aircraft simply because the engine diameter exceeds the wing thickness. However, aircraft like the Nimrod MRA4 (first flight 2004) as seen in figure 4.13 are still designed nowadays proving that the challenges of wing-inlets can be solved and wing inlets are a feasible option for the airflow of the cooler in the cruiser's heat cycle. The three disadvantages for in-wing engines mentioned above are all less applicable to the in-wing heat exchanger of the cruiser:

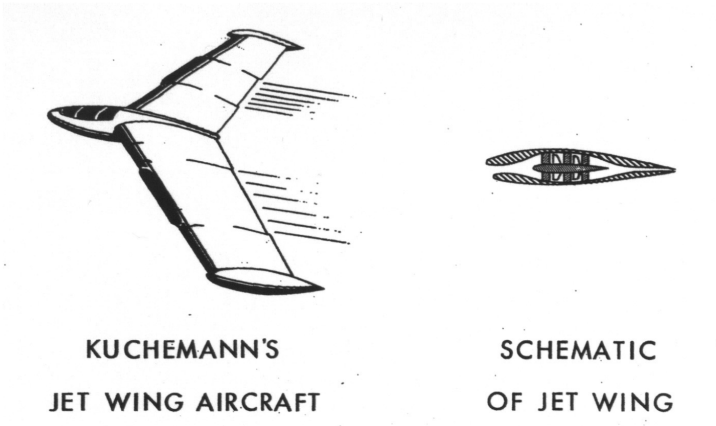

Figure 4.12: Illustration of the jet wing configuration, from [49]

- **Maintenance:** whereas replacing an in-wing engine entails a lot more effort than replacing a podded engine, the additional work required for the heat exchanger is minimal. Maintaining the inside of the PCHE is an enormous effort, regardless of its placement on the aircraft, because the entire heat cycle has to be drained and the heat exchanger has to be taken apart. Moreover, because there are no moving parts in the PCHE, the maintenance intervals will be extremely long
- **Safety:** because the heat exchanging process does not involve the burning of fuel, like a jet engine, the risk of fires and explosions is virtually non-existent
- **Design:** whereas regular inlets such as the Nimrod's have to be able to function under a wide variety of flow conditions (velocities, inflow angles, etc.) between take-off, cruise, and landing, the cruiser's inlets are only active during cruise. In this flight phase the range of inlet conditions is very limited, which reduces the complexity of the inlet design

Figure 4.13: BAE Systems Nimrod MRA4 using in-wing engines, licensed by Ronnie Macdonald under CC BY 2.0 (Creative Commons)

The result of the air passing through the inlet, being heated by the CO_2 in the cooler, and being ejected out of the outlet can be seen as a large subsonic, low temperature ramjet. Depending on the mass flow of air, the outlet temperature after the cooler, and the pressure losses in the cooler this ramjet can be designed to compensate for the ram drag power loss due to the air inlet and possibly even provide additional thrust. This could then be used in subsequent design iterations to decrease the reactor power required during thrust and save reactor weight. Although the exact design of the inlets, outlets, and ducting is outside the scope of this research two pointers for their design are presented in the following points.

- As mentioned above, the cruiser's cooler only has to be active when the heat cycle is powering the aircraft, which is during cruise. For take-off and landing the cruiser depends on regular engine operation and the inlet and outlets in the wing surface could cause a serious performance penalty in those stages of the flight. Therefore it is advised to construct the leading and trailing edges out of morphing material, which allows the slots to be open during cruise and closed when the cooler in not active. These morphing structures can then also be used to (partly) replace the control surfaces on the wing
- The proposed system requires in-wing ducting to transport the air to and from the PCHE. The additional weight is to be included into the calculations after careful design of the ducting. Sources such

as [51] suggest estimating ducting weight as a factor of the heat exchanger weight, but other factors such as mass flow might play an important role as well

This concludes the sections that deal with the theory of component design. Before performing the final optimisation two steps have yet to be taken: the grid search calculations of the heat cycle and, before that, the definition of the search regime for each variable involved in the calculations. This is the subject of the following section.

4.2.6. BOUNDS AND CONSTRAINTS

As with any optimisation it is important to determine what the solution space of the problem is. This section states the values and sources of the bounds on the variables in the calculations and the constraints that limit the outcome of the calculations as well as explaining where the limitations stem from.

Table 4.4 displays the range of values in between which the variables are varied during the grid search to discover the lightest option, as well as the parts of the calculations in which each variable is found. For some of the entries an explanation of the choice of bounds is presented in the following paragraphs.

The pressure in the CO_2 cycle is varied between 100 and 700 bar. The lower value is selected to be slightly above the critical point to capture the lower end of the regimes of pipe thickness and compressor strength. The upper bound of the pressure regime originates from [42], which lists it as the maximum operating pressure of PCHE's.

The input dimension of the PCHE's depends on which PCHE is under consideration. The heater is situated inside the containment vessel and any excessive dimension would increase the size of the entire containment vessel. Therefore it has bounds between 0.5 and 3 m. The cooler on the other hand will not be able to perform its task at that size, as mentioned in section 4.1.2. Because the cruiser wing has ample room to accommodate it, the cooler's bounds can be set between 4 and 10 m. The regenerator bounds are estimated to be 1 and 8 m. Heatric currently manufactures PCHE's in standard blocks of 0.6 x 0.6 x 1.5 m maximum, but for large orders any size can be selected. Moreover, multiple of these blocks can be welded together to achieve the dimensions mentioned above.

The choice of bounds for the mass flows of air and LBE in the cooler and heater, respectively, are based on educated guesses and preliminary test calculations. The air mass flow is made dependent on the CO_2 mass flow to ensure proper heat exchange throughout the large range of possible CO_2 mass flows found in the grid search. The LBE mass flows are set between 1000, which is an arbitrary low value, and 12800 kg/s. The latter value is chosen to be able to compare the heater's size that would be necessary to accommodate the baseline LBE-cooled reactor SVBR-100[52], which uses said mass flow of LBE to cool its core.

Variable	Value(s)	Location
Cycle maximum pressure: P	$[1\ ,\ 7]\cdot 10^7$ Pa	Cycle calculations
PCHE frontal dimension: h_{HEX}	Variable according to space	PCHE calculations
Channel diameters: d_{CH}	$[0.2\ ,\ 5]\cdot 10^{-3}$ m[42]	PCHE calculations
LBE mass flow: $\dot{m}_{LBE}$	[1000 , 12800] kg/s	Heater
Air mass flow: $\dot{m}_{air}$	$[0.8\ ,\ 4]\cdot \dot{m}_{CO_2}$	Cooler

Table 4.4: Bounding values on the calculation variables

During the calculations, the value of different variables changes depending on the input that is given. This results in a number of constraints that are enforced during the calculations. These are given in table 4.5 along with the parts of the calculations in which each constraint is tested. An explanation for the choice of values is presented in the following paragraphs.

The maximum temperature that is not to be exceeded anywhere in the cycle during the calculations is set at 1023 K. This is due to the maximum achievable temperature of LBE that prevents accelerated chemical attack on the structural steels that contain it. From the information in section 2.4.1 it is assumed that advances in material science and perfection of the oxidation control will have raised the maximum achievable temperature slightly by the time the cruiser is set to fly and therefore the assumption of 1023 K is made.

Without any restriction on the length of the PCHE, the most optimal configuration is usually found to be a wide, very short heat exchanger because this minimises the length of each control volume. However, this is an infeasible configuration in reality due to the thermal stresses resulting from the temperature gradients in the PCHE. For that reason a reasonable minimal length constraint has to be added into the calculations. This is estimated at the given 0.3m.

The minimum thickness of the PCHE side wall is set at an estimated 1 mm and the wall thickness between fluid channels on the same plate is set at a minimum of 0.1 mm. These values are selected as reasonable values from a safety and manufacturing standpoint.

The minimum plate thickness of 0.5 mm is given in [34].

The restrictions that have been placed on fluid velocities stem from the need to limit the pressure drops in the components. In piping 30 m/s is an often-used velocity in industry, whereas in PCHE's the small channels call for a lower CO_2 flow velocity, which is set to 10 m/s in this study. The maximum flow velocity of LBE has been mentioned earlier in section 2.4.1. The determination of the flow velocity of the air in the cooler channels is based on the outcome of preliminary tests since no maximum velocity tests have been done using air inside a PCHE. Since the pressure drop is not included into the calculations as a penalty factor, like it is done for CO_2, an artificial limit is needed to prevent excessive pressure drops. This limit is set at M 0.3 because lower limits yield very large heat exchangers and higher limits would be inadvisable due to compressibility effects in the airflow.

The final restriction also applies to the cooler and limits the maximum possible incoming mass flow of air by means of the available inlet area on the wing leading edge. From the model shown in figure 4.1 it is estimated that a slot of maximum 30 m^2 is able to be cut in the leading edge, which limits the air mass flow at cruise conditions to 2577 kg/s.

Constraint	Value	Location
Maximum temperature: T_{max}	1023 K	Cycle calculations and heater
Minimum PCHE length: l_{HEX}	0.3 m	PCHE calculations
Minimum PCHE side wall thickness: $t_{sw,min}$	$1{\cdot}10^{-3}$ m	PCHE geometry calculations
Minimum PCHE wall thickness: $t_{w,min}$	$1{\cdot}10^{-4}$ m	PCHE geometry calculations
Minimum PCHE plate thickness: $t_{pl,min}$	$5{\cdot}10^{-4}$ m	PCHE geometry calculations
Maximum CO_2 flow velocity: V_{max} , CO_2 piping	30 m/s	Piping calculations
Maximum CO_2 flow velocity: V_{max} , CO_2 PCHE	10 m/s	PCHE calculations
Maximum air flow Mach number: V_{max} , air PCHE	M 0.3	Cooler calculations
Maximum LBE flow velocity: V_{max} , LBE	3 m/s	Heater calculations
Maximum cooler air inlet area: $A_{inlet,max}$	40 m^2	Cooler air mass flow

Table 4.5: Constraints governing the calculations

The bounds are easily enforced in the calculations by setting the values to be tested in the grid search for-loops to values within the bounds. The constraints are enforced through constant testing. At each instance that the constrained variable is calculated it is tested against the value mentioned in table 4.5 and if the test fails the calculation code throws an error indicating that this set of input values does not yield a feasible component or cycle. The only exceptions to this procedure are the constraints on the PCHE structural thickness values: after the stress calculations, the resulting thickness is compared to the constraint value and the maximum of these two is used in further calculations.

4.2.7. DETERMINING OPTIMUM FROM GRID SEARCH MINIMUM

The component weights from the PCHE and piping calculations per cycle grid point have to be combined into a total weight so that a minimum weight grid point can be selected. This point is then used as starting point for a more detailed search to find the absolute optimal design point. As for any optimisation problem, an optimisation objective is needed. As stated in the thesis requirements in section 1.3, the weight of the heat cycle is the main optimisation objective. However, the optimisation of the cycle is of a multi-disciplinary nature because it also involves the efficiency of the cycle. Section 4.2.1 introduced the penalty factor that has to be included to link the pressure drop in a component to the increase in reactor weight. This factor is also valid for combining two cycles of different input efficiencies. This also increases the reactor output needed, which induces additional weight to be added to the total cycle weight to form the optimisation objective J in equation 4.13.

$$J = W + PP \cdot \Delta Q_{reac} \tag{4.13}$$

In this W is the cycle or component physical weight, PP is the selected power penalty, and ΔQ_{reac} is the additional required reactor power. From pressure losses, this additional power is calculated using the change in enthalpy, which is a function of the pressure. So with the change in pressure the enthalpy of the flow after the compressor is updated and the change in enthalpy gives the additional compressor power. This then has to be multiplied by $\frac{1}{\eta_{hc}}$ to correct for the cycle efficiency in order to reach the final value of the additional reactor power.

In the grid search processes the component pressure losses are summed and compared to the overall assumption of cycle pressure losses that was made during the cycle calculations explained in section 4.2.1. Any pressure loss above the assumed percentage is converted to a power penalty that is added to the total weight. Because the pressure loss in the cycle is given as a percentage of the compressor output pressure, the additional compressor power is quite insignificant for reasonable values of the pressure loss. For example, the additional power required to recover an excess pressure loss of 0.5% above the assumed pressure loss in a 60 MPa 45% efficient cycle requires only 0.3 MW of extra reactor power.

The determination of this power penalty factor is both vital for the final outcome of the optimisation process and hard to determine. For an accurate determination of the power penalty factor a weight estimate of a weight-optimised shielding and reactor vessel should be known. Because this is currently unavailable for an LBE reactor, educated guesses have been made that result in the indicated 1000 kg of penalty weight per MW of additional reactor power required. This value is approximately equal to the slope of the graph shown in figure 4.14, which is copied from a technical report written during the ANP research period that uses a helium-cooled reactor[13]. Note that this graph only displays the shielding weight and the reactor weight still has to be added to that. Another source of information that is used for determining the power penalty are the characteristics of the Russian-built SVBR-100 LBE-cooled reactor[52]. In this document the power of the reactor is listed as 280 MW at a modular weight of 280 tons, from which the slope of 1000 kg/MW results. The fact that these slopes match seems remarkable because reactor technology has advanced considerably since the publication of the ANP document. It also seems to disprove the statement made in previous decisions (section 2.4) that LBE-cooled reactors would save shielding weight due to the inherent shielding properties of the coolant. However, this can be explained by noting that the SVBR reactor has not been designed with an optimised shield, whereas the reactor design in the ANP report does include a minimised weight shielding vessel. To be conservative the power penalty has been chosen to remain at 1000 kg/MW for this thesis, because estimating the potential savings of optimised shielding design for an LBE reactor is not feasible with the limited information available. However, in future design iterations a detailed reactor and shielding design could yield a lower slope.

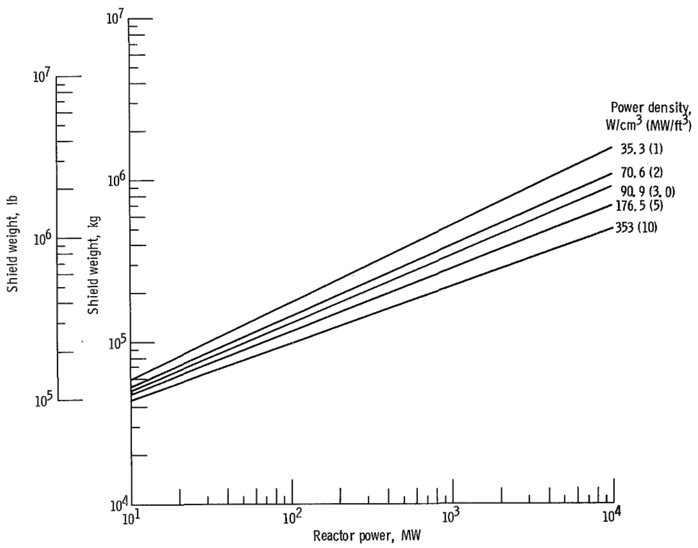

Figure 4.14: Graph showing relation between optimised shielding weight and reactor power, from [13]

The results of the grid search include the following weight components, which are added and compared to find the lowest objective weight and the corresponding set of input parameters to be fed into the final optimisation.

- Component weights for the cycle components
  - Cooler
  - Heater
  - Regenerator(s)
  - Piping
- Fluid weights of the cycle fluids
  - CO_2 in the piping
  - CO_2 in the heat exchangers' channels
  - LBE in the heater channels
  - Air in the cooler channels
- Power penalties from the following sources
  - Variations in overall cycle efficiency
  - Variations in overall cycle pressure losses

The power penalty weight that is derived from the overall cycle efficiency comes into play when comparing two different cycles in the determination of the grid search minimum and during the optimisation. If one of the cycles has a higher efficiency than the other, the reactor in that cycle has to provide less power to the heater of the cycle to achieve the same turbine power output. As a result the reactor in the less efficient cycle is heavier by an amount that is determined by the power penalty factor multiplied by the difference in required reactor power between the two cycles.

The optimisation is done using the *fmincon* function in Matlab with the choice of bounds during the optimisation being dictated by the grid search. In this optimisation the Sequential Quadratic Programming (SQP) algorithm is used because of its ability to recover from errors during the calculations, which are thrown if one of the constraints of table 4.5 is broken. The cycle pressure and efficiency inputs are chosen such that the search regime during the optimisation is limited to the area around the minimum weight cycle grid point. The bounds for the individual components are determined by the grid search as well. The component set-up corresponding to the minimum component weight at the optimal cycle grid point is taken as the input per component, after which the bounds of each of the component's variables are set to the values that flank the optimum value in the component variable grid search input vector. A UML diagram of the optimisation process is found in figure 4.15. This again shows the link to the component calculation codes mentioned earlier.

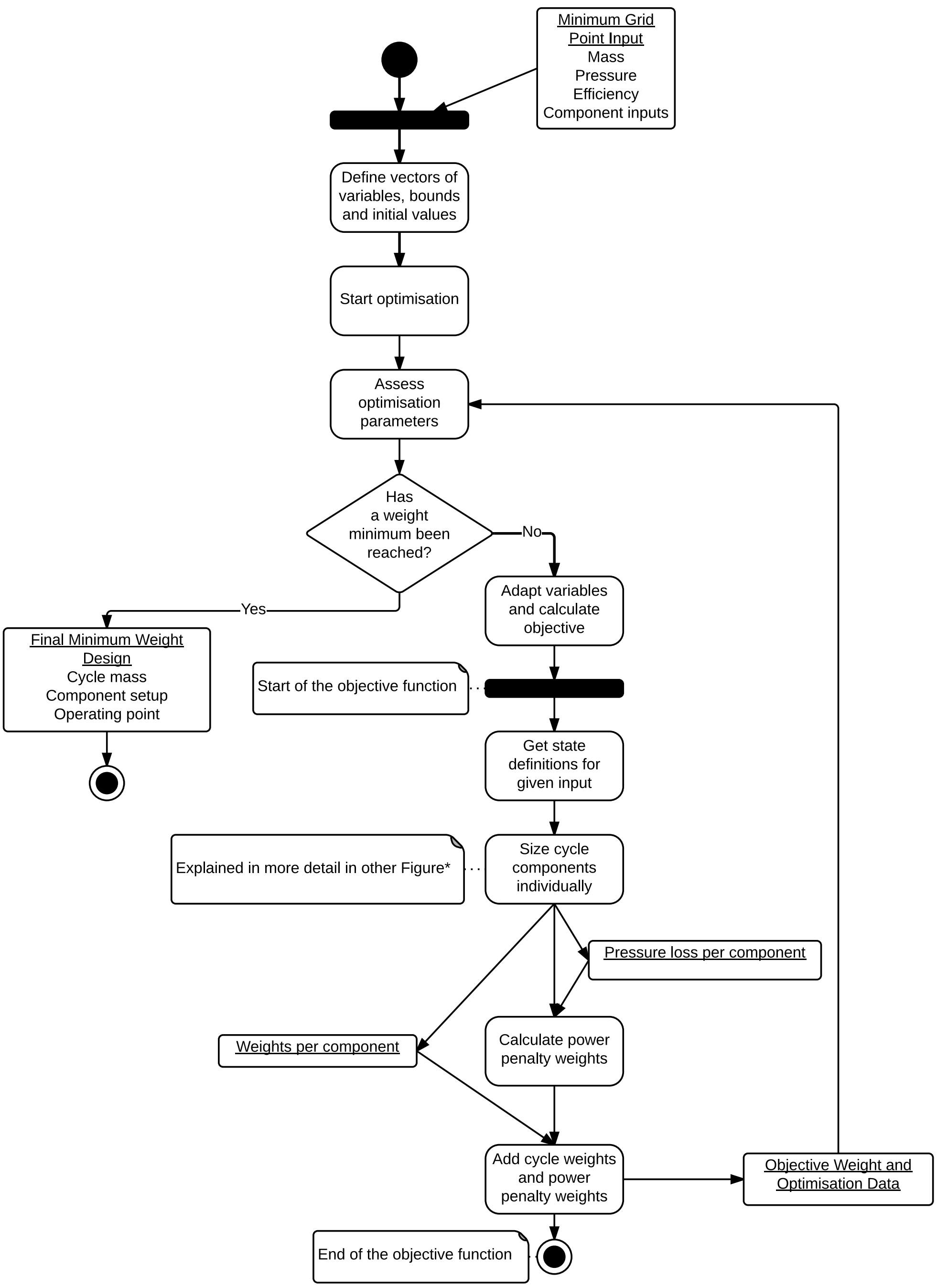

Figure 4.15: UML diagram of the overall optimisation Matlab code. *: see figure 4.7

4.3. CALCULATION METHOD FOR THE OPEN CYCLE SET-UP

The calculation method used to determine the weight of the heat cycle in the open cycle set-up consists of two distinct parts, each detailed in the following sections. The process starts with the engine design, which determines the inputs for the second step performed in the heat exchanger design code.

4.3.1. ENGINE DESIGN

The engine sizing for the open cycle is done in the engine modelling software *GasTurb 11*. Because the open cycle uses a single engine to house the nuclear-powered heat cycle as well as the fuel burning cycle used for take-off and landing a geared unmixed flow turbofan setup is selected, as suggested in previous deliverables of the *RECREATE* research group[6]. In impression of the general layout of such an engine is provided in figure 4.16.

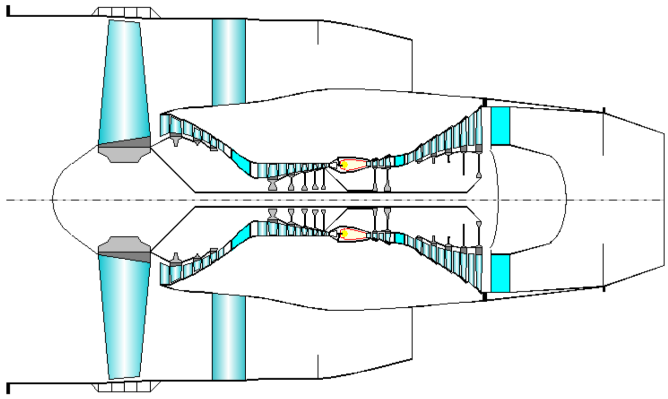

Figure 4.16: Example schematic of a geared turbofan engine as provided in GasTurb

Starting from this choice of general setup, parameters can be changed to match the range of possible inputs supplied by the FLiBe heat cycle. The main limitation is the achievable temperature, which is limited at 1023 K by the LBE, which heats the FLiBe, which then heats the air. The maximum achievable air temperature after the two heat exchanging processes (LBE to FLiBe in one HEX and FLiBe to air in the second) is unknown at this stage so the choice is made to optimise the engine for three TIT's and carry out the heat exchanger design for each of those to determine which is the optimal value. The selected engine air TIT's are 973 K, 948 K, and 923 K. These values are selected to allow a maximum temperature difference of 50, 75, and 100 degrees, respectively, between the air leaving the heat exchanger and the maximum possible temperature within the heat cycle, which is 1023 K. Temperature differences smaller than 50 degrees are expected to be too small to result in a compact heat exchanger because of the difference between the heat transfer properties of air and FLiBe. Because these properties air much poorer for air, a relatively large temperature difference is needed to achieve efficient heat transfer. The upper limit is set at 100 degrees because the temperature of the air entering the turbine is then set at 923. Lower turbine inlet temperatures result in a larger required engine air mass flow to generate the required thrust and it is expected that temperatures lower than 923 K result in sub-optimal engine designs. If the results of the calculations indicate that a higher or lower temperature difference could be beneficial, these are easily investigated. GasTurb has a built-in optimiser, which allows for the user to enter the objective variable as well as the range in which the other variables can be altered.

In order to use the code for the calculation of cruise power generation, an important alterations has to be performed. In this flight phase there is no fuel burning in the engine, the air is simply heated by routing it through the heat exchanger. This increases its temperature but not its heat capacity, which is the case for a fuel burning engine. The difference in the properties of the air before and after burning influence the calculations of the turbine conditions and through that the final thrust of the engine. To minimise the error caused by this difference the heating value HV of the fuel can be raised to unrealistically high values (in this study 100,000 MJ/kg is used, with the normal value being around 43). This ensures that the proper amount of energy is delivered to the airflow while the fuel flow is even more negligible than it usually is. As a result the thermodynamic properties of the air remain unchanged and the engine model is an accurate representation of cruise operations.

With the accuracy of the engine model verified, the setup for the optimisations can commence. The selected objective function is the fuel mass flow, which can be converted to the heater power using equation 4.14.

$$Q_{he} = HV \cdot \dot{m}_{fuel} \tag{4.14}$$

The variables selected to create the design space are:

- Fan and compressor pressure ratios (PR)
- Engine bypass ratio (BPR)
- Air mass flow

The resulting optimisation is restricted by two constraints:

- **$Th_{eng} \geq$ 110.77 kN:** This value stems from dividing the cycle power from equation 4.1 by the airspeed to gain the force delivered per cycle. This values then has to be halved to find the required thrust per engine
- **$d_{eng} \leq$ 3.5 m:** If left unconstrained, the resulting engine could become unrealistically large. This value is typical of the largest turbofan engines currently in production

The outcome of the engine optimisations contains the following values that are used in the design of the heat exchanger:

- **Q_{he}:** As mentioned, the fuel flow from the engine model is converted to the heater power required
- **Vol_{burner} and l_{burner}:** Dividing the available volume of the fuel burner by its length, a value for the required frontal area is found. Taking the root of this value yields the upper limit of h_{he} that allows the heat exchanger to be placed inside the engine casing. If the heat exchanger code does not converge for this value, the heat exchanger has to be placed in the back of the cruiser, as mentioned in section 4.1.1
- **T_{CE}, P_{CE}, $\dot{m}_{air}$:** The values at the station that represents burner entry in the engine models are the values used as input for the heat exchanger. The input air mass flow of the PCHE depends on whether or not the heat exchanger fits inside the engine. If that is the case, the input mass flow is equal to the value from the engine optimisations, if not it is double this value. In that case it is more efficient to use a single heater for each cycle because of fixed weights that are present for each heat exchanger, which will be saved if the two heaters are combined. The airflow from the engines then merged before the heat exchanger and split again before being led back into the engine turbine
- **m_{eng}:** The geometry calculation in GasTurb also allows the mass of the resulting engine design to be calculated. This is stored to add to the heat cycle mass in later stages of the calculations

4.3.2. HEAT EXCHANGER DESIGN

Starting from the input values as dictated by the engine design, the heat exchanger design code is similar to that used in the grid search step of the closed cycle design. The input variables are looped over for several values and the lightest option is selected. Therefore the general calculation scheme is not repeated here, as it can be found in section 4.2.4, with the characteristic equations for FLiBe being presented in equation 4.12.

What is different are some of the limits from table 4.5 and some additional input that is required. The constraints that have changed are:

- **T_{max}:** Within this secondary heater (LBE to FLiBe being the primary heater) the temperature will not be allowed to go up to 1023 K because it is impossible for the FLiBe to have that temperature due to the temperature difference that is required in the primary heater. Therefore, this is relaxed to 1013 K
- **$V_{FLiBe,max}$:** The limit for FLiBe flow velocity is set at 6 m/s because is it does not have the same restrictions as LBE but is still a dense liquid, which limits the maximum achievable speed
- **$\Delta P_{air,max}$:** Unlike the cooler of section 4.2.5, the pressure loss of the airflow is restricted in these calculations. From the GasTurb model a value of 0.96 is selected for the burner pressure ratio. This corresponds to a 4% pressure loss limit in the PCHE, above which the PCHE design code will throw an error and discard the set of input values

The additional input to the PCHE code are varying mass flows of FLiBe between 100 and 5000 kg/s and differing input temperature differences between the air inflow and the FLiBe outflow. These are set to vary between 100 and 310 K. These substantial design ranges are necessary due to the lack of previous work on similar heat exchangers. Therefore, it is unknown in advance where in the design space the feasible designs are located, let alone the optimal ones.

Using the given input and bounds the FLiBe heater design code calculates the usual minimal weight, the set of geometrical input values that result in that weight, as well as the input and output temperature of the FLiBe that is necessary as input for the primary heater.

Now that all calculation methods have been specified the following chapter presents the results of each step that lead up to the final outcome of this thesis.

5
Results of the Heat Cycle Calculations

This chapter discusses the results obtained by running the design codes discussed in the previous chapter. In the end it presents the final optimal design, which is used to complete the goal of this study: assess the feasibility of designing a heat cycle for the nuclear cruiser within the available weight budget. This optimal design outcome contains the cycle layout, the values of the cycle inputs, and the values of the component inputs of that cycle that yield the minimum weight heat cycle.

5.1. Open cycle results

The results of the engine optimisations and the heat exchanger design process are detailed in the following sections, respectively.

5.1.1. Open cycle engine optimisation results

The engine optimisations in GasTurb, which are explained in section 4.3.1 yield very similar results for the three selected turbine inlet temperatures of 973 K, 948 K, and 923 K. The values of the output variables are shown in table 5.1.

TIT [K]	**Th [kN]**	**BPR [-]**	**$\dot{m}_{air}$ [kg/s]**	**PR outer fan [-]**	**PR inner fan [-]**	**PR comp 1 [-]**
973	101.77	1.69	569	1.79	1.57	1.44
948	101.77	1.01	475	1.79	1.57	1.43
923	101.77	1.52	602	1.84	1.56	1.32
TIT [K]	**PR comp 2 [-]**	**$T_{CE,he}$ [K]**	**$P_{CE,he}$ [kPa]**	**Q_{he} [MW]**	**h allowance [m]**	
973	6.48	569	490	92.6	1.81	
948	6.49	568	487	97.0	1.92	
923	6.72	559	460	93.8	2.01	

Table 5.1: Output values for the open cycle engine optimisation from GasTurb

Inspection of the resulting engines reveals the optimal engine geometry for TIT = 973 K to be of the form shown in figure 5.1. It is clearly visible that the burner cans protrude out of their designed casing and into the bypass flow. To counter this problem, a standard geometry input value linking can width to can length is changed from 0.25 to 0.15. This results in the engine shown in figure 5.2. In this set-up there is an even smaller allowance for the heat exchanger dimension, which for the 973 K engine decreases h from 1.8 m to 1.4 m.

Further inspection of the actual output reveals that the engines require a very large core mass flow in order to generate enough energy from the relatively low TIT airflow to provide ample thrust. Compared to current engines like the GE90, the obtained GasTurb models are similar in diameter but have a BPR of just over 1 instead of 8. This also stands in vast contrast with the engine design of the *RECREATE* deliverable[6], which has a BPR of 6. The small bypass ratio results in an inefficient engine, which deteriorates fuel efficiency during

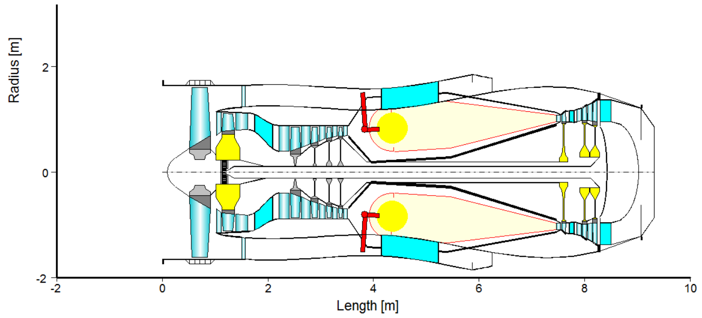

Figure 5.1: Engine geometry output for optimal open cycle engine at TIT = 973 K

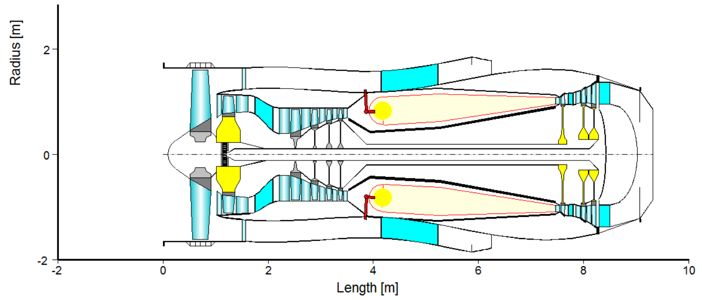

Figure 5.2: Updated engine geometry for optimal open cycle engine at TIT = 973 K

flight phases in which the cruiser is powered by chemical fuel. This results in a higher required backup fuel volume, which adds weight and changes the assumed weight breakdown of the cruiser as shown in figure 1.7.

Because of the complications that arise in the engine design, the open cycle is discarded as a feasible candidate at this point in the study. It has to be noted, however, that the problems are mainly due to the low TIT that is allowed by the reactor choice. If future designs were to employ a higher temperature reactor option, the open cycle should be taken back into consideration. To provide a starting point for those calculations and prove the feasibility of this heat cycle choice, the FLiBe to air heat exchangers have been designed nevertheless, albeit only in the grid search process in stead of a full optimisation. The results of this can be found in the following section.

5.1.2. OPEN CYCLE HEX GRID SEARCH RESULTS

The first test to be done is to check the possibility of including the heat exchangers in the engine pod design. This means that the PCHE calculation code has to converge for an input of h of 1.4 m for 973 K. All calculations within the grid of FLiBe mass flows, channel diameters, and input temperature differences fail for this set-up either producing an error of insufficient temperature difference between the flows or excessive pressure losses due to the necessary length of the heat exchanger. Therefore, the grid search is repeated without the restriction in h and with the input mass flow of air doubled to simulate a single heater for both engines, which places this heat exchanger outside the engine pods.

The grid search for the minimal weight set-up of the heater yields the output values that are presented in table 5.2 for the three air exit temperatures listed above.

TIT [K]	$\mathbf{m}_{he}$ [10^3 kg]	h [m]	$\mathbf{d}_{CH,H}$ [mm]	$\mathbf{d}_{CH,C}$ [mm]	$\dot{m}_{FLiBe}$ [kg/s]	ΔT_{in} [K]	$\mathbf{T}_{FLiBe,HE}$ [K]
973	18.1	4	3.5	5	500	190	787
948	18.7	4	5	5	1000	190	773
923	18.6	4	2	5	100	220	917

Table 5.2: Optimal output values for the open cycle heat exchanger grid search

Even though the piping and additional equipment for the open cycle is not taken into further consideration, the weights listed for the FLiBe to air heat exchanger provide hope for the feasibility of this cycle in itself. As said, in this study the open cycle is not applicable due to the engine design difficulties it entails but in other similar design problems where the temperature allowance is higher the open cycle could provide a very lightweight system and should be designed in further detail.

5.2. CLOSED CYCLE GRID SEARCH RESULTS

This section gives the results of the closed cycle grid searches, starting with the determination of the cycle search regime and continuing with the results of the individual components grid searches. It ends with the determination of the minimum weight design from the grid search data.

5.2.1. CYCLE RANGE DETERMINATION

The first step in the calculations is testing the range of input pressures and efficiencies for which the cycle calculation routine of section 4.2.1 gives feasible answers. Feasibility in this case is defined by the absence of errors caused by either of the following points:

- FluidProp or cycle errors, which result from an inability to converge to a solution in the cycle calculations
- Component powers. At low efficiencies the regenerators are superfluous in the cycle, which reflects in very small or even negative regenerator powers in the output of the cycle calculations
- Maximum CO_2 temperature higher than 1023 K, which is the maximum temperature allowance of the LBE heating the CO_2, as set in section 4.2.6. Because the cycle calculations are set up to find the minimum possible TIT, any set of inputs that needs a temperature higher than this 1023 K before converging to a cycle is infeasible and is left out of grid search calculations

Several assumptions have to be made before the thermodynamics of the cycle can be calculated. These are listed in table 5.3, and are mostly equal to those made by Noriega[36]. The exception is the initial assumption of the pressure loss, which is lowered from 2% to 1% to account for the decreased pressure loss resulting from the use of airfoil-finned PCHE's.

Input	**Value**
η_{cm}, compressor efficiency [-]	0.85
η_{tr}, turbine efficiency [-]	0.934
η_{he}, heater efficiency [-]	0.99
$P_{in,cm}$, compressor inlet pressure [MPa]	7.4
$T_{in,cm}$, compressor inlet temperature [K]	304.4
ΔP_{tot}, cycle total pressure loss assumption [%]	1

Table 5.3: Input assumptions affecting the cycle calculations

The tested cycle inputs are given by the following vectors of input values: $P = [1, 2, ..., 7] \cdot 10^7$ Pa, $\eta = [0.2, 0.25, ..., 0.7]$. The resulting ranges of feasible inputs are shown in figures 5.3 and 5.4 for regenerative and recompression cycles, respectively. In the plot of the regenerative cycle, two valid cycle grid points are marked for further reference in other results of this section. One is at the low pressure, low efficiency end of the grid ($[P, \eta] = [1 \cdot 10^7$ Pa , 0.2]) and is marked by a plus sign, whilst the other lies at the high pressure, high efficiency end ($[P, \eta] = [7 \cdot 10^7$ Pa , 0.45]) and is marked by a cross.

Using the information from the cycle calculations, matrices are filled with cycle outputs per grid point for use in component grid search calculations. A plotted example of these values is found in figure 5.5, which depicts the CO_2 mass flow in the regenerative cycle option as a function of the pressure and efficiency input. In this figure the points are the actual outcome of the calculations and the surface is constructed using fitted data generated by those points. It shows that lower values for the efficiency require much higher mass flows to generate the required power output and the same can be said for low pressure values. The variation between the maximum mass flow of 2300 kg/s at input $\eta = 0.2$ and $P = 10^7$ Pa and the minimum of 281 kg/s at $\eta = 0.45$ and $P = 7 \cdot 10^7$ Pa proves especially important for the design of the heat exchangers, which is treated in the following sections.

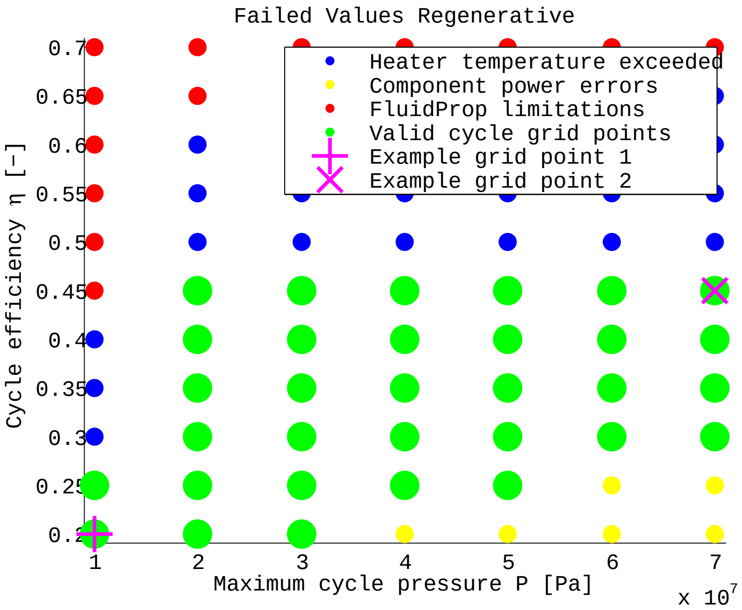

Figure 5.3: Results of the cycle calculations range test for regenerative cycles

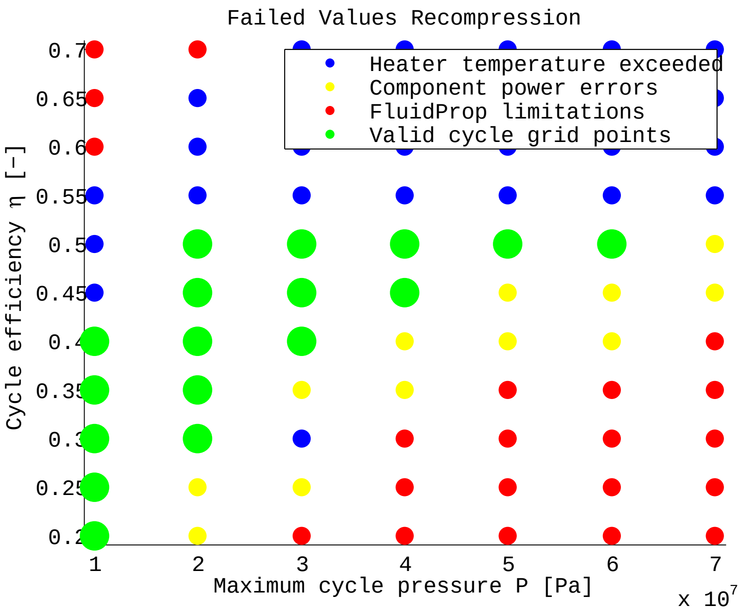

Figure 5.4: Results of the cycle calculations range test for recompression cycles

5.2.2. PIPING GRID SEARCH RESULTS

From the optimisation process explained in section 4.2.3 the weight of the piping is calculated for each grid point in both the regenerative and the recompression cycle. The resulting trends are shown in figures 5.6 and 5.7, respectively. Table 5.4 gives some typical values for input and output of the piping of a regenerative cycle at the η = 0.45 and P = $7{\cdot}10^7$ grid point. Because the band of feasible recompression cycles is quite narrow for low pressure inputs it is impossible to plot the results for this cycle option as a surface. In stead they are shown as a 2D scatter plot with the colours of the data points indicating their weight.

The dependence of piping weight on the cycle inputs inputs is clear from figures 5.6 and 5.7, with minimum weights being found generally in high efficiency, high pressure cycles. The fact that higher pressures

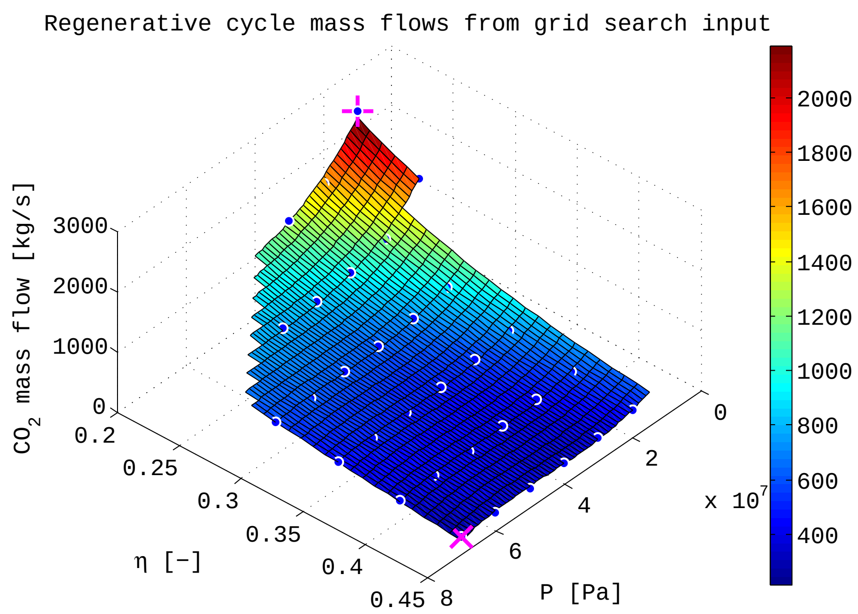

Figure 5.5: Variation of regenerative cycle CO_2 mass flow with varying grid search input

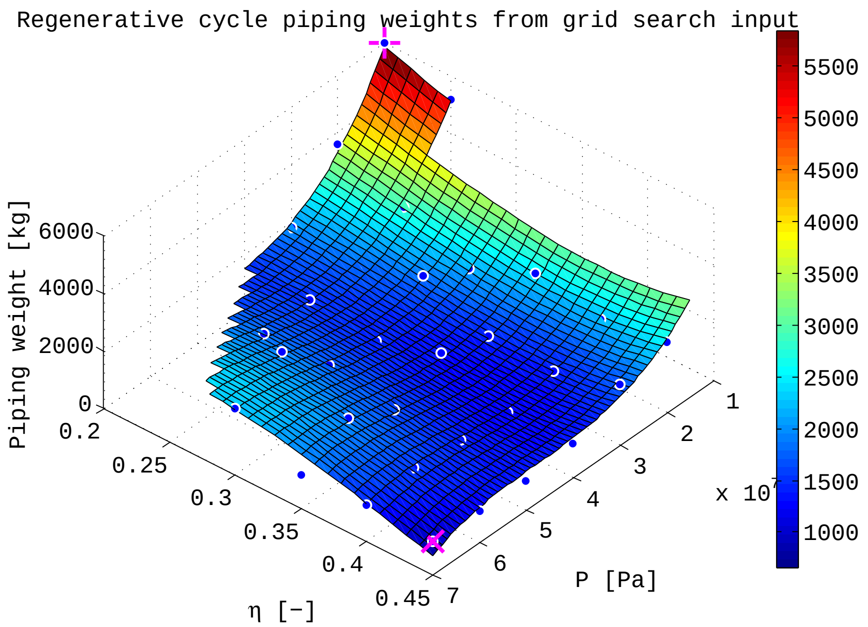

Figure 5.6: Variation of regenerative cycle piping weight with varying grid search input

lead to lower piping weight may seem counter-intuitive but it has to be kept in mind that the mass flow for those cycles is lower, which is why smaller diameter piping is possible. Because of this, despite the increased pressure requiring a higher thickness-to-diameter ratio, the overall weight will be low.

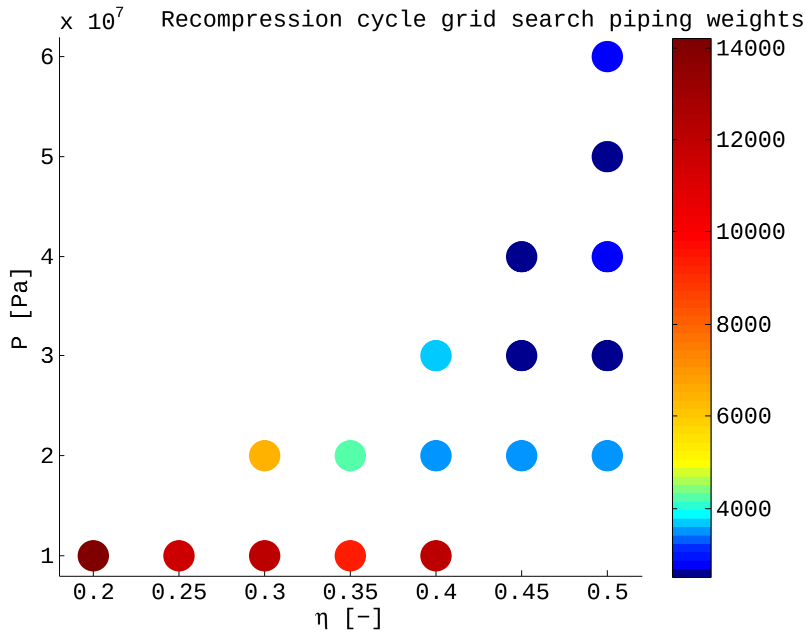

Figure 5.7: Variation of recompression cycle piping weight with varying grid search input

Output	**Value(s)**
Assumed length per pipe [m]	[5, 1, 3.5, 2.5, 2, 2.5]
Internal radius r_i per pipe [cm]	[15.1, 11.5, 8.8, 9.6, 33.6, 23.0]
Wall thickness t_w per pipe [mm]	[2.7, 21.4, 16.6, 22.1, 6.3, 4.2]
Total piping mass m_{piping} [kg]	1176
Total pressure loss ΔP_{tot} [kPa]	47.9

Table 5.4: Example of piping grid search output for a regenerative cycle at the $\eta = 0.45$ and $P = 7 \cdot 10^7$ grid point

Accompanying table 5.4 the following notes have to be made:

- The pipes in this regenerative cycle are numbered as in figure 5.8:
    1. Cooler to compressor
    2. Compressor to regenerator (cold side)
    3. Regenerator to heater
    4. Heater to turbine
    5. Turbine to regenerator (hot side)
    6. Regenerator to cooler
- The assumption of thin-walled pipes is indeed not valid, as indicated especially in pipes 2 and 4, which have t/r ratios of 0.18 and 0.23, whereas the threshold for the thin-walled assumption lies at 0.05
- With the overall cycle pressure loss assumption of 1% of the cycle maximum pressure being 700 kPa in this case, the 47.9 kPa pressure loss in the piping falls well within the range of acceptable values

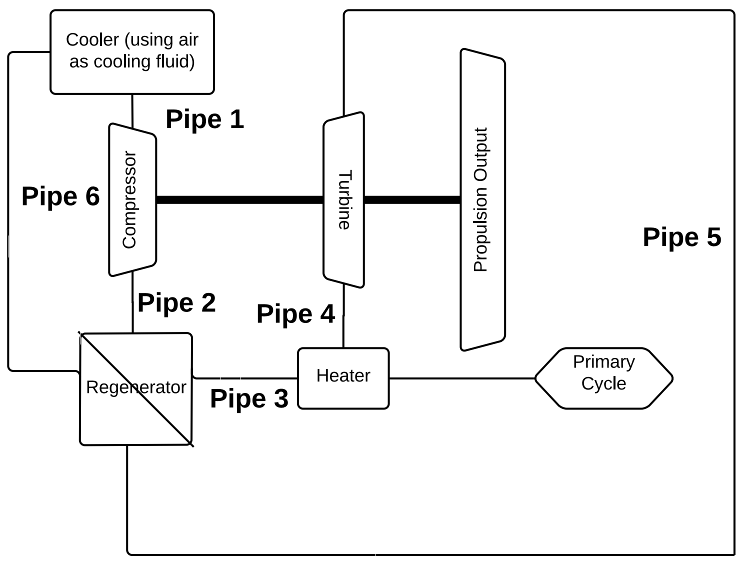

Figure 5.8: Schematic of the regenerative cycle showing the numbering of the pipes

5.2.3. REGENERATOR GRID SEARCH RESULTS

There are three sets of results to be discussed in this section: one regenerator design for the regenerative cycle option and two for the recompression cycle. Figure 5.9 presents the data points and resulting fitted surface for the regenerative cycle component, of which the lowest data point also serves as an example for the output values of the code, as shown in table 5.5. The recompression components are shown in figure 5.10 for regenerator 1, and figure 5.11 for regenerator 2.

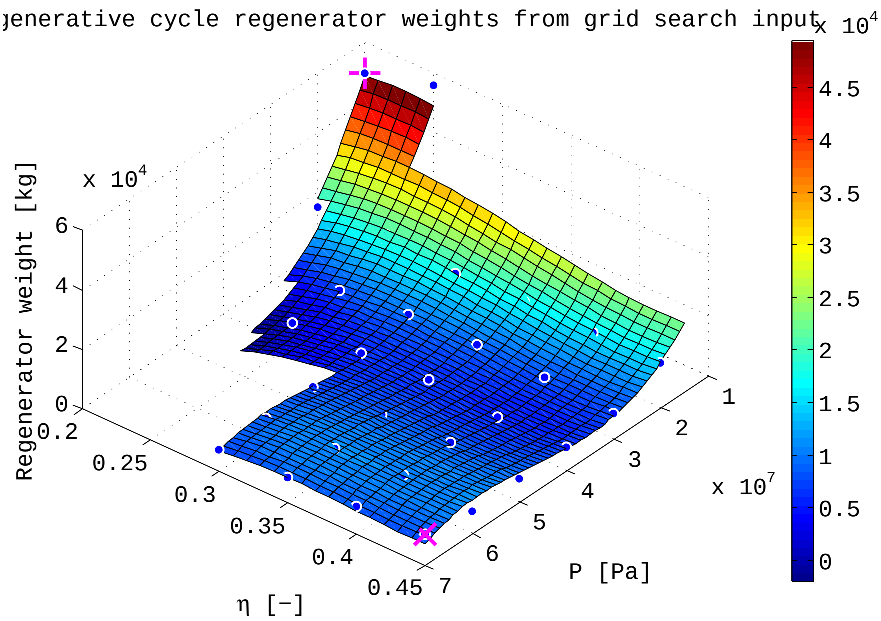

Figure 5.9: Variation of regenerative cycle regenerator weight with varying grid search input

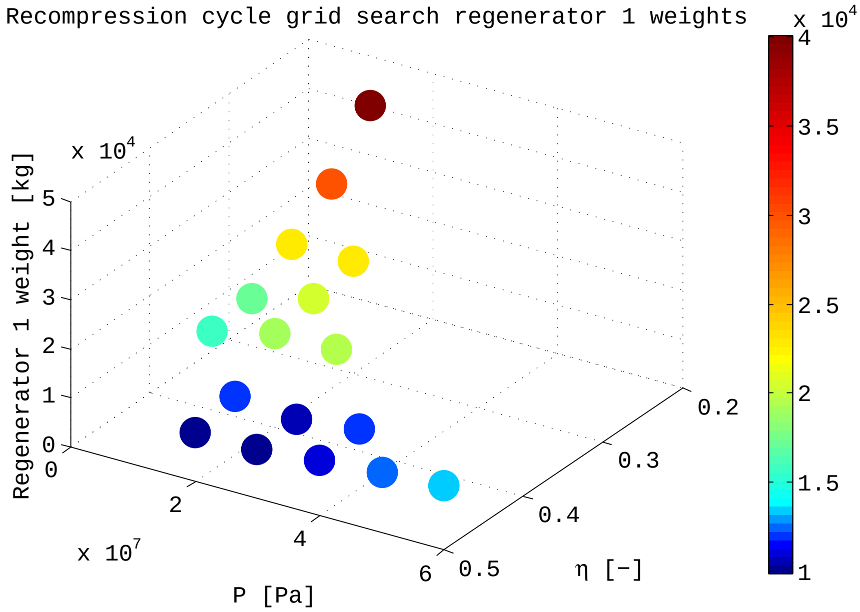

Figure 5.10: Variation of recompression cycle regenerator 1 weight with varying grid search input

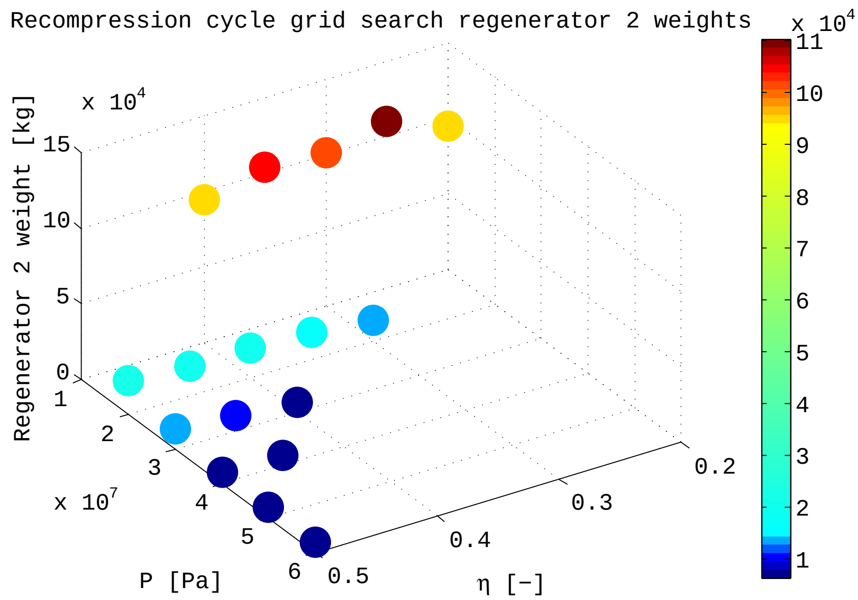

Figure 5.11: Variation of recompression cycle regenerator 2 weight with varying grid search input

Noteworthy information that can be gathered from these results includes:

- Similar to the trends shown in the piping results the points at low pressure and efficiency inputs yield the highest regenerator weight due to the high mass flow that has to be accommodated. An example of the results is found in the heat exchanger dimension output. For the minimum regenerator weight grid point shown in table 5.5 the frontal dimension output by the grid search is 2 m, whereas for the minimum weight regenerator for the cycle of inputs $\eta = 0.2$ and $P = 10^7$ h = 5 m

Output	Value
PCHE frontal dimension h [m]	2
Hot channel diameter $d_{CH,H}$ [mm]	2
Cold channel diameter $d_{CH,C}$ [mm]	2
Regenerator mass m_{reg} [kg]	7032
Total regenerator pressure loss ΔP_{tot} [kPa]	17.6

Table 5.5: Example of regenerator grid search output for a regenerative cycle at the η = 0.3 and P = $6{\cdot}10^7$ grid point

- The effect of higher mass flow is even more profoundly present in the trends shown in figure 5.11 for regenerator 2 of the recompression cycle. Besides the total mass flow in the cycle being higher, the fraction of the flow that flows through this regenerator is also higher. For high efficiency, high pressure cycles α is around 0.2 but this rises up to 0.5 for the lowest pressure inputs. The second lowest pressure input already decreases this fraction to 0.3, which is why there is such a large distinction between the regenerator weights on the low pressure side of figure 5.11
- With the overall cycle pressure loss assumption of 1% of the cycle maximum pressure being 600 kPa for the minimum weight regenerative cycle grid point, the 17.6 kPa pressure loss in the listed design falls well within the range of acceptable values. However, due to the grid search method and the resulting stepwise variations in channel diameter inputs some design points yield pressure losses of close to 200 kPa. The fact that these designs can still come out as the most optimal design for that grid point is the result of the relatively small effect that the pressure loss has on the objective function, as explained in section 4.2.7. The next best set of input values is then such that the resulting heat exchanger is so much larger and thereby heavier that the additional weight diminishes the reduced power penalty weight that is gained from lowering the pressure losses
- The cycle grid point at which the minimum component weight occurs is different for the regenerators than for the piping as found in section 5.2.2. This indicates that the determination of the overall minimum grid point in section 5.2.6 is indeed a trade-off over all components in which not every component will have the lightest possible setup

5.2.4. HEATER GRID SEARCH RESULTS

The weight trends of the heaters with varying grid search inputs are shown in figures 5.12 and 5.13 for regenerative and recompression cycles, respectively. Again, a sample output table shows the characteristics of the regenerative minimum heater weight grid point, which lies at η = 0.35 and P = $7{\cdot}10^7$. This information is found in table 5.6.

Output	Value
PCHE frontal dimension h [m]	1
Hot channel diameter $d_{CH,H}$ [mm]	0.5
Cold channel diameter $d_{CH,C}$ [mm]	1
Heater mass m_{he} [kg]	2178
LBE mass flow $\dot{m}_{LBE}$ [kg/s]	2500
CO_2 mass flow ΔP_{CO_2} [kPa]	112

Table 5.6: Example of heater grid search output for a regenerative cycle at the η = 0.35 and P = $7{\cdot}10^7$ grid point

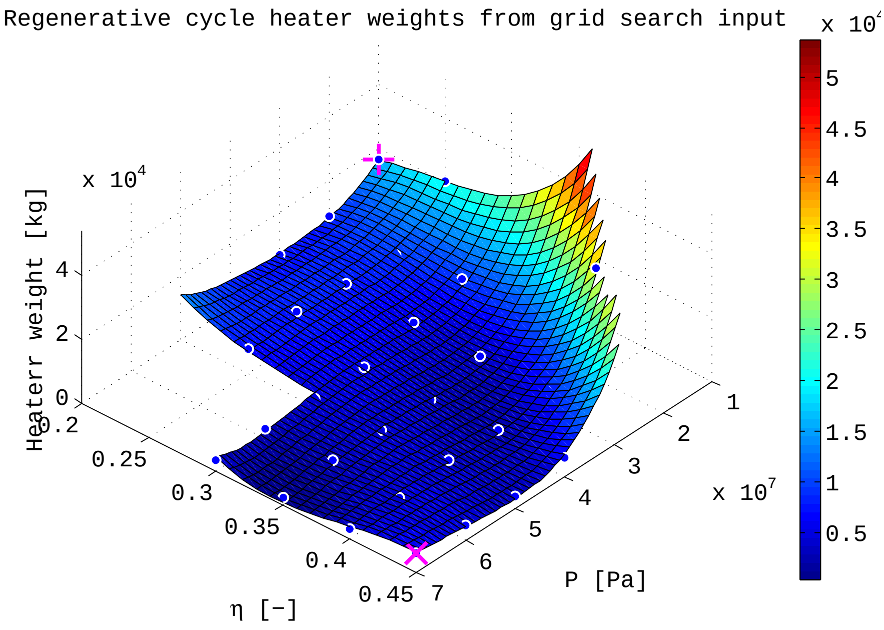

Figure 5.12: Variation of regenerative cycle heater weight with varying grid search input

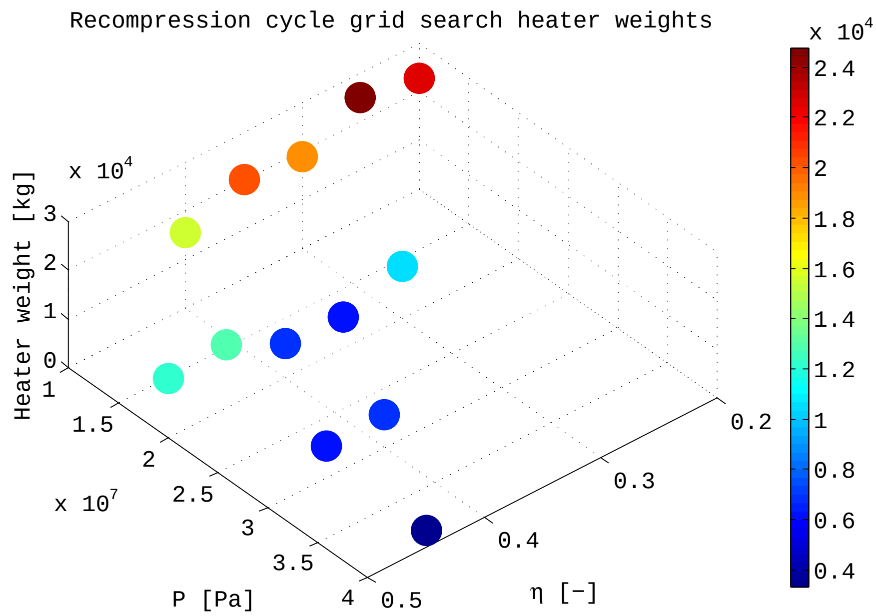

Figure 5.13: Variation of recompression cycle heater weight with varying grid search input

The most important statements that can be made after examination of the results are:

- As for the piping and regenerators, the high mass flow effects are clearly visible in the heater weights
- The maximum pressure listed in figure 5.13 for the recompression cycle is 40 MPa, even though there are feasible cycle results up to 60 MPa. In fact, at $\eta = 0.5$ only the feasible cycle option using $P = 2{\cdot}10^7$ is shown in the results. The reason for the other heater designs not converging is found in their CO_2 output temperatures. At $\eta = 0.5$ and $P = 2{\cdot}10^7$, for example, the cycle results gathered in section 5.2.1

require the CO_2 to exit the heater at 994 K. Even though this lies within the bounds of the cycle calculations, it proves not to be feasible to produce a heater that is capable of providing the required power within the bounds set by the grid search. All points that encounter this problem are therefore left out of consideration when determining the overall minimum grid point

- Because of the beneficial heat transfer properties of both LBE and s-CO_2 the heaters can indeed be compact, as expected. The heat exchanger of typical dimension h = 1 m should fit comfortably in the reactor vessel and no additional weight penalty has to be added to account for a necessary increase in size of the reactor vessel

5.2.5. COOLER GRID SEARCH RESULTS

Figures 5.14 and 5.15 depict the data points as well as the fitted surfaces that show the variation of cooler weight with cycle inputs for regenerative and recompression cycles, respectively. The shape of the area of feasible design points for recompression cycle coolers allows for this graph to also be a 3D surface plot. Table 5.7 shows the values of the variables that are presented by the calculation code as output of the regenerative cycle cooler grid search. Again, the minimum component weight grid point is selected, which lies at η = 0.45 and P = $6{\cdot}10^7$ for the cooler.

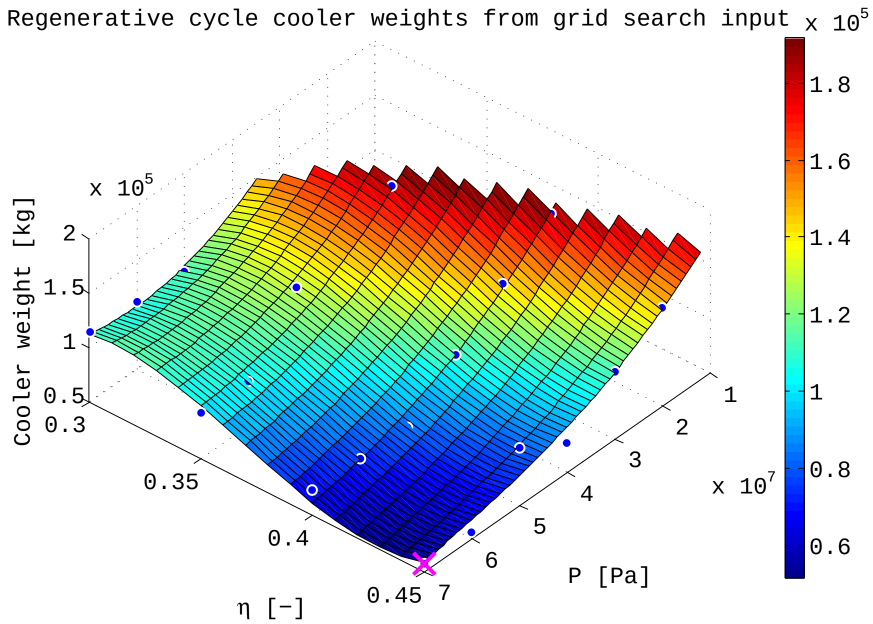

Figure 5.14: Variation of regenerative cycle cooler weight with varying grid search input

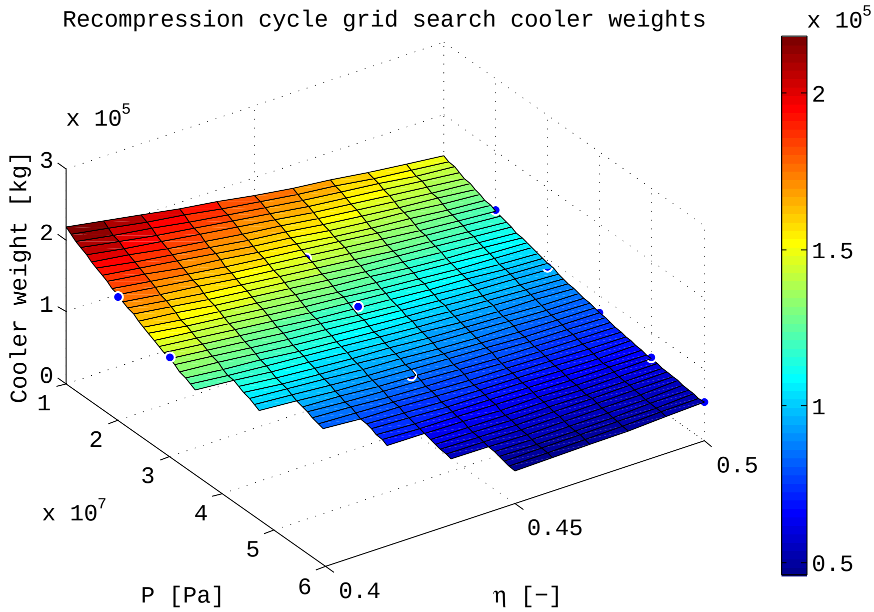

Figure 5.15: Variation of recompression cycle cooler weight with varying grid search input

Output	**Value**
PCHE frontal dimension h [m]	7
Hot channel diameter $d_{CH,H}$ [mm]	5
Cold channel diameter $d_{CH,C}$ [mm]	5
Mass flows ratio $\frac{\dot{m}_{air}}{\dot{m}_{CO_2}}$ [-]	2
Air mass flow $\dot{m}_{air}$ [kg/s]	592
Air inlet area on wing A_{inlet} [m^2]	6.9
Mach number of air at cooler inlet $M_{air,in}$ [-]	0.2
Air temperature at cooler outlet $T_{air,out}$ [K]	364
Cooler mass m_{co} [10^3 kg]	55.7
CO_2 pressure loss ΔP_{CO_2} [Pa]	13.2
Air pressure loss fraction $\frac{\Delta P_{air}}{P_{air,in}}$ [-]	0.2

Table 5.7: Example of cooler grid search output for a regenerative cycle at the $\eta = 0.45$ and $P = 6 \cdot 10^7$ grid point

Based on the presented results the following statements can be made regarding the cooler design in the grid search:

- Due to the poor heat transfer properties of air, the cooler is indeed by far the largest component in the heat cycle. The bound on h has been put at 11 m and even this high bound is not met by many of the grid points, which is why the ranges on the axes of figures 5.14 and 5.15 are reduced with respect to other components. Again, the cycle grid points at which there is no converging cooler design are left out in further design steps because, even though the cycle is feasible at that point, the components do not converge so a physical design of that cycle is not possible within the bounds set in this study
- The pressure loss on the CO_2 side of the heat exchanger is extremely small, which is a result of the low flow velocity in the CO_2 channels. The cooler design is dictated by the air flowing through it in the sense that the CO_2 is always capable of supplying enough heat but the air is causing the code to produce errors by:
    - Exceeding the air flow velocity bound, which happens at high air mass flows when the cooler dimension or flow channel diameter input is too small

  - Reducing the temperature difference between air and CO_2 flows too much. This stops the heat exchanging process and is caused by insufficient air mass flow

  The end result is that the heat exchangers which contain enough air at sufficiently low speed are so large that the mass flow of CO_2 is divided over a much larger area of flow channels than for other heat exchangers, even in a double cold banking set-up

- Due to the high flow velocity in the air channels, the pressure drop on that side of the heat exchanger is very large. At this point in the calculations, no limit is imposed on the airflow pressure loss but it is important when determining the possible additional thrust

- The additional output parameters of cooler inlet Mach number of the airflow $M_{air,in}$ and the cooler outlet temperature of the air $T_{air,out}$ are required in the output because they have to be entered into the GasTurb subsonic ramjet model that is used to determine the cooler airflow thrust contribution

- The airflow is limited by the available area of cooler channels and the bound on PCHE airflow velocity. Therefore, the inlet area only comes out as 6.9 m^2, which is nowhere near the available 30 m^2 that is set as the bound in section 4.2.6. This results in a beneficial reduction of the complexity of the cruiser wing design because only a small portion of the wing leading edge has to accommodate an inlet

5.2.6. MINIMUM WEIGHT GRID POINT DETERMINATION

With the outcomes of the component grid searches, the overall minimum points can be determined for the regenerative and recompression cycles. The steps taken to achieve this are:

1. Load the weight and pressure loss results of the component grid searches into the working memory of the Matlab code as matrices of which each entry corresponds to a grid point

2. Calculate the power penalty weights that are incurred by the additional heater power and excess pressure losses, as explained in section 4.2.7

3. Add all weights per grid point

4. Discard all grid points at which any of the components did not produce a feasible design such as the restrictions mentioned for the cooler

5. Find the point of minimum total weight and retrieve the necessary information for that point. This includes the grid cycle inputs and the weight breakdown that leads up to the total weight

There are two main results per cycle to be displayed here: a surface plot showing the variation of the overall cycle weight with varying cycle inputs and a pie chart showing the minimum weight grid point and the contribution of each heat cycle component to the total weight. For the recompression cycle the surface plot is shown in figure 5.16 and the weight breakdown pie chart in figure 5.17. The figures of the regenerative cycle are figure 5.18 for the surface plot and figure 5.19 for the pie chart.

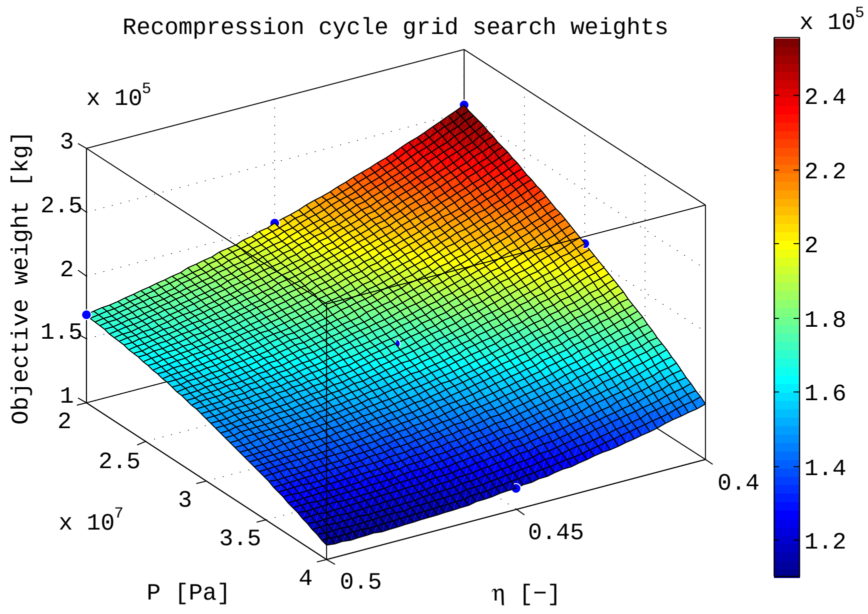

Figure 5.16: Variation of recompression cycle total weight with varying grid search input

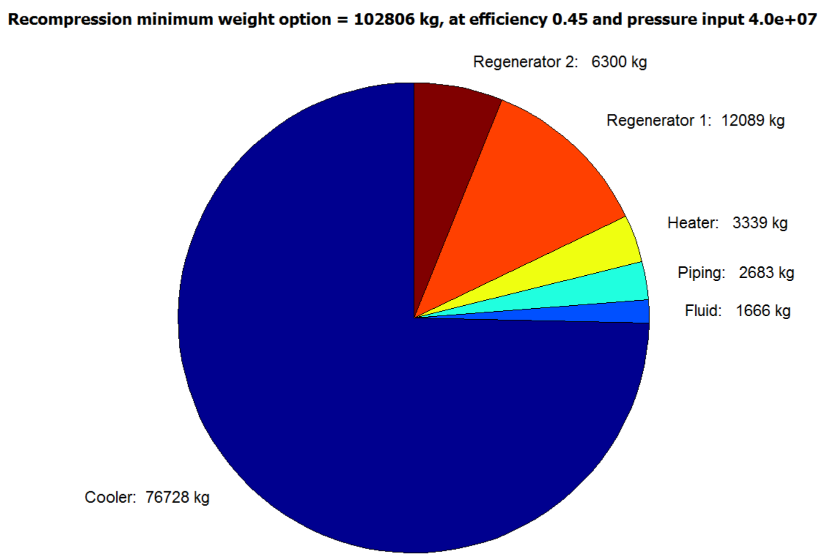

Figure 5.17: Pie chart with the breakdown of the recompression cycle total weight at the minimum weight grid search point

What can be gathered from the overall results of the grid searches is:

- The range for feasible cycle and components design is much larger for the regenerative cycle options. The recompression cycle had fewer valid cycle points to begin with and lost more of them due to unfeasible component designs such as the cooler and heater
- Not shown in the graphs but nevertheless noteworthy are the results of the overall pressure drop penalty. Even though the effect on the objective function is small due to the considerations mentioned in section 4.2.7, there is a clear distinction between regenerative cycles and recompression cycles. The increased number of components and pipes in a recompression cycle cause the total pressure drop in those cycles to be notably higher than the regenerative cycles' total pressure drops. Whereas the 1% pressure drop assumption made at the beginning of the cycle calculations proves to be overestimating

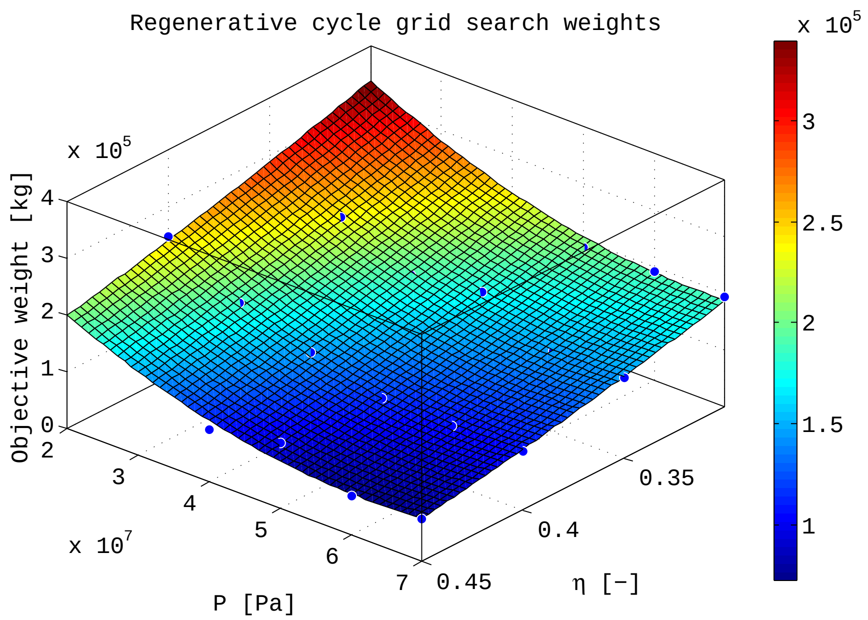

Figure 5.18: Variation of regenerative cycle total weight with varying grid search input

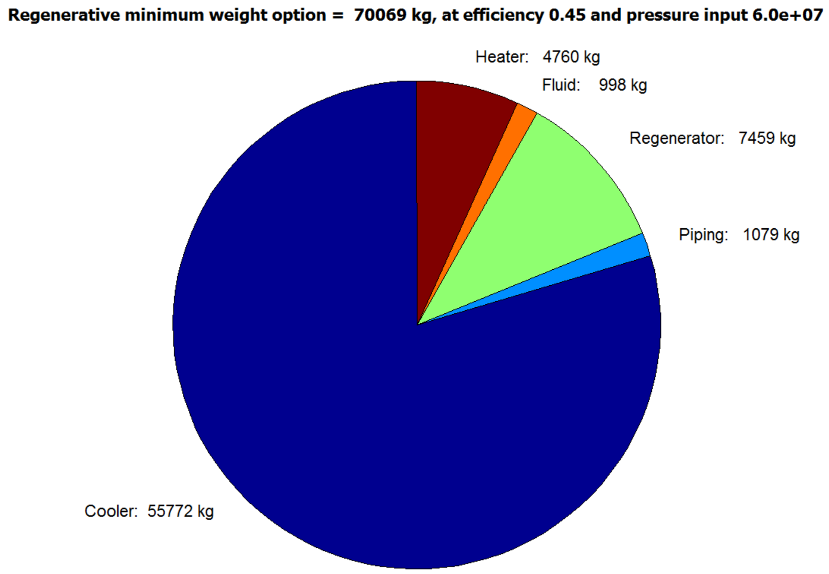

Figure 5.19: Pie chart with the breakdown of the regenerative cycle total weight at the minimum weight grid search point

the actual pressure drop for all but one of the grid points of the regenerative cycle, it is a significant underestimation for all but two of the recompression cycle's grid points. The actual pressure drop percentages for the regenerative cycle range between 0.12 and 1.8% with an average of 0.43% and between 0.58 and 4.7% for the recompression cycle with an average of 1.9%. These discrepancies do not influence the final result significantly as shown by the fact that the maximum pressure loss penalty incurred is 1700 kg for a recompression grid point of which the total objective weight is 168,000 kg. However, future iterations of this study should include varying pressure loss assumptions for the regenerative and recompression cycle

- The minimum weight grid points are located at η = 0.45 and P = 40 MPa for the recompression cycle and at $\eta = 0.45$ and P = 60 MPa for the regenerative cycle. The values of the total weight at those points are about 103,000 kg and 70,000 kg respectively

- The weight breakdowns show that the cooler is by far the biggest contributor to the cycle weight in either case, with its weight constituting almost 75% of the total cycle for the recompression cycle and even close to 80% for the regenerative cycle. Because of the higher mass flows present in the recompression cycle its components are almost consistently higher for each of the components at each of the points. In the shown pie charts, only the heater of the recompression cycle is lighter than that of the regenerative cycle. This is due to the recompression heater having CO_2 channels with a diameter of 2 mm, whereas the heater of the minimum weight regenerative cycle grid point configuration has channel diameters of 1 mm
- Even at the minimum weight grid point the recompression cycle already exceeds the heat cycle weight budget of 100,000 kg set in the requirements of section 1.3. Remember that the weight of turbines, compressors and additional systems has not even been taken into account here. As a result of this and the vast difference between the weight of the recompression cycle and that of the regenerative cycle it is decided not to pursue further optimisation for the recompression cycle. So the optimisations of the following section are only performed from a starting point given by the regenerative data, which is the point $\eta = 0.45$ and P = 60 MPa.

5.3. CLOSED CYCLE OPTIMISATION RESULTS

Starting from the minimum weight grid point of the regenerative cycle at $\eta = 0.45$ and P = 60 MPa the optimisation sets out to find the overall optimal cycle and component set-ups for the nuclear cruiser's heat cycle. For the optimisation the input vectors and bounds are determined from the inputs of the grid cycle calculations. Because the variables are varied in steps during the grid search, the final optimum can assumed to lie within the area directly around the minimum point for each of the variables. This area is bounded by the two adjacent input values of the variable that are tested in the grid search. For example, the value of the cycle efficiency that resulted in the minimum weight cycle during the grid search is 0.45, which is entered into the input vector of the optimisation. The cycle efficiency is varied in step sizes of 0.05 during the grid search. This means that the points closest to 0.45 that the calculations have been performed for are 0.4 and 0.5. These are then used as the lower and upper bounds for the optimisation. This process is similar for each variable.

The resulting vectors of inputs, lower bounds, and upper bounds are shown in table 5.8. It can be seen that most of the inputs fall perfectly between their respective bounds, which shows that the grid search has performed its duty and the assumed grids are chosen correctly. The only exceptions are the channel diameters of the cooler, which are set to 5 mm by the grid search. This is equal to the upper bound, which means that the actual most optimal configuration may be beyond the bounds set during the grid search. Therefore, future studies should investigate the possibility of increasing channel diameters of PCHE's beyond the maximum 5 mm that is currently applied. This problem could already be solved by the inclusion of airfoil-finned heat exchangers because that set-up abandons the distinct fluid channels. The exact result of this change on component weight and dimensions are unknown at this point, so this study continues with the well-defined fluid channels with a diameter limit of 5 mm. To ensure that optimisation function runs, the upper bound of a variable cannot be equal to its initial value. To counter the problem, the upper bound for the cooler channel diameters is raised slightly to 10^{-10} m above 5 mm. This increase is big enough to avoid errors in the optimisation code, yet small enough to not influence the final result.

To ease the optimisation process, it is useful to normalise these vectors so that all lower bounds can be set to 0 and all upper bounds to 1. The resulting input vector is listed in table 5.9. The objective function output is normalised by dividing its outcomes throughout the optimisation process by the value of the objective function that results from the grid search.

	$\mathbf{P}_{hc}$ [MPa]	η_{hc} [-]	$\mathbf{r}_{i,pipes}$ [cm]	$\dot{m}_{air}$ [kg/s]	
Upper bound	70	0.5	[50, 50, 50, 50, 50, 50]	888	
Input	60	0.45	[13, 15, 9.6, 11, 23, 18]	592	
Lower bound	50	0.4	[5, 5, 5, 5, 5, 5]	296	
	$\mathbf{h}_{co}$ [m]	**$\mathbf{d}_{CH,C,co}$ [mm]**	**$\mathbf{d}_{CH,H,co}$ [mm]**	**$\dot{m}_{LBE}$ [kg/s]**	**$\mathbf{h}_{he}$ [m]**
Upper bound	8	5	5	5000	2
Input	7	5	5	2500	1
Lower bound	6	3.5	3.5	1000	0.5
	$\mathbf{d}_{CH,C,he}$ [mm]	**$\mathbf{d}_{CH,H,he}$ [mm]**	**$\mathbf{h}_{reg}$ [m]**	**$\mathbf{d}_{CH,C,reg}$ [mm]**	**$\mathbf{d}_{CH,H,reg}$ [mm]**
Upper bound	2	1	3	2	2
Input	1	0.5	2	1	1
Lower bound	0.5	0.2	1	0.5	0.5

Table 5.8: Vectors of input values and bounds that result from the grid search minimum weight grid point setup

Normalised	$\mathbf{P}_{hc}$ [-]	η_{hc} [-]	$\mathbf{r}_{i,pipes}$ [-]	$\dot{m}_{air}$ [-]	
Input	0.5	0.5	[0.09, 0.1, 0.05, 0.07, 0.19, 0.14]	0.5	
Normalised	**$\mathbf{h}_{co}$ [-]**	**$\mathbf{d}_{CH,C,co}$ [-]**	**$\mathbf{d}_{CH,H,co}$ [-]**	**$\dot{m}_{LBE}$ [-]**	**$\mathbf{h}_{he}$ [-]**
Input	0.5	1	1	0.38	0.33
Normalised	**$\mathbf{d}_{CH,C,he}$ [-]**	**$\mathbf{d}_{CH,H,he}$ [-]**	**$\mathbf{h}_{reg}$ [-]**	**$\mathbf{d}_{CH,C,reg}$ [-]**	**$\mathbf{d}_{CH,H,reg}$ [-]**
Input	0.33	0.38	0.5	0.33	0.33

Table 5.9: Vector of normalised input values

The progress of the optimisation is visualised by its convergence from the normalised starting point to the final optimal value in figure 5.20. This normalised output shows an improvement by the optimisation of almost 8% from the result of the grid search. Even though the fractional difference is not very large, the absolute improvement in objective function from around 70,000 kg to 64,200 kg, which represents a weight saving of around 6000 kg, is worth this additional computation effort. The other important part of the output is the final value of the optimisation variables shown graphically in figure 5.21 and numerically in table 5.10, in which the final value of the variables is compared to their initial values. This shows that all variables, except for the cooler channel diameters, undergo changes during the optimisation. The only reason that those diameters do not change is that their optimal point most likely lies somewhere beyond the upper bound, as explained at the beginning of this section. Another interesting trend that seems to be consistently present in the output is that the fractional decrease in heat exchanger dimensions has an almost 1:1 correlation to the increase in heat cycle efficiency around the minimum grid point. Although the optimisation has only been performed once so there is no evidence in this study to fully prove this statement under different circumstances, it is noteworthy that all three of the heat exchangers' frontal dimension variables decrease by the exact 7.5% that the heat cycle efficiency variable increases.

The final values of the optimisation variables are needed as the input for the code that states the final heat cycle design. In this code, the cycle variables of pressure and efficiency are used to generate the final value of the CO_2 mass flow, component powers, and the cycle's thermodynamic variations. The geometrical inputs for the components are then used along with the outcome of the cycle computations to generate the final sizes and weights for all components. The result is shown in section 5.5.

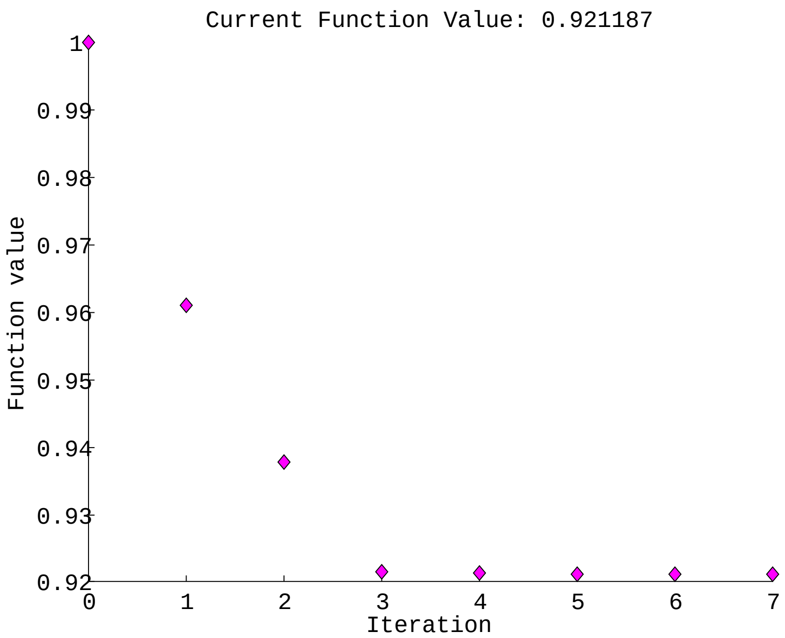

Figure 5.20: Convergence history on the regenerative cycle final optimisation

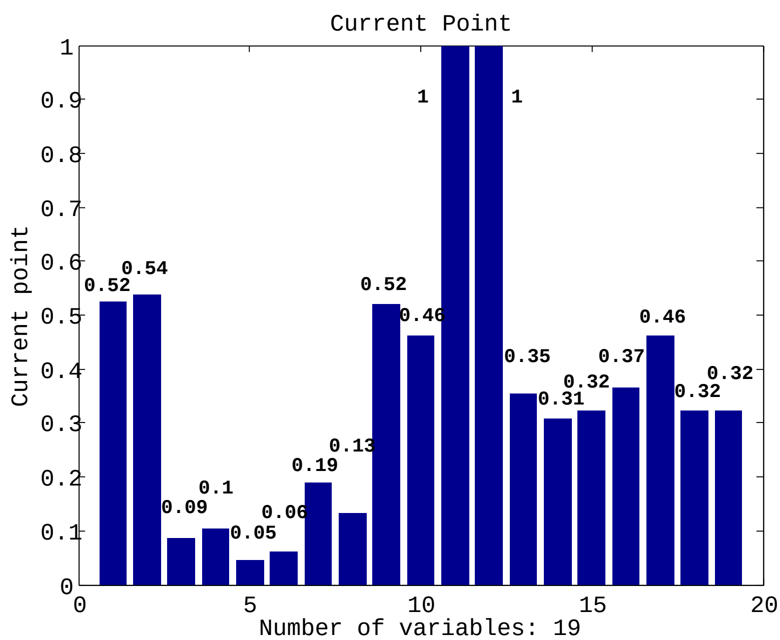

Figure 5.21: Final normalised values of the optimisation variables

Normalised	$\mathbf{P}_{hc}$ [-]	η_{hc} [-]	$\mathbf{r}_{i,pipes}$ [-]	$\dot{m}_{air}$ [-]	
Output	0.52	0.54	[0.09, 0.1, 0.05, 0.06, 0.19, 0.13]	0.52	
Difference [%]	4.9	7.5	[-2.5, -2.8, -7.5, -7.3, -0.5, -0.7]	4.2	
Normalised	$\mathbf{h}_{co}$ [-]	$\mathbf{d}_{CH,C,co}$ [-]	$\mathbf{d}_{CH,H,co}$ [-]	$\dot{m}_{LBE}$ [-]	$\mathbf{h}_{he}$ [-]
Output	0.46	1	1	0.35	0.31
Difference [%]	-7.5	0	0	-5.6	-7.5
Normalised	$\mathbf{d}_{CH,C,he}$ [-]	$\mathbf{d}_{CH,H,he}$ [-]	$\mathbf{h}_{reg}$ [-]	$\mathbf{d}_{CH,C,reg}$ [-]	$\mathbf{d}_{CH,H,reg}$ [-]
Output	0.32	0.37	0.46	0.32	0.32
Difference [%]	-3	-2.4	-7.5	-2.9	-3

Table 5.10: Vector of normalised output values and the variation from the input vector

5.4. VALIDATION OF THE RESULTS

Theoretical validation of the results gathered from this thesis is hard because nothing similar has ever been done. No documentation has been found of PCHE design with the intent of minimising component weight while using different fluids. The same goes for weight estimation of entire heat cycles and minimum weight modern nuclear reactors. By basing as many of the calculations as possible on validated research, the outcome of this research should also be realistic or at the very least provide a good indication of what an actual minimum weight design would be. This is achieved by employing formulas and methods from other research and combining them to reach the final goal of a minimum weight heat cycle for the nuclear cruiser. However, extensive amounts of theoretical and practical research will have to be done in the future to validate the results presented in this thesis. This additional research includes:

- Scale mock-up tests of the heat cycle and its components
- CFD analysis coupled to finite element calculations to test airfoil-finned PCHE's on both structural integrity as well as heat exchanging performance and pressure losses
- Heat exchanger performance tests in denser fluids such as LBE and FLiBe to be able to include pressure loss calculations for those fluids in future design codes

For the time being, checks of the validity of the results of the present study, without this additional research having been performed, comes from inspecting trends in the results and ensuring that they coincide with realistic expectations. An example of this process is determining the causes for errors in PCHE calculations. Narrow channels tend to fail to converge because of flow velocity-related errors due to the high mass flow per unit area. A cooler with relatively low air mass flows on the other hand fails in temperature or pressure-related calculations caused by excessive flow lengths needed to transfer the proper amount of heat.

5.5. FINAL DESIGN SPECIFICATION

The output of the optimisation is converted to an actual design of the final heat cycle for the nuclear cruiser. The first resulting design is the thermodynamic behaviour of the heat cycle itself. Using the final input of η = 0.454 and P = 60.5 MPa the T-s diagram of the heat cycle is shown in figure 5.22. The accompanying values of pressure, temperature and mass flow for each cycle point is listed in table 5.11, with the order of the cycle points equal to the pipes of section 5.2.2. The numbers in brackets represent the numbering adopted in Noriega's thesis and depicted in figure 3.9. The pressure values clearly show the assumption of the assumed pressure losses in the cycle calculations being concentrated at the compressor and turbine inlets. Future research could be made more accurate by replacing this assumption and assume a pressure loss per component in stead.

Using an analogous series of steps as used throughout the calculations, now the final design of the components are presented. For each component a table of component outputs is presented, starting with the piping in table 5.12, followed by the regenerator in table 5.13, the heater in table 5.14, and the cooler in table 5.15. In these tables the values that are situated at a bound limit are highlighted by underlining them, showing that future researches should investigate the possibility of extending the bounds to reach other designs that may prove to result in even lower weights.

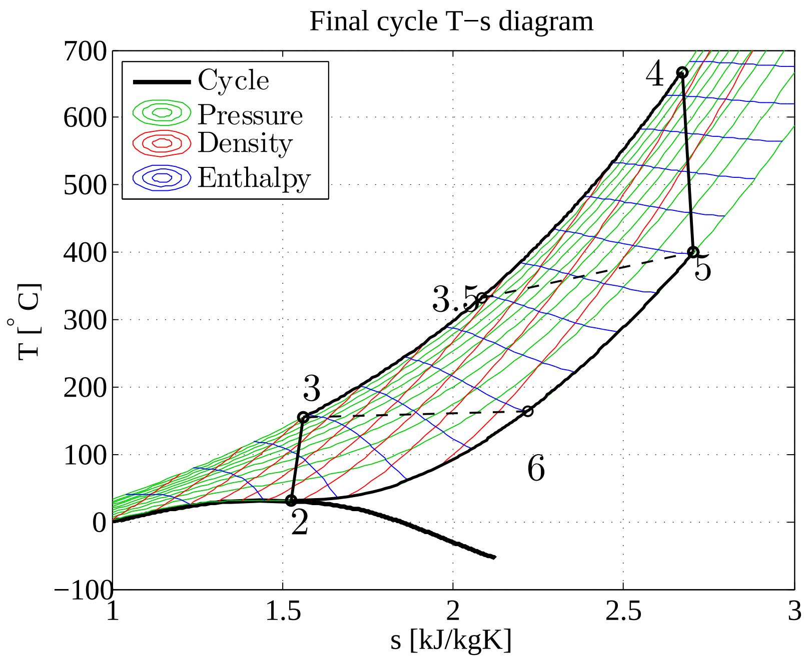

Figure 5.22: T-s diagram of the optimal heat cycle

	Compressor in (2)	Compressor out (3)	Heater in (3.5)
Pressure [MPa]	7.4	60.5	60.5
Temperature [K]	304	428	606
Density [kg/m^3]	369	739	472
Mass flow [kg/s]	291	291	291
	Heater out (4)	**Turbine out (5)**	**Cooler in (6)**
Pressure [MPa]	59.9	7.5	7.5
Temperature [K]	940	673	438
Density [kg/m^3]	290	59	100
Mass flow [kg/s]	291	291	291

Table 5.11: Thermodynamic variables at the cycle points of the optimal heat cycle

Pipe number	1	2	3	4	5	6
Length [m]	5	1	3.5	2.5	2	2.5
Internal radius [cm]	13	15	9	11	23	18
Wall thickness [mm]	2	24	15	21	4	3
Flow velocity [m/s]	15	6	22	28	<u>30</u>	<u>30</u>
Pressure loss [kPa]	7	0.4	21	12	1	3
Pipe weight [kg]	79	195	274	313	102	74
Contained CO_2 [kg]	100	52	45	26	19	25
Total pressure loss [kPa]			45			
Total CO_2 weight [kg]			267			
Total piping weight [kg]			1037			

Table 5.12: Design output for the piping of the optimal heat cycle

Variable	**h**	**l**	**d**$_{CH,C}$	**d**$_{CH,H}$	**V**$_{CO_2,C}$	**V**$_{CO_2,H}$
Value	1.9 m	0.3 m	1 mm	1 mm	1 m/s	8 m/s
Variable	$\#CH,C$	$\#CH,H$	**t**$_{w,C}$	**t**$_{w,H}$	**t**$_{pl,C}$	**t**$_{pl,H}$
Value	1.6·10^6	1.6·10^6	0.2 mm	0.2 mm	*0.5 mm*	0.5 mm
Variable	**t**$_{sw}$	ΔP_C	ΔP_H	ΔP_{tot}	**m**$_{CO_2,reg}$	**m**$_{reg}$
Value	1 mm	4 kPa	24 kPa	28 kPa	138 kg	7072 kg

Table 5.13: Design output for the regenerator of the optimal heat cycle

Variable	**h**	**l**	**d**$_{CH,C}$	**d**$_{CH,H}$	$\#CH,C$	$\#CH,H$
Value	1 m	0.7 m	1 mm	0.5 mm	0.3·10^6	1.2·10^6
Variable	**t**$_{sw}$	**t**$_{w,C}$	**t**$_{w,H}$	**t**$_{pl,C}$	**t**$_{pl,H}$	$\dot{m}_{LBE}$
Value	1 mm	0.3 mm	0.1 mm	0.5 mm	0.5 mm	2416 kg/s
Variable	**V**$_{CO_2}$	**V**$_{LBE}$	**T**$_{HL}$	ΔP_{CO_2}	**m**$_{CO_2,he}$	**m**$_{he}$
Value	9 m/s	2 m/s	998 K	186 kPa	32 kg	4208 kg

Table 5.14: Design output for the heater of the optimal heat cycle

Variable	**h**	**l**	**d**$_{CH,C}$	**d**$_{CH,H}$	**T**$_{CL}$
Value	7 m	0.3 m	5 mm	5 mm	360 K
Variable	**t**$_{sw}$	**t**$_{w,C}$	**t**$_{w,H}$	**t**$_{pl,C}$	**t**$_{pl,H}$
Value	1 mm	0.1 mm	0.1 mm	0.5 mm	0.5 mm
Variable	**V**$_{CO_2}$	**M**$_{air,in}$	ΔP_{CO_2}	$\frac{\Delta P_{air}}{P_{air,in}}$	**A**$_{inlet}$
Value	0.3 m/s	0.3	13 Pa	0.2	7 m^2
Variable	$\#CH,C$	$\#CH,H$	$\dot{m}_{air}$	**m**$_{CO_2,co}$	**m**$_{co}$
Value	2·10^6	1·10^6	605 kg/s	502 kg	52371 kg

Table 5.15: Design output for the cooler of the optimal heat cycle

All the individual component results are combined to determine the overall cycle results, as shown in table 5.16. The breakdown of the total weight of the optimal cycle is depicted in a pie chart in figure 5.23. It is apparent from the total values that the initial pressure loss assumption is overestimating the total pressure loss of all components in the final cycle. As a result, the objective function value is slightly lower than the combined component weight.

Variable	ΔP_{tot}	**Pressure penalty**	$Q_{reac,pp}$	m_{pp}
Value	258 kPa	-346 kPa	-0.3 MW	- 344 kg
Variable	m_{coms}	m_{CO_2}	m_{tot}	**Objective function**
Value [kg]	64688	938	65626	65282

Table 5.16: Design output for the overall optimal heat cycle

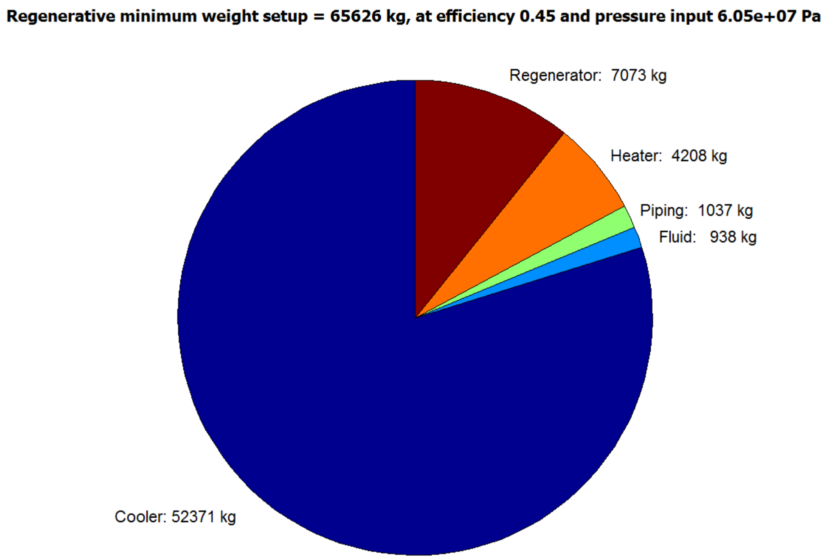

Figure 5.23: Weight distribution of the optimal weight final design

As stated in section 4.2.5, the cooling air mass flow can be used to generate thrust. For the ideal set-up the resulting gross thrust amounts to almost 112 MW, but due to excessive pressure losses in the cooler the resulting net thrust is negative because the ram drag created by the inlet is higher than the produced thrust. In order to try and compensate for this two remedies are attempted, which are explained below along with their impact on the design.

- **Adding a compressor before the heat exchanger:** increasing the pressure of the air flowing into the PCHE should benefit heat exchange and result in a smaller cooler. However, the additional work performed by the compressor also raises the temperature of the incoming air, which proves to be detrimental for cooler performance. Even at small pressure ratios the increased temperature of the air diminishes the gain in effectiveness due to the increase in pressure, which is shown in increased cooler weights and more failures in the design code. These failures are caused by the air heating up too quickly so that heat exchange happens very slowly causing the pressure to drop due to the long control volumes that are necessary to reach the set control volume power or even reverses, at which point the code is set to throw an error

- **Decreasing the allowed pressure loss of the air:** manually setting a limit on the air pressure loss in the cooler design code by throwing an error when the pressure loss exceeds a set value also proved not to work. This value is deduced from the GasTurb model of the subsonic low-temperature ramjet setup mentioned in section 4.2.5. By decreasing the pressure ratio and monitoring its effect on the thrust output, the point of 0 thrust is found to be around a pressure loss of 10% depending on air mass flow and cooler outlet temperature. When this limit is entered into the cooler design code and the cooler grid search is ran, it shows drastic increases in cooler weight and dimensions. Taking the minimum cooler weight grid point of the regenerative cycles as an example, the relevant values are presented in table 5.17. This table shows that, despite the net thrust being close to 0, the decreased power penalty weight is not enough to compensate for the additional cooler mass

Variable	**ΔP allowed = P$_{in}$**	**ΔP allowed = 0.1 P$_{in}$**
h [m]	7	8
$\frac{\Delta P}{P_{in}}$ [%]	18.3	9.3
m_{co} [10^3 kg]	56.75	81.71
Th_{net} [kN]	-31.63	-5.33
ΔQ_{hc} [MW]	7.47	1.26
m_{PP} [10^3 kg]	16.6	2.8
Δm_{tot} [10^3 kg]	0	11.2

Table 5.17: Table comparing efficiency of solutions for trying to increase cooler thrust

So, for now it seems most beneficial to complete the design process using the set-up as it sits and let the main propulsion system compensate for the power lost due to the cooler airflow inlet. The final visual result of the heat cycle components as they are present in the wing is shown in figure 5.24. On the left side of the figure the outer skin is visible to provide an idea of the scale and placement of the final components, on the right side the heat cycle components are depicted. An annotated close-up of the heat cycle is shown in figure 5.25 to indicate which body represents which (heat cycle) component. An extra note has to be made explaining the contents of the cyan coloured containment vessel, which is on the left the cylindrical reactor vessel and the block on the right is the LBE-to-CO_2 heater.

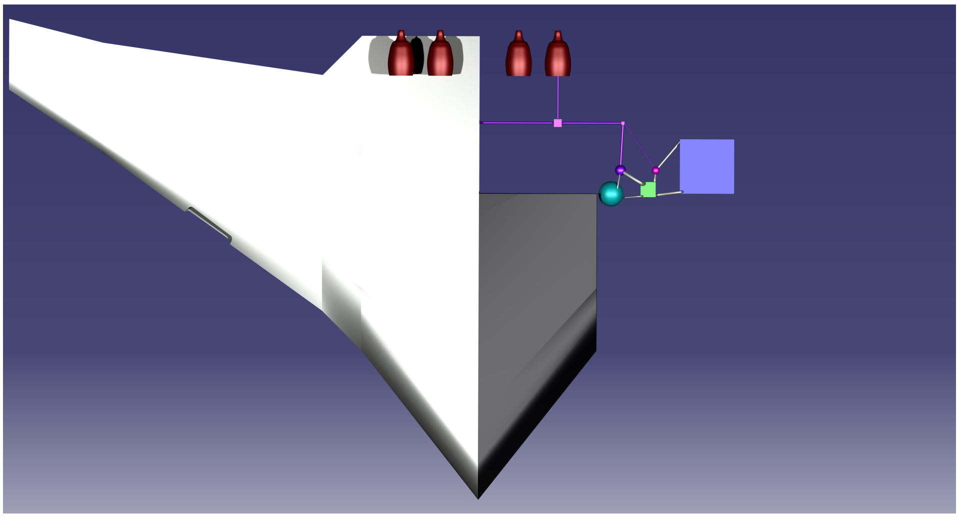

Figure 5.24: Sketch of the final to-scale regenerative cycle component placement in cruiser wing

From this model the assumptions of the pipe lengths are checked and the results are shown in table 5.18. The differences between the assumed and the actual pipe lengths are fairly large and require some additional analysis. The main reason for the pipe lengths in the final design being so much larger than the assumed values lies in the assumption in the CATIA rendering that the pipes exit the heat exchangers at a tangent to the horizontal faces. As can be seen in the rendering, this requires the pipes to contain additional curvatures in order to link up the components. These add significant length to each pipe, skewing the final result. The assumption of how the pipes are connected to the heat exchangers stems from the fact that it is unknown what the optimal way is to merge the pipes into the PCHE channels at minimum weight and minimum pressure loss. The present situation is easy to render because it does not require the design of additional merging ducts between the heat exchangers and the pipes. Future design iterations should update this assumption and come up with an optimal in- and outflow design of the PCHE, which is likely to reduce pipe lengths by eliminating the complex curvatures of the present assumption.

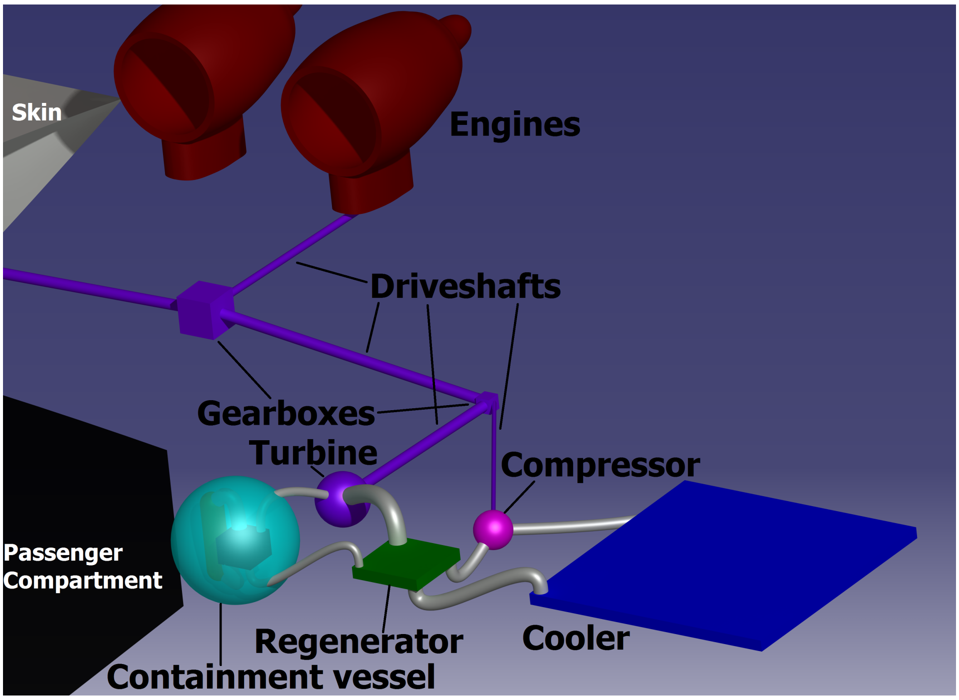

Figure 5.25: Close-up of the final heat cycle with annotations

Pipe number	**1**	**2**	**3**	**4**	**5**	**6**
Assumed length [m]	5	1	3.5	2.5	2	2.5
Length from final CATIA model [m]	4.7	1.6	4.1	2.9	3.4	4.2
Difference [%]	-6	64	16	16	68	67

Table 5.18: Check of the assumed piping lengths from the initial model using measurements from the final setup of figure 5.24

Remembering the weight budget set in section 1.3 the outcome of the calculations leaves 34,400 kg for all components that have not been sized such as the driveshafts, turbomachinery, and systems to hold the piping in place. Even though accurate design work and calculations are needed to ensure that this excess weight budget is sufficient to accommodate these parts, instinctively it seems feasible.

6

ADDITIONAL SPECIFIC SAFETY ASPECTS FOR A NUCLEAR-POWERED AIRCRAFT

Apart from the safety considerations that have already been dealt with in previous chapters, some remaining issues still have to be discussed. These are treated in this chapter, along with suggestions of possible solutions for these issues. Most of these suggestions are not developed into detailed designs or plans, as they are meant to provide a starting point for future projects and as an indication of what specific issues arise when designing and operating a nuclear-powered aircraft. To better understand the danger of a malfunctioning reactor, the chapter starts off with a short description of the infamous concept of reactor meltdown.

6.1. REACTOR MELTDOWN

For understanding the events leading up to a meltdown, it is important to know how nuclear reactions produce heat. When a large atom such as uranium fissions it forms two smaller atoms, free neutrons and heat. The free neutrons can react with other large atoms to cause them to fission, thereby releasing more heat. If enough unstable large atoms are gathered in the fuel rods of a reactor the reaction becomes self-sustaining, which is the normal working of nuclear reactors. A state of constant heat production is reached when a stable nuclear chain reaction has been reached. This happens when exactly one free neutron from any fissioned heavy atom causes the fissioning of a next heavy atom. The produced heat is then lead away by the fluid in the reactor's heat cycle to drive a turbine and generate power. To shut down a reactor, control rods are inserted between the fuel rods. These rods are made of neutron absorbing materials so that the free neutrons do not interact with other atoms and the nuclear reaction stops. However, even after active fission has stopped the fission materials in the fuel elements still generate heat due to their residual radioactivity. This heat, produced after reactor shutdown, is called the reactor's afterheat. Now suppose that the cooling system has failed following an accident or coolant leak. In this situation the heat produced in the fuel rods is not evacuated, causing the fuel rods to heat up. If the fuel rods reach a critical temperature, which is determined by the melting temperature of the structural alloy used in their construction, the fuel rods begin to lose their structural integrity and eventually melt. The molten fuel element material then leaks away from the control rods and forms a pool at the lowest point of the reactor vessel. This pool can support a nuclear reaction of its own if it reaches so-called critical mass because of the absence of control material. To prevent this, active insertion of so-called poisoning materials such as boric acid has to be performed. But even if the pool does not sustain nuclear reactions, in the absence of active cooling the afterheat can keep the pool molten on the containment vessel. The wall of the containment vessel can eventually also melt, causing the pool to leak through and start eating away at subsequent barriers. If all barriers are breached before the molten material has been cooled, a full release of radioactive material takes place. This has to be prevented at all costs and during all possible crash and malfunction conditions on the nuclear cruiser to achieve the necessary safety levels.

6.2. IN-FLIGHT REACTOR PROBLEMS

If there is a malfunction in the reactor or the heat cycle, the aircraft structure and its valuable contents (passengers and cargo) should remain safe. The safest way of ensuring this in case of a significant issue concerning these critical systems is to shut down the nuclear propulsion system in order to avoid further damage to the system. The aircraft should then be able to use the remaining reactor system of the dual-reactor set-up and the emergency fuel-powered option for the faulty reactor cycle in order to reach an airport to perform an emergency landing. The specifics of this backup system are treated in section 3.4. After landing and evacuation of the aircraft, specialised teams can then investigate and, if necessary, repair the reactor system. There are two distinct options to deal with the disengagement of the faulty reactor and subsequent switch from nuclear power to emergency fuel: the faulty reactor can be jettisoned from the aircraft altogether or it can simply be shut down but remain on board. The advantages and disadvantages of both these options are discussed in the following sections. A schematic summary of the options and final decision is portrayed in figure 6.1. In this figure, the two options are each presented at a side of the decision block. For each of them, the additional design challenges are presented in the square blocks and their consequences in separate block below the square blocks. The selected options are indicated by underlined text and bold lines.

6.2.1. JETTISON THE REACTOR

In order to decrease the danger to the aircraft and the passengers, crew and cargo, inside the faulty reactor may be jettisoned from the aircraft. The jettison would encompass everything that is inside the shielding, so not only the reactor but also the primary heat cycle and any additional systems. This has the advantage that all nuclear material of the faulty cycle is removed from the aircraft. This obviously increases safety to the passengers because any deterioration of conditions inside the reactor (such as meltdown) does not affect them. It also prevents further damage of systems by the afterheat produced after the reactor has been shut down. On the other hand, there are additional systems needed to ensure a safe jettison of the reactor. Apart from the obvious skin panels that need to be able to open in flight (as opposed to only on land during reactor maintenance), the shielding needs to be attached to a jettison system. Investigations mentioned in [17] state that these systems alone add approximately 5% to the weight of the nuclear system. The additional space needed for the system also has to be taken into account during the design of the reactor bay. On top of that there are the additional systems needed for a safe landing of the jettisoned reactor. To decrease the impact on the ground some kind of deceleration device must be added. As shown in figure 6.1 three main options can be identified for this deceleration. Options that decrease impact speed such as a parachute, options that decrease the impact itself like airbags, or not including any systems and use only the containment vessel to prevent core damage. The final option is viable since the containment vessel should be designed to cope with any impact, as described in section 6.3, but for an already faulty reactor the impact should be as mild as possible to prevent accidental criticality of core material. Therefore, a parachute is deemed the most appropriate option. Because the location of jettison cannot be specified beforehand, the reactor has to be equipped for landing on both water as well as land. For any surface, however, the reactor must be able to withstand the impact at the design speed of the parachute. For water landings, there is the need for flotation equipment to ease recovery of the reactor. In case the reactor lands on solid ground, a system is needed to ensure that the afterheat produced by the reactor is dealt with to prevent meltdown. This problem is dealt with in more detail in section 6.3.1. Another effect of jettisoning the reactor system is the sudden change in weight (distribution) of the cruiser. Due to the large density of the reactor and other contents of the shield, a highly concentrated mass is present at that location. If this is suddenly removed, the entire balance of the aircraft is disturbed. This means that, in order for jettison to be an option, the reactor has to be at a very carefully determined location, preferably as near to the centre of gravity of the aircraft as possible. In his thesis, Chiozzi[8] proposes to place the nuclear reactor in the nose of the aircraft, directly underneath the cockpit. If the reactor were to be jettisoned from that position, the shift in centre of gravity would be big enough to cause the aircraft to become unstable and stall immediately. Another suggested position for the reactors, mentioned in [8] and [53], is in both wing roots, flanking the cabin. Even though this is a much better proposition considering longitudinal stability, it might still present significant problems in lateral stability, with large aileron deflections needed to overcome the lateral shift in centre of gravity. The placement of the reactors in the wing roots does ensure that the pipes carrying the heat cycle fluid do not have to run the throughout the entire aircraft and have to be routed around the passenger cabin and fuselage loading facilities. Finally there is the problem of opening the reactor hatch in order to perform the jettison. This hatch has to be opened and closed in order to retain the aerodynamic design of the cruiser and ensure safe flight and adequate performance. Detaching the hatch before jettison, like the canopy of a fighter aircraft, is not a feasible option. This would leave a large permanent hole in the outer skin of the aircraft, which severely decreases the lift to drag ratio. A final consideration has to be made regarding the mechanics of the containment vessel upon leaving its bay. If the moving panels would open sideways, like the doors on a bomber aircraft, the vessel could damage down-stream structure. Due to its size, a significant portion of the reactor is already subjected to the high-speed airflow around the aircraft before the entire vessel is clear of the aircraft structure. This airflow then results in a velocity difference between the vessel and the aircraft, which can result in the vessel damaging aircraft structure in case of inaccurate design or unexpected aircraft attitude. A more appropriate option would be to open a hatch against the airflow, like the cargo door at the back of military transport aircraft, and let the containment vessel roll down this hatch. That shields the vessel from the airflow until it is a sufficient distance from the aircraft. All the options presented above assume the reactor to be positioned near the lower skin at a convenient location in the aircraft before jettison. Before jettison the reactor vessel could be automatically transported inside the aircraft to such a location but the weight and complexity of such a system, as well as the added risks for aircraft stability and passenger safety diminish the applicability of such a system. As a result of the above consideration, the jettison option puts additional constraints on the positioning of the containment vessel.

6.2.2. SHUT DOWN THE REACTOR ON BOARD

The other option for continued flight on emergency systems is to only shut down the reactor but keep it on board. This option clearly dictates the final destination of the faulty reactor, being a specialised facility where the emergency landing is performed. This seems to dismiss the need for specialised pick-up teams to potentially recover a jettisoned reactor from the middle of the ocean. However, in case of a crash on water, such capabilities are still needed, as well as the need for flotation of the reactor vessel. By carrying the reactor to an airbase in any situation except for a catastrophic failure of the aircraft due to impact or explosion, the shutdown option also decreases the risk of the general public or even malicious organisations being able to come into contact with radioactive materials. However, keeping a faulty reactor on board does pose some additional problems that need to be solved. Even though the probability of accidental criticality after shutdown and other unforeseen reactor problems is reduced in future reactor types, afterheat will still be produced by the reactor after shutdown. An active cooling system is needed to backup the primary cooling cycle, of which it has to be assumed that it no longer functions.

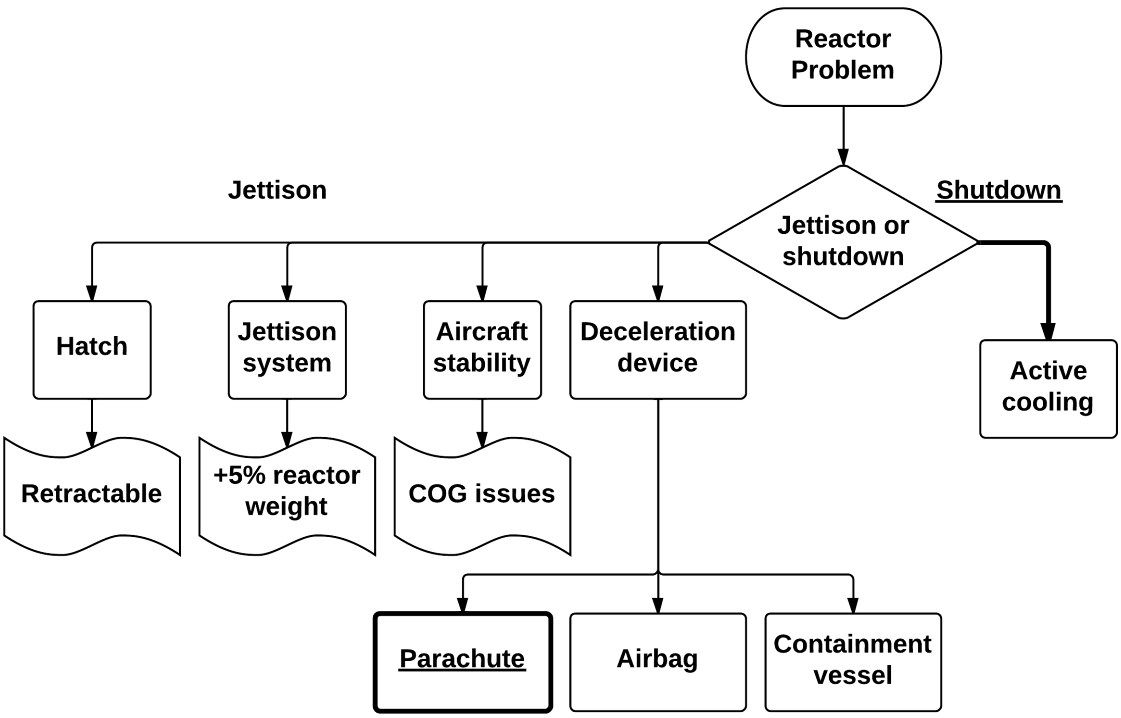

Figure 6.1: Option tree for dealing with in-flight reactor problems, showing the problems and design challenges for the two design options

To structure the decision-making process for choosing the most ideal option to deal with in-flight reactor problems, some criteria have to be chosen on which the two options can be graded. The selected criteria and which options has the best characteristics in each of them are shortly elaborated on in the following bullet points. The information is also found in table 6.1.

- **Passenger safety:** Because the reactor is detached from the aircraft, and removed from the vicinity of the passengers, the jettison option is best in terms of passenger safety.
- **Environmental safety:** The shutdown option takes the faulty reactor directly to a specialised repair facility, whereas after jettisoning recovery teams can take a significant time to reach the reactor. In this time, the environment and any people near the crash site could be in danger. Therefore, the shutdown option performs best in this category.
- **Additional design work:** The changes that have to be incorporated in the aircraft design for the jettison option include the jettison system itself, the hatch that allows the reactor to move away from the aircraft, and the parachute or other deceleration device. The need for jettison also restricts the design space for the positioning of the reactor. In case of the shutdown option the active cooling system needs to be designed. But it might be useful to include such a system also for the jettison option to reduce the number of jettisons that have to be performed. In that case, this design work would even be part of the general design process and would fall outside the scope of this criterion. The natural conclusion is that shutting down the reactor but keeping it on board has an advantage over jettisoning it according to this criterion.
- **Flight safety:** Provided that the consequences of the reactor problem can be contained within the containment vessel, the shutdown option has no effect on flight safety. In case of jettisoning, the sudden change in weight or even centre of gravity can pose a serious issue with regards to stability and controllability. Thus, the jettison option ranks below the shutdown option.

After considering the pros and cons of both options, it becomes clear that each of them has problems that cannot readily be solved. Despite that, the number and severity of these issues is deemed to be larger for the jettison option. Therefore, it is considered to be more feasible for designers of a nuclear cruiser aircraft to only include the shutdown system to deal with in-flight reactor problems.

Criterion	Jettison	Shutdown
Passenger safety	+	-
Environmental safety	-	+
Additional design work	-	+
Flight safety	-	+

Table 6.1: Decision table for dealing with in-flight reactor problems

In order to retrieve the reactor vessel after a crash, it is important that it has its own GPS locator. Because the reactor may have rolled away from the rest of the wreckage during or after the impact, it can have a different location than the rest of the aircraft and the black boxes. A clear example of this is given in the hypothetical case of the cruiser crashing into a hillside and the reactor vessel rolling down after being released from its surrounding structure. Also consider the case of a water landing where the reactor floats and has been swept away by ocean currents. Using the transmitted location, the dedicated recovery teams can locate the reactor and retrieve it to bring it back to a maintenance plant for repairs or safe disposal of the nuclear material. The transport vessel used by these teams needs to be equipped with additional cooling systems and sealed chambers to store the reactor and prevent meltdowns from occurring on the way to the maintenance plant.

6.3. CRASH DESIGN

One very common association people have when hearing about nuclear-powered aircraft is that it will explode like an atomic bomb in case of a crash. This fear is understandable but completely unfounded. In an atomic bomb the nuclear material is highly enriched and compressed to critical mass by a small preliminary explosion. This causes a very high amount of neutron interactions, which releases the nuclear energy at a very high rate[54]. None of these three conditions is present in a regular nuclear reactor (aboard the aircraft but also the current reactors on land): the nuclear material is commonly enriched to only a small percentage (below 10% currently), whereas weapons-grade uranium is 90+% enriched. Furthermore, the required density of the fuel to reach critical mass will not be reached in a regular reactor under any circumstances because the reactor contents will expand faster than the density can rise, so that it will never reach this state. In an atomic bomb, this process is forced by a leading explosion in a confined chamber inside its shell. This chamber then contains the resulting chain reaction as long as possible before releasing all this stored energy in the massive explosion. Finally, a normal reactor has control rods and other control mechanisms (as mentioned in section 6.1) to prevent the necessary chain reaction of neutrons from taking place.

That being said, there are of course many dangers that still remain in case the nuclear cruiser would crash. Any breach of the containment vessel could release radiation and nuclear debris into the environment. Therefore, it is vital this does not occur under any crash condition. The most critical situation would be a head-on mid-air collision with another aircraft at cruise speed. Instinctively, this is the case because of the fact that two bodies colliding at cruise speed will have the same effect as one of them crashing into a solid object at two times cruise velocity. However, a simple consideration of Newton's third law shows this to be an incorrect assumption. Indeed, the impact force is doubled but this higher force is taken up by two bodies, in stead of just one. Therefore the impact force on the reactor is approximately equal for a mid-air collision at cruise speed than it is for a crash into solid terrain at cruise speed. The reason that a mid-air collision is still more critical than a crash into the ground is the effects after the crash. If a reactor vessel were to rupture at the site of an impact with terrain, the nuclear waste would spill onto a relatively small area of land. If such a rupture would occur during cruise, on the other hand, the spill would cover a vast area. Especially if the aircraft continues to fly after the accident, the trail of nuclear material could stretch over the entire flight path, until this vessel is repaired after landing. Considering that no control or monitoring system will ever be 100% certain of preventing crashes, the reactor needs to be designed such that it will survive even this most critical crash condition.

According to [12] there are four paths to absorb the energy of a crash before the reactor vessel ruptures:

- Deformation of the soil upon which the impact takes place
- Deformation of the aircraft structure
- Working of a specialised impact energy absorption system
- Deformation of the material surrounding the reactor assembly, which includes the containment vessel and shielding

Because of the risks involved it is important to consider the worst-case scenario, regardless of how unrealistic it might seem, when designing the impact safety systems. The two items that can vary in the above list are the amount of energy absorbed by deformation of the soil and the aircraft structure. Suppose the aircraft would impact straight into a granite mountain face, rendering the energy absorption by the terrain to be negligible. Now consider the distribution of aircraft structure around the reactor. Regardless of the position of the reactor, there will always be directions where there is considerably less aircraft structure present to absorb impact energy. In the proposed location in the wing root, these directions would be directly above and below the reactor. Moreover, the structure that is present may already have been weakened by previous incidents. Combined with the uncertainty that exists about the attitude of the aircraft during the crash, it is essential to protect the reactor equally in every direction: a 4π steradian impact energy absorption system is needed.

For land-based nuclear reactors, the reactor impact analyses are performed for the building around the containment vessel. In the design of the nuclear system considered for the cruiser aircraft, the usual reinforced concrete dome is left out. Therefore the crash survivability in the worst-case scenario described above is up to the ability of the containment vessel, possibly aided by specialised systems to prevent the reactor contents from being released. Other potential sources of information could lie in researches performed in benefit of the design of nuclear ships and submarines. However, the information that is found on the crash protection of these vessels considers the structure of the vessel to be the main barrier for reactor damage. This assumption can be made due to the inherent strength of ship and submarine hulls as well as the low impact velocities. For aircraft, especially in the worst-case scenario described above, these assumptions are not met and therefore the containment vessel itself has to be researched further. During the days of the ANP programme, the importance of crash survival was already understood. During this programme multiple tests were done to investigate the possibility of protecting the reactor vessel by constructing the containment vessel out of materials that can absorb the energy of a crash by deforming without cracking. Using rocket-propelled sleds giant blocks of concrete were impacted into spherical models of different sizes, weights, and composition at varying speeds and the deformation of the models was measured [55–59]. Using the gathered data as well as dimensional analysis, a formula was devised that predicts the deformation of these models in [60, 61]. The resulting predictive curve is shown in figure 6.2. This curve is constructed for a 5.18 m diameter sphere with the additional properties as mentioned in the caption.

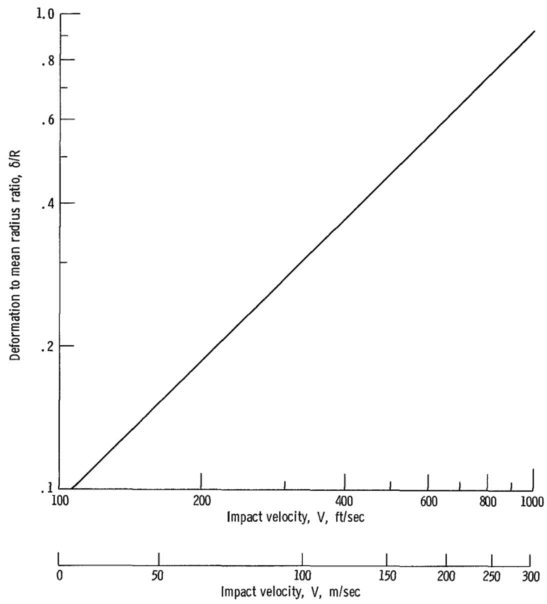

Figure 6.2: Deflection to mean radius ratio versus impact velocity correlation applied to a predetermined sphere with wall thickness: 7.62 cm, mean radius: 2.55 m, mean radius to thickness ratio: 33.5, sphere material density: 8030 kg/cm^3, ultimate stress: 6.9 $\cdot 10^8$ N/m^2, material: AISI 304 stainless steel, from [60]

For models up to 3 feet and 1305 pounds (about 0.9 m and 592 kg)[59], this relation appears to be correct in predicting that the tested models will change their shape by approximately the calculated amount without structural failure that would allow leakage of any kind. Even during tests performed at 1055 feet/s (322 m/s or Mach 0.95 at sea level, which is much faster than the design speed of the cruiser), the models proved to be leak-tight after impact [58]. But the largest model tested during these trials is still nowhere near the size of the reactor vessel on the cruiser. It is unknown what effect the change in size will have on the impact dynamics, even though [61] suggests that the non-dimensional approach makes it more probable that the formula mentioned above will hold for larger vessels as well. *"That assumption implies that no new variables are involved in the impact deformation of the large sphere. Data from large sphere-impact tests are needed to expand the range of application of the correlation equation and to improve the reliability of predicting the impact-deformation of large spherical containment shells"*[60]. Even if this were the case and the containment vessel of the cruiser's reactor would be constructed out of stainless steel, which proved to be the most resilient option during the tests, figure 6.2 shows that the non-dimensional deformation δ/r_{CV} would still be around 0.9 at the envisioned cruiser speed. To get an idea of what the resulting vessel would look like, figure 6.3 shows one of the test models after impact. Even though this kind of impact could be survivable in terms of leaking of the containment vessel, the resulting deformation can cause the core to become supercritical. Therefore, a passive system has to be devised that inserts neutron absorbing material into the core in case of excessive deformation. Additionally it might be worth determining what energy absorption device would present an effective extra barrier for absorbing impact energy, which decreases the deformation of the containment vessel.

Another side of American research during the ANP programme was focused on determining which lightweight impact energy absorption device would be applicable for protecting an aircraft's nuclear reactor. Efforts soon concentrated on *frangible tubes* because tests showed this system to have the highest specific energy absorption coefficient, measured in the unit Nm/kg [62]. The system, as portrayed in figure 6.4, consists of a tube that is slid over a die. The bottom of the die is curved so that, as the tube is pushed down on it, the tube ex-

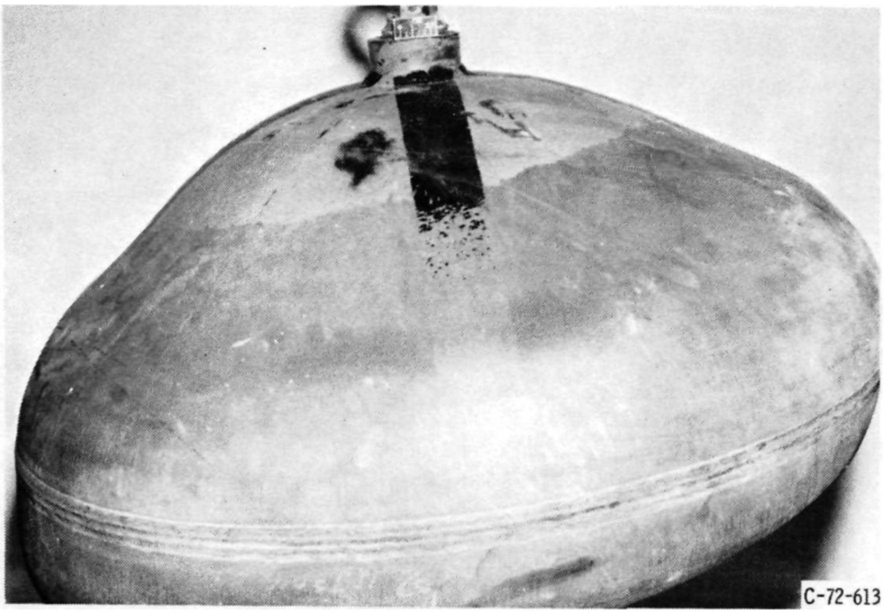

Figure 6.3: Resulting shape of a test vessel after 322 m/s impact, from [58]

pands radially. If the tube is pushed down further, it cracks and subsequently breaks up or franges into small pieces. This process uses the friction between tube and die, and plastic deformation of the tubes to absorb the impact energy[63].

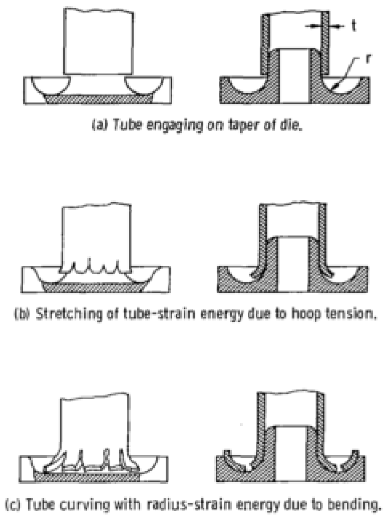

Figure 6.4: The franging process for frangible tubes, from [64]

The tubes can be added to the outside of the containment vessel as an extra layer or they can be incorporated into the contents of the containment vessel. A big advantage is that frangible tubes present a passive security in case of impact. Just like the deformation of the containment vessel, no activation system or switch is needed for providing protection. Other options like airbag-type devices do need such an addition, which always possesses a risk of failing to operate. However, the frangible tubes also have distinct disadvantages; firstly, the allowable tolerances in its design and production are small. As illustrated in [65], the size of the tube and die have to be designed, constructed, and assembled under very strict scrutiny in order for the system to operate. Any misalignment will prevent the designed cracking and franging, which severely inhibits energy absorption. Then there is the somewhat related issue of uni-directionality. If the applied force is slanted by as little as 5° from the parallel of the tube, energy absorption decreases drastically as the tube will cease to frange and buckle instead. Therefore, the tubes would need to be applied to the vessel in bundles in order to provide sufficient protection to the reactor in any crash direction. This solution could be replaced or enhanced by adding a plate on top of the tube to gain more control over the direction of the load that is led into the tube. The large amount of tubes or extra plates needed for this, increases the weight of the impact absorption system.

The above tests and considerations for survivability of the containment vessel in case of a crash only apply if there would be no pipes protruding the vessel. In the nuclear cruiser, at least two pipes will violate this assumption: the pipe carrying cold fluid in the secondary cycle towards the primary heat exchanger and the pipe carrying the heated fluid to the turbine or secondary heat exchanger. In case of an accident these pipes could be destroyed, leaving two holes in the containment wall that nullify all previous efforts for ensuring a leak-tight vessel. The solution to this problem lies in so-called fast acting valves that close the pipes if necessary. The original design for such a system is described in [66], but a lighter design was deemed possible and the resulting redesign is treated in [11]. This shows two options slide and pin, as portrayed in figures 6.5 and 6.6, respectively. For the example of a pipe with a diameter of 10 inches (0.254m), the slide option proved to be the lightest at 4565 pounds per valve (or 2071kg), compared to 6390 (2898kg) for the pin valve and around 17000 (7711kg) for the original design. In case of an accident requiring the containment vessel to be completely sealed, a small explosive charge is set off in the firing chamber of the valve system. The resulting overpressure translates the pin or slide so that the flow in the fluid pipe is blocked. Because of this, a possible removal of the piping outside the containment vessel has no effects on the contents of the containment vessel.

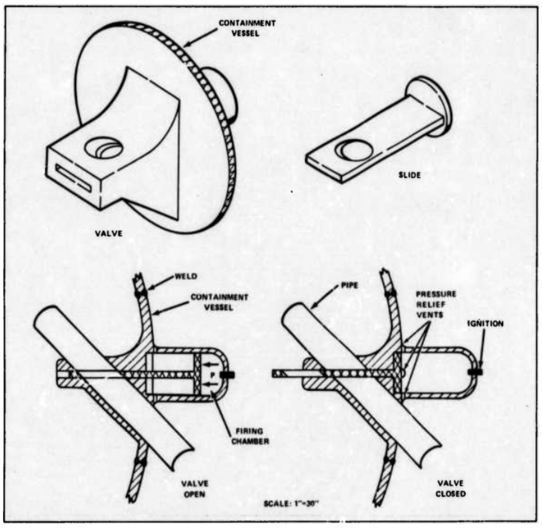

Figure 6.5: Fast acting shutdown valves: the slide option, as proposed in [11]

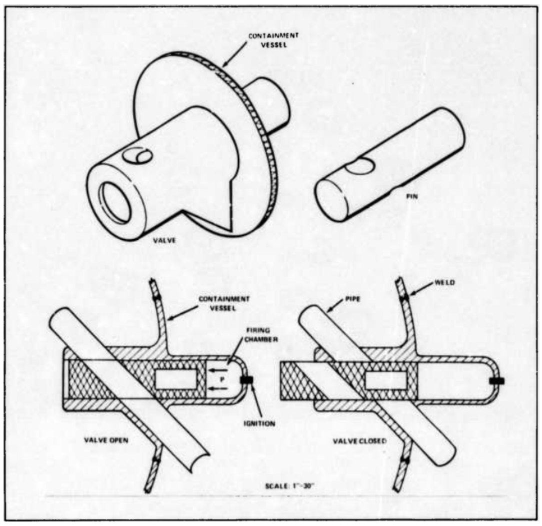

Figure 6.6: Fast acting shutdown valves: the pin option, as proposed in [11]

6.3.1. POST-CRASH HEAT MANAGEMENT

Containing the reactor contents in case of a crash is not the only consideration to be made for the containment vessel. Another set of challenges arises after the reactor has come to a halt on the ground. Even though passive poisoning systems will have shut down the nuclear reaction, heat is still produced as is explained in section 6.1. After a crash, this process can be intensified because the fuel rods and other parts inside the vessel have become dislodged. Combined with the deformation of the vessel this can lead to pools of liquid core material forming on the bottom of the vessel. The resulting concentration of heat puts extra strain on the vessels. If the reactor lands in water, the heat is exchanged between the vessel and its surroundings, which decreases the risk of vessel damage. A more critical situation arises if the reactor impacts on dry land and ends up at the bottom of an impact crater. As discussed in [12, 67], a partially buried reactor has a higher risk of meltdowns and the subsequent release of core material because of the insulating capabilities of the soil. This is especially important for the liquid pool of core material since it will always pool at the lowest point where the vessel is in contact with soil. To counter this effect, some form of active cooling is needed to cool the vessels and the materials inside. In stationary reactors this function is fulfilled by sprinkler systems, but for the cruiser's reactor it has to be assumed that it has rolled completely free of the surrounding structure and no piping for the active cooling has survived outside of containment vessel. Further studies are needed to explore the options for systems to prevent full meltdown caused by latent heat long enough for the recovery crews to reach the reactor after a crash.

6.4. AIRCRAFT MOVEMENT EFFECTS

In contrast to ordinary heat cycles of nuclear power plants, there is no stationary frame of reference on the nuclear cruiser. As the aircraft performs manoeuvres or encounters turbulence the heat cycle and reactor, along with their respective contents, are subjected to distinct accelerations in all directions. This causes a variety of problems that have to be kept in mind during future design steps of a nuclear-powered aircraft. Among the most important problems are movements of piping and fluid sloshing. The current studies of these problems for heat cycles in power stations are performed for accelerations caused by seismic events, but the underlying principle can also be applied to accelerations due to the causes mentioned above. The two main problems are now briefly discussed in the following paragraphs.

The system of fluid-filled pipes in the nuclear cruiser is excited by to several kinds of motion. Due to the size of the different components, the heat cycle is spread out over a significant area inside the cruiser structure. During flight, the fuselage and wings of the cruiser move with respect to each other in response to the aerodynamic loading. The pipes of the heat cycle, as well as the attachments to the components have to be able to flex to accommodate this motion. This also adds a fatigue component to the loads that the piping has to be designed for. Recalling the layout of the cycle, as presented in figure 4.1, especially the long pipes running to and from the cooler in the wing will be subjected to large motions between their endpoints. Another source of concern in the design of the piping for the heat cycle is vibration. Caused by turbulence, control input, or engine operation the cruiser can be excited in a certain frequency. The contents of the cruiser is also excited in this frequency if there is no damping present between the cruiser structure and the component in question. Vibrations can be the source of accelerated fatigue occurring and therefore has to be taken into account specifically during the design, as is already done for current aircraft. For the heat cycle this is especially difficult due to the presence of large amounts of liquid with different physical and thermodynamic characteristics, which influence the response. If the excitation frequency is close enough to the natural frequency of a pipe and the fluid within the pipe will begin vibrating uncontrollably, which can lead to destruction of the structure[68]. In contrast to the relative motion problem, resonance can affect all the pipes in the heat cycle, short as well as long. Differences in length, diameter, weight, and contents will make each pipe sensitive to a different frequency of excitation so careful study into every possible vibration has to be carried out. Vibrations and resonance can be prevented by adequate support of the piping and maybe even active damping mechanisms to prevent resonance from occurring.

Resonance of the fluid and piping, as described above, is not the only problem that is linked to fluid motion induced by external accelerations. Especially for the high density coolants that have been selected for the *RECREATE* nuclear cruiser design, coolant inertia has to be taken into account in future design steps. When a vessel or pipe is filled with a liquid and then subjected to an external acceleration, the inertia of the liquid will cause it to have a delayed response to this acceleration. Depending on the pattern of the acceleration (single sudden impact or periodic vibration) different responses can be induced in the fluid, each with its own set of resulting forces and moments on the heat cycle and its components[69]. On top of this, the movement of a body of fluid from one side of a vessel to the other side results in a shift of mass and an additional acceleration on impact with the structure at the far side of the vessel. If the container is large enough, such as a reactor vessel, this sloshing of the fluid negatively affects the controlability of the cruiser. This sloshing problem is also present in conventional aircraft where the fuel tanks in the wings are the sources of large fluid inertia during aircraft motion. To prevent excessive sloshing of the fuel the tanks are divided into smaller portions by using various types of baffles and one-way valves to stop the fuel from moving around in large quantities and over large distances. In order to use such devices in the nuclear cruiser, a detailed investigation is needed into the accelerations that the system has to be able to handle and the allowable resulting fluid motion that does not endanger the cruiser's controlability. The design of the anti-sloshing mechanisms should then be focused on reducing fluid motion to below this set limit, while minimising the pressure loss that is introduced by including these systems in the pipes and components of the heat cycle.

7

Conclusions and Recommendations

Coming to a conclusion on the feasibility of the nuclear cruiser, as proposed by the RECREATE research group, has now become possible using the results of the decision processes and calculations presented in this thesis report. The three most important factors that are used to define feasibility at the beginning of the report are repeated in the following sections, along with a determination of the extent to which they are fulfilled.

7.1. Conclusions on the heat cycle's ability to power the nuclear cruiser

Using the total weight of the aircraft as an input to the calculations, along with the selected cruise conditions, the heat cycle design is able to provide the propulsive power needed to maintain those cruise conditions. To achieve this goal, the heat cycle has a double closed cycle layout using two working fluids to convert the heat generated in the reactor core to propulsive shaft power. This study is limited to the determination of cruise propulsion requirements because safety restrictions as well as reactor physics prohibit the use of nuclear power to perform take-off and landing operations.

The first cycle is the cycle that cools the reactor core and transfers its heat to a heat exchanger, where it is passed on to the second cycle. The first cycle is fully enveloped by the shielding containment vessel because of its direct contact with nuclear by-products and radiation. Because of its excellent heat transfer properties and inherent nuclear shielding capabilities molten lead-bismuth eutectic (LBE) is selected as the working fluid of this primary cycle after a trade-off including other options like sodium and water. The shielding properties of the lead in LBE should decrease the required shielding weight of the reactor, however its corrosive properties at elevated temperatures limits the maximum temperature in the primary cycle to 1023 K.

From the primary cycle's heat exchanger the power is transferred to the secondary cycle, for which supercritical CO_2 (s-CO_2) is selected as the working fluid. A big advantage of s-CO_2 as the working fluid in this cycle is the reduced size of the turbomachinery (compressors and turbines) needed, when compared to those employed in cycles using other fluid options such as water or helium. Moreover, s-CO_2 is non-corrosive and is able to provide a high efficiency cycle at limited temperatures, which provides a good combination with the restrictions set by the LBE of the primary cycle. The secondary cycle has a simple regenerative layout, containing a compressor, regenerator, heater, turbine, and cooler to achieve the necessary thermodynamic variations in the CO_2.

The secondary cycle has a closed set-up, meaning that a turbine is used to provide the propulsive work. Open cycle set-ups, using a series of two heat exchangers to heat up the airflow in an engine pod much like a jet's fuel burner, have also been investigated. But these have been found to be ineffective due to the low available temperature output by the LBE primary cycle. If higher temperatures are available, due to a different primary cycle fluid or more effective corrosion prevention techniques in LBE for example, the small number of components does make the open cycle a feasible alternative because the heat exchanger weight is significantly lower than the combined weight of the heat cycle components of the closed cycle.

The design of the final cycle has been optimised to fit into the wing root of previous cruiser designs so that the aerodynamic efficiency of the design is retained and the initial weight distributions are still valid.

7.2. CONCLUSIONS ON HEAT CYCLE SAFETY

The safety of the cruiser is ensured by employing safety factors throughout the mechanical design and considering back-up propulsion options in case the nuclear reactor develops a problem that forces it to shut down. In this case, a fuel burner is present in a detour of the heat cycle that replaces the primary heat exchanger as the heat source of the s-CO_2 cycle. Also the choice of LBE as the primary cycle fluid enhances safety by providing additional shielding as well as increased safety in case of a puncture of one of the pipes between the reactor core and the primary heat exchanger. For gaseous coolants such a leak would completely drain the system or even cause a catastrophic failure of the pipe, whereas the LBE solidifies when exiting the pipe, thereby sealing the puncture.

Other safety measures have been implemented into the overall design by for example investigating the optimal manner of dealing with a faulty reactor. Jettison of the reactor has been considered but found to be ineffective at increasing the safety of the entire project. Other qualitative safety investigations have been performed into the crash safety of the nuclear containment vessel, aircraft motion effects, and cruiser operations such as routing. An important safety aspect for the outcome of this research is the choice for a dual reactor, dual heat cycle setup. This retains half of the propulsive power in case one of the heat cycles fails, with the driveshafts linking both heat cycles to their respective engines are routed such that there is no asymmetric thrust that results from one cycle being inactive.

Because this research is only a portion of the conceptual design of the nuclear cruiser, many of these investigations do not exceed the qualitative stage and full designs of the systems can only be done once a reactor design has been completed.

7.3. CONCLUSIONS ON MEETING THE CRUISER WEIGHT BUDGET

To minimise the weight of the heat cycle a process of calculations is used to determine which combination of heat cycle and component inputs leads to a minimum weight set-up. This process starts with a grid search over a set of cycle inputs to determine the minimum possible weight per component at each of the grid points. These minimum weight components are then added and the resulting cycle weights are compared to find the cycle grid point at which the lowest total weight is present. This cycle point, and the accompanying component input values, are then used as input for a final optimisation around that minimum weight grid point to end up with an overall minimum weight heat cycle. In this process, the weight is linked to the cycle efficiency through a so-called power penalty procedure, which allows pressure and efficiency losses in the design to be converted to additional required reactor power, and eventually additional reactor weight. Therefore, the final results do not necessarily provide the lightest heat cycle components but the lightest overall propulsion system weight.

The heat exchanging components, being the cooler, heater, and regenerator, are all designed as printed circuit heat exchangers (PCHE's) to minimise component size and weight. Employing airfoil-finned fluid channels in stead of a zigzag configuration minimises the component pressure drop, thereby minimising the additional compressor work needed, which in turn decreases the power penalty. Due to the lack of available literature the sizing of s-CO_2 turbomachinery is not part of the present research, assuming only that its weight will not be of significant influence on the final design due to the reduced size of these components for the selected fluid. A detailed design of the driveshafts is also omitted from this thesis because driveshaft weight optimisation has been performed in other fields already, whereas heat cycle weight optimisation still requires specific attention.

From the initial design by RECREATE of the nuclear cruiser, a weight budget of 200,000 kg is reserved for the heat cycles. Dividing this by 2, to account for the dual cycle set-up yields a weight allowance for each heat cycle of 100,000 kg. The optimal cycle found after the optimisation results in a cycle weight of around 65,600 kg, which includes the weight of the components in the heat cycle, the piping linking the components, the total weight of the s-CO_2 needed for the cycle to be operated. This leaves 34,400 kg for the systems that have not been included in the weight optimisations in this research, most importantly the turbomachinery and driveshafts. This excess weight budget is deemed to be sufficient to accommodate these additional systems. Therefore, the research is concluded by stating that the design of a heat cycle for the nuclear cruiser as dictated by the requirements set in the RECREATE research project is indeed feasible. This opens opportunities for further research, which is also necessary to be able to confirm the outcome of the calculations. These future investigations can benefit from a number of recommendations that can be given at the end of this research, as discussed in the following sections.

This now leaves only the requirement compliance matrix to be discussed to mark the completion of this study. The requirements that are set in the introduction in section 1.3 are repeated in table 7.1, along with the method of compliance of each requirement and the part of the report that treats the method.

Requirement	Method of compliance
Capacity: 1000 passengers	Preliminary aircraft design seating arrangements
Range: > 60,000 nm	Nuclear power ensures extended operation
Maximum Take Off Mass: 2,000,000 lb	Input into the power calculations
Cruise Speed: M = 0.8	Input into the power and cooler air mass flow calculations
L/D: > 20	Input into the power calculations
Maximum radiation levels: $1 \cdot 10^{-3}$ Sievert/year	Safety considerations are implemented at every design step
Entry into service: Before 2100	Technology readiness assessments of all applied concepts
Propulsion: Hybrid nuclear/chemical fuel	Applied in heat cycle selection
Requirement	**Location**
Capacity: 1000 passengers	Figure 1.5
Range: > 60,000 nm	Chapter 2
Maximum Take Off Mass: 2,000,000 lb	Section 4.2.1
Cruise Speed: M = 0.8	Sections 4.2.1 and 4.2.5
L/D: > 20	Section 4.2.1
Maximum radiation levels: $1 \cdot 10^{-3}$ Sievert/year	Throughout the report
Entry into service: Before 2100	Throughout the report
Propulsion: Hybrid nuclear/chemical fuel	Section 3.4

Table 7.1: Requirement compliance matrix

7.4. RECOMMENDATIONS FOR FURTHER WORK

The recommendations that are given to future research depend on what the purpose of the research in question is: if this is to go further into the research to specifically design a nuclear-powered aircraft, the applicable advices are presented in section 7.4.1, if the researcher is interested in optimising heat cycles and PCHE's they should read section 7.4.2, if the research strives to reiterate the results of this thesis the pointers are presented in section 7.4.3, and for people preparing to use the calculation codes that have been used in this thesis, the appropriate recommendations are in section 7.4.4.

7.4.1. RECOMMENDATIONS FOR RESEARCHING NUCLEAR AIRCRAFT

For researches that strive to design nuclear aircraft the most important advice is to consider the safety aspects mentioned throughout this research, specifically in section 1.1 and chapter 6. Safety is paramount in the design of any aircraft, and of any nuclear installation so the combination of the two makes it important for all designers of nuclear aircraft to read up on suggested safety risks and possible solutions.

The presented research includes significant uncertainties due to the fact that the reactor and shielding design is not coupled to the heat cycle design. For other researches striving to design a nuclear-powered aircraft, these two areas should be connected as soon as possible in the design process. In that way the effect of choosing a different reactor coolant with, for example, a higher temperature allowance on the overall cycle weight can be investigated more easily. This could also result in making the open cycle a more feasible option due to the increase in coolant temperature. It also allows for the qualitative safety aspect that have been discussed in this thesis to be elaborated into more detailed design suggestions of actual safety systems because the reactor size and weight is known simultaneously with the aircraft design.

7.4.2. RECOMMENDATIONS FOR RESEARCHING HEAT CYCLES AND PCHE'S

For researches using this research as a source of information for investigations into heat cycles and PCHE design, the following points are important to keep in mind.

- In the PCHE calculations future research should update the PCHE geometry from the current set-up, which is based on a zigzag channel set-up, to a set-up based on open flow plates linked by the airfoil fins. In this configuration, the airfoil fins provide the structural link between the plates and should be designed to provide adequate strength, while simultaneously optimising their fluid-dynamical shape to reduce pressure losses. Their performance should be verified in all possible configurations and fluid types by CFD simulations and/or practical experiments

- For the LBE-to-CO_2 heater calculations, the input temperature difference between the hot and cold fluid is fixed at 10 °C in this research. Future research should include the temperature difference as a variable to see whether a higher difference could yield a more efficient heat exchange and result in a lighter cycle

- For now, thermal stresses are not taken into account in the PCHE calculations. Thermal stresses are induced by temperature differences within a component, which causes one side of the component to expand more than the other side, causing internal stresses. Because of the short heat exchanger lengths that stem from the optimisations, thermal stresses could be significant in the heat exchangers and should therefore be taken into consideration in future design iterations. This could shift the optimal PCHE design point away from the shortest possible options that consistently result from the optimisations in this research

- Some of the bounds seem to limit the component optimisation consistently. Especially some of the PCHE thickness limitations should be researched further to see whether reducing their minimum value is an option because this may save considerable weight in future iterations

- Using the results from this thesis, a more accurate representation of the heat cycle's thermodynamics can be made in future researches. The pressure losses, for example, are now concentrated at the turbine and compressor inlets and could be entered as an assumed value at each component based on the results of this thesis as long as the cycle inputs of required power output, compressor outlet pressure, and efficiency are similar to those used in this research. This should result in a more accurate representation of the thermodynamic states throughout the cycle and of component designs

7.4.3. RECOMMENDATIONS FOR CONTINUING THE RESEARCH OF THIS THESIS

The results of this thesis can be used as a starting point for another iteration of the cruiser heat cycle design and the design of the aircraft as a whole. When doing so, the following points should be taken into account.

- More in-depth research should include detailed calculations for flight phases other than cruise. This results in changes in power requirements, cooler air inlet temperature, and air mass flow, amongst others, which have an effect on the design of the propulsion system. Also the sensitivity of the cycle to changes in cruise conditions such as temporary decreases in altitude or velocity to perform a certain task has to be determined. The cycle should be able to provide enough thrust during such phases to minimise the fuel burn of the alternative propulsion systems.

- In this thesis the driveshafts and turbomachinery have been left out of the design work. These could be included the next iteration of the design codes so that their weight can also be taken into account in order to come up with a more complete picture of the cycle weight. Future research into the cruiser design also should include an accurate design of the reactor and containment vessels. Their weight has not been determined in this thesis. Therefore, also the influence of the reactor power on the reactor weight, called the power penalty in this research, is unknown. This power penalty factor is also an important input that has to be determined more accurately in future design iterations

- If the weights of the turbomachinery, reactors, and driveshafts are known in the following iteration of the cruiser design, the overall design process should be redone with the weight results from this thesis combined with the determinations for the components that have been left out in this thesis. The resulting total weight can be lower or higher than the weight budget set in the current requirements as well as allow different budgets for each system. The resulting difference in weight leads to a change in required reactor power, which changes the optimal input of the heat cycle calculations. The resulting new design will again yield an updated weight and corresponding heat cycle power requirements. The heat cycle optimisation process can then be redone to yield a new optimum for the updated power output. This entire set of tasks should be repeated until it yields converged design, in which aircraft weight and optimised heat cycle design are consistent with each other. This design can then be used for more detailed design work

- A more detailed design investigation of the subsonic low temperature ramjet propulsion system around the cooler should be conducted in further studies. The ideal situation would be to link the ramjet model to the cooler design code and directly be able to calculate the thrust from the input and output states of the airflow from the cooler. Currently, the additional thrust gained from using the cooler airflow for propulsion from the wing's trailing edge is not considered in the calculations of power requirements. In the future iterations of the reactor and heat cycle optimisation, this additional thrust could be deducted from the thrust requirements from the engines driven by the heat cycle. This in turn reduces the reactor power required during cruise, and with that also the reactor weight. Linking all these models together results in a more complete determination of the optimal design point in which all thrust contributions are added and the reactor weight is also included into the calculations

- More investigation is needed to accurately design the cooler air intakes and outlets and the ducting linking them to the heat exchanger. The ducting for the cooler air flow also has to be designed in detail to ensure the assumed efficiency can be reached and to estimate the ducting weight, which should then be added to the total cycle weight

7.4.4. RECOMMENDATIONS FOR USING THE CALCULATION CODES OF THIS THESIS

The code performing the calculations for the cycle components is very computationally expensive. Due to the iterative nature of the PCHE calculations, the repeated calls to the thermodynamic fluid library, and the large number of subvariables, a full optimisation around a feasible point can take hours to even days to run. This could be significantly reduced if the fluid library was replaced by look-up tables or analytical functions. These look-up tables are being developed but were not yet available during this thesis. From the results of this thesis, which was more exploratory in nature, the search regimes in future design iterations can be reduced to lessen the computation time.

Further recommendations and statements to better understand the codes can be found in the code report starting from chapter 8. Any researcher intending to use or alter the code is advised to read this code report.

Part 2

Code Documentation

8
Explanation of the Code and its Layout

The calculation code developed in this thesis has the function of optimising a heat cycle for minimum weight, using a set of input values and restrictions. It takes into account heat exchangers and piping, but ignores the contributions due to compressors, turbines, and driveshafts. It is set up to perform this optimisation in two steps, starting with a grid search to determine an approximate minimum before advancing to an optimisation around that point. This enhances the user's understanding of the trends and thermodynamic processes at play.

Although this study uses the code to design a heat cycle for a nuclear cruiser, it is open to be adapted for designing other minimum weight heat cycles as well, but only after careful assessment of the validity of the equations and methods that are used in the calculations.

This code report focusses mainly on explaining the closed cycle calculation codes using Matlab because they have been used most during the calculations. Also, the design of the open cycle FLiBe-to-air heater is similar to the design of the PCHE's of the closed cycle code so additional explanations are unnecessary. The engine design process using GasTurb of the open cycle engine has already been explained in section 4.3.1.

A copy of the code and the results obtained for this thesis can be retrieved from the FPP department secretariat at the faculty Aerospace Engineering of Delft University of Technology.

8.1. Code layout

A UML schematic of the layout of the overall code is found in figure 4.4. From this figure and the other UML diagrams of figure 4.7 and figure 4.15 the big lines of the calculation process become clear. Each part of the code has its own goal for which it requires a distinct set of input variables, which is performed by a number of functions, and which results in a certain output. These aspects are explained for each of the three main parts of the code, as depicted in figure 4.4: cycle calculations, grid search, optimisation. For each of the codes used, the run time on an eight core 2.4 GHz processor has been recorded and is also supplied below.

8.1.1. Cycle calculations code explanation

- **Function:** Determine the range of feasible cycles in a grid of cycle input variables and for each feasible grid point, export properties of the CO_2 cycle to be used by other calculations
- **Steps:** In a predetermined grid of cycle inputs, first a range test is performed to check which combinations of efficiency and pressure inputs yield feasible cycles. Then these feasible cycles are simulated and the resulting thermodynamic parameters are stored in the workspace
- **Method:** Cycle calculation codes as provided in Noriega's thesis[36]
- **Input:** Required cycle output power, feasibility limitations for the heat cycle such as temperature restrictions, assumptions for the component efficiencies and cycle pressure loss
- **Variables:** Cycle efficiency, cycle maximum pressure

- **Output:** Range of feasible cycle inputs, thermodynamic properties of the CO_2 at different stations in the cycle and the required component powers per cycle grid point
- **Run times:**
  - **Range test:** 0:04:33 on 8 cores
  - **Cycle calculations:** 0:01:08 on 1 core for regenerative, 0:00:31 on 1 core for recompression

8.1.2. GRID SEARCH CODE EXPLANATION

The grid search code contains three main parts: PCHE component grid searches, piping optimisations, determination of the overall minimum weight grid point. Each of these are explained in the following bulleted lists, which are structured as in section 8.1.1. The basics of the component grid searches are equal for heaters, coolers, and regenerators alike. Therefore, they are treated in the same list, with notable differences being mentioned at each relevant bullet.

→ ***PCHE component grid search:***

- **Function:** Provide minimum weight component set-ups at each feasible cycle grid point
- **Steps:** For each of the cycle grid points, loop over the variables in predetermined intervals and design the PCHE for the resulting input using the appropriate PCHE design code
- **Method:** Component calculation codes adapted from the codes used in Noriega's thesis[36] and a calling code to enforce the loops
- **Input:** Feasible range of grid points, required component power, thermodynamic fluid properties, power penalty factor and compressor efficiency from input file
  - The cooler also requires input for the airflow, provided by the input file in the form of altitude and Mach number
- **Variables:** Component frontal dimension, channel diameters, banking parameter
  - The cooler and heater also allow variations in the mass flow of the air and LBE, respectively
- **Output:** Minimum component weight for each cycle grid point, along with the value of the variables that resulted in this minimum. Other outputs are the component pressure loss and weight of the fluid contained in the PCHE channels
  - The cooler also outputs the pressure and temperature of the airflow as it leaves the PCHE for use in the GasTurb model of the subsonic low-temperature ramjet, as well as the inlet area that is needed on the leading edge of the wing to allow the mass flow of air to enter
- **Run times:**
  - **Regenerators:** 0:46:19 on 8 cores for regenerative, 0:44:05 on 8 cores for both regenerators of the recompression cycle
  - **Heaters:** 2:02:06 on 8 cores for regenerative, 0:54:35 on 8 cores for recompression
  - **Coolers:** 11:04:47 on 8 cores for regenerative, 6:44:00 on 8 cores for recompression

→ ***Piping grid search:***

- **Function:** Provide minimum weight piping set-ups at each feasible cycle grid point
- **Steps:** For each of the cycle grid points, calculate piping weight and pressure loss using varying values of the variables to minimise the objective weight of the piping
- **Method:** Piping pressure loss calculation codes adapted from the codes used in Noriega's thesis[36], stress calculation codes and an optimisation process that calls both of these codes in series to obtain their respective contributions to the objective weight

- **Input:** Feasible range of grid points, thermodynamic fluid properties, length per pipe, power penalty factor and compressor efficiency from input file

- **Variables:** Internal radius for each pipe

- **Output:** Minimum piping weight for each cycle grid point, along with the value of the internal radius for each pipe that resulted in this minimum. Other outputs are the pressure loss and weight of the fluid contained in the PCHE channels

- **Run times:** 0:21:01 on 1 core for regenerative, 0:13:04 on 1 core for recompression

→ ***Overall grid search:***

- **Function:** Find the minimum weight grid point

- **Steps:** Load all the component data obtained in the component and piping grid search, along with cycle data. Then add all the contributions to the objective weight per cycle grid point and find the lowest objective weight grid point

- **Input:** Cycle data, component grid search output, piping grid search output, power penalty factor and compressor efficiency from input file

- **Output:** Minimum objective weight cycle grid point, along with the breakdown of the total weight of the cycle at that point

- **Run time:** A few seconds

8.1.3. OPTIMISATION CODE EXPLANATION

- **Function:** Perform the concluding optimisation of the heat cycle and present the final heat cycle design

- **Steps:** Using the minimum weight grid point as a starting point, vary the cycle and component variables to reach the overall minimum weight cycle. Then export the final values of the variables to a design code that displays the final result

- **Method:** Optimisation code using the *fmincon* function in Matlab. Cycle and component calculation codes as before

- **Input:** Minimum weight grid point and corresponding configuration of cycle and components

- **Variables:** Cycle efficiency, cycle maximum pressure, component variables

- **Output:** Overall minimum weight cycle, with corresponding component designs

- **Run time:** 1:06:02 on 8 cores for the optimisation, final design takes a few seconds

8.2. PARALLEL COMPUTATIONS

Because of the large number of calculations and the independent nature of many of the calculations parts, parallel computing may be employed to speed up the calculation process. This has been investigated in several stages of the code and this section presents the results of these investigations. This also provides a rationale for the choice of parallel computing set-up in the codes. For grid searches always put the variable with the largest number of variations as the innermost loop and use *parfor* on that loop. The division of cores is also an option for using parallel computing. Opening multiple instances of Matlab and assigning each instance a fraction of the available cores means that two codes can be run at the same time. However, it is found that running the codes in series from a single instance with the maximum amount of cores is faster. The final investigation that has been done for parallel computing is during the optimisation, which is detailed in the following section.

8.2.1. PARALLEL COMPUTING IN THE OPTIMISATION STEP

The optimisation code uses a main function, which varies the input and calls the objective function. In the objective function the heat cycle calculations and component designs are executed to obtain the objective weight. Because the design of each component in the heat cycle is independent of the outcome of the other components, this part of the calculations can be performed in two ways. The objective function can calculate the components' weights individually and then add them, or each component can be optimised for each iteration of the objective function. The latter is referred to as double optimisation. In case of double optimisation, each iteration provides an optimum design for each individual component, whereas the prior case of single optimisation may contain sub-optimal component solutions for intermediate results. The optimisation process then has three possible locations for including parallel processing, which are investigated:

1. In the main function as a standard option of the *fmincon* function in Matlab. This causes each core to calculate the objective function with a specific set of input values, whilst the other cores calculate the objective function for a different set of values
2. In the optimisation of each component in the objective function using the same method as mentioned in the previous point
3. By including a parfor loop in the objective function to loop over the different components

A test code was written and altered to include each of these options, as well as all possible combinations to study their effect on the run time of the optimisation process. The set-up of the problem was equal in each run, as were the outcomes. The resulting observations are presented in table 8.1, where the notation of the options is defined as follows. The first word indicates whether a double or a single optimisation set-up is used. The following three letters are either y or n, indicating whether each of the three options for including parallel computing has been applied. For example, *doubleyyn* indicates the use of the additional optimisation option inside the objective function, where both optimisations are run with the parallel option in fmincon enabled, whilst the looping of the different components is done in series. Note that single optimisation set-ups only have two letters at the end of their names because the second option from the list is not included by definition. As can be seen from table 8.1, the single optimisation using parallel computing on in the main function call

Parallel option	**Run time [hh:mm:ss]**	**Saving** [%]
Doublennn	06:47:43	0%
Doubleynn	06:23:30	6%
Doubleyny	04:22:42	36%
Doublenny	04:55:05	28%
Doublenyn	05:41:08	16%
Doubleyyn	05:28:18	19%
Doublenyy	05:36:02	18%
Doubleyyy	05:22:36	21%
Singlenn	05:56:38	13%
Singleyn	02:11:57	68%
Singleyy	02:15:58	67%
Singleny	05:01:22	26%

Table 8.1: Results of the variation of placement of parallel computing functions in the optimisation process on the run time of the process

is most beneficial in terms of run time. Therefore, this configuration is used in the calculation codes of this thesis.

9
USER MANUAL FOR FUTURE USERS

This user manual describes how to operate the calculation codes to end up with the final answer that is presented in this thesis. After that it describes the process that is required for handling varying input parameters so that other research is able to use the code for the optimisation of heat cycles.

9.1. USING THE CURRENT CODE

The following sections indicate the order in which to run the Matlab calculation codes to reach a final minimum weight heat cycle design for the nuclear cruiser.

9.1.1. CLOSED CYCLE CALCULATIONS

The code is made up of several subcodes, each dealing with a distinct part of the overall calculations. The file names of the code in the Matlab folder are numbered to indicate the intended order of running the codes. The intended order of running is listed below, along with a short summary of the information for each part of the code from section 8.1 and the file name of the code to be run at each step. Note that the *XXX* in the file names indicates that two versions are present in the folder: one labelled *REC* for recompression and one labelled *REG* for regenerative calculations. The file names usually start with an A to ensure they are on top of the folder's file list to ease the selection of the files to run, which is also aided by the numbering of subfolders.

- A. **Start up:** Initiates FluidProp and sets up figure output for optimal coupling into LaTeX documents. File name: A_STARTUP.m
- B. **Input determination:** Uses values of the input variables and assumptions to determine the required cycle output power. Also stores the values of the input and assumptions for use in other calculations and performs material maximum stress calculations. File name: B_INPUTS.m
- 1a. **Range test:** Retrieves the required cycle power and assumptions to determine the grid of feasible cycles, for which the component calculations are to be computed in the grid search. File name: Range_test.m
- 1b. **Cycle calculations:** Performs cycle calculations to determine values of pressure, temperature, mass flow, and component powers for the grid points selected in the range test. These values are used as input during the component grid search calculations. File name: Fill_cycle_matrix_XXX.m
- 2. **Piping calculations:** Minimises piping weight per cycle grid point using the input from the cycle calculations and optimising the piping set-up using the internal radius per pipe as a variable. File name: A_OPTIM_PIPE_XXX.m
- 3. **Component calculations:** Designs the components of each heat cycle grid point to find an initial minimum weight set-up for use in the optimisations. This is done by varying the component input variables over a series of structured values in a multi-dimensional component grid search. This components included in this are:
    - a. Heater. File name: A_HE_SURF_LBEtoCO2_XXX.m

   b. Cooler. File name: A_CO_SURF_XXX_Ramjet.m
   c. Regenerator. The two instances for the recompression cycle can be run separately using the numbered files RG(1/2)_SURF_REC.m or combined using A_RG_SURF_RUNNER_REC.m. The file to run for the grid search of the regenerative cycle is A_RG1_SURF_REG.m

4. **Grid search:** Combines the output of the component grid searches to find the overall minimum weight cycle grid point. File name: A_GridSearchXXX.m

5. **Optimisation:** Initiates an optimisation starting from the grid search minimum grid point and using the set-up from that point as the vector of initial values. Starting from this step, the codes are only used for the regenerative cycle because at the previous step it has been found that the recompression cycle's weight discards it as a feasible set-up in this study. File name: OPTIM_WXXXnorm.m

6. **Final design:** Finalises the design process by running the cycle and component calculation codes using the vector of final values that results from the optimisation process. File name: FinalDesignReg.m

7. **GasTurb cooler ramjet design:** Uses the output values of the cooler design to determine the net thrust or drag contribution that arises from the process of inflow-heating-outflow by means of a subsonic low-temperature ramjet design optimisation

For now, these steps have to be initiated individually to allow the user to inspect each step's results before using those results in the following step. Because validation material for the majority of the calculations is not present, it is important to consider the expected trend and outcome of each of the calculations prior to running the code. After the run, the inspection of the outcome variables has to be focussed on checking whether these expectations have been met. If this is not the case, careful inspection of the calculation code and inputs has to be performed to ensure that the discrepancies between expectations and results is due to the inaccuracy of the expectations rather than mistakes in the code or inputs. Once the user is satisfied that the results are feasible, the Matlab workspace is saved so that the results of the calculations can be retrieved in following calculations. Because this study has paved the way by exploring the search regime for each variable, future studies have a better indication of a feasible starting point. This opens the door to automation of the entire process by linking the steps to each other and automatically saving relevant variables, in stead of requiring the user to check the variables before storing them and manually starting the next section of the code.

The user has to ensure that workspaces are saved under the same name as the names that are used in the code to retrieve variables from the intended workspace. If a different file name is used to store the workspace, the code has to be altered to reflect this new name. The same goes for renaming variables in these workspaces, as their names are also used in the call to retrieve specific information from a saved workspace.

9.1.2. OPEN CYCLE CALCULATIONS

The calculation process for the open cycle requires the following steps:

A. **Start up:** Initiates FluidProp and sets up figure output for optimal coupling into LaTeX documents. File name: A_STARTUP.m

B. **Input determination:** Uses values of the input variables and assumptions to determine the required cycle output power. Also stores the values of the input and assumptions for use in other calculations and performs material maximum stress calculations. File name: B_INPUTS.m

1. **Engine designs:** Optimises engine designs for different TITs in GasTurb to minimise required heater power, whilst keeping the engine diameter and air mass flow within set limits. Store appropriate outcome values in an Excel sheet to be able to retrieve the values in future calculations

2. **PCHE heater calculations:** Designs the heater of each engine design to find an initial minimum weight set-up for use in the optimisations. This is done by varying the PCHE input variables over a series of structured values in a multi-dimensional component grid search, using the inputs, which include air mass flow and required heater power, from the GasTurb optimisation. For now, only the FLiBe-to-air heater code has been used. The LBE-to-FLiBe heater design code is present but its results are not included in this thesis. File name: HE_SURF_Flibe_to_Air_Hrange.m

3. **Heater optimisation:** Performs an optimisation starting from the grid search minimum grid point of the previous step and using the set-up from that point as the vector of initial values. The code for this is not present in the folder that is available from the FPP secretariat because the open cycle concept has been dismissed in this thesis after step 2, rendering further optimisation useless

9.2. ALTERING CODE FOR VARYING INPUT

When using the code in other research, the inputs or design limitations may differ from those used in this thesis. The process of adapting the code to cater to these differences is described for a series of examples of alterations at different levels of the code below. Because of the limited literature available on PCHE design and computations at the time of this report, it is important for each future research to conduct an investigation into the state of the art of PCHE research before starting the research. When making any alterations to the code, ensure that the equations and statements are valid for the combination of fluid and PCHE configuration at hand.

- **Aircraft weight change:** If the cruiser overall weight budget changes from the current 1 million kg, the entire calculation has to be redone. This starts at the changing of the value of variable W in B_INPUTS.m. Then this code has to be rerun in order to update the power that is required from the cycle. After that, all steps from sections 9.1.1 and 9.1.2 are taken again because the change in cycle power has an influence on all its components. If the change in weight is modest, the bounds of the grid search can remain the same, but for big changes an update of the search regime might be necessary. This is obvious from the result of the grid search if one of the variables of the minimum grid point set-up is at a bound for that variable. For example, if a regenerator frontal dimension loops between 1 m and 4 m and the minimum weight grid point is found at 4 m, the upper bound of the search regime should be shifted to 5 m to investigate whether a further optimum is possible, before advancing to the optimisation
- **Different fluid:** If a change in trade-off parameters yields a different fluid for one of the heat cycles, the calculation codes have to be updated accordingly. This is done by including a new code to get the section properties of the heat exchanger using the fluid. This new code has the same form as the codes named GET_SEC_PROP_XXX.m, where XXX represents the fluid in question. The call to this code then has to be implemented into the design code of all heat exchangers that use the new fluid. If the new fluid is present in the FluidProp library, the new fluid has to be initiated in A_STARTUP. After this the relevant properties can be easily retrieved, as is done for CO_2 and air in this thesis. If the new fluid is not present in FluidProp, the appropriate formulas have to be found in literature just like has been done for FLiBe and LBE in this study. Once this is done, the cycle calculations have to be redone starting from the component grid search step. In this process, the properties of the new fluid have to be taken into account when determining the relevant limitations of the grid search. Maximum temperatures might have to be updated, as well as maximum flow velocities. A change of heat transfer properties between the current fluid and the new fluid might result in smaller or larger heat exchangers, which has to be reflected in the grid search bounds, or in a change in the desired banking parameter
- **Increased temperature allowance:** If a different primary cycle fluid or improved corrosion resistance of components results in a temperature allowance higher than the current 1023 K, this bound has to be updated throughout the calculations, starting in the range test, then the cycle property calculations, and the error statements in the PCHE design codes of the heater. For the open cycle, the GasTurb design studies have to be redone with higher TIT allowances, in order to check whether the new maximum TIT results in possible engine designs that are be closer to the assumed engine of the nuclear cruiser. If this is the case, the open cycle has become a feasible alternative to the closed cycle of this thesis and the design codes for the final steps described in section 9.1.2 have to be completed in order to design the heat cycle of the open configuration
- **Changes in engine design:** Any changes that apply to the engine design in GasTurb, such as an increase in engine diameter allowance or enforcing additional limits, are easily applied by changing the limits of the optimisation processes in GasTurb. Care has to be taken to ensure that the initial engine design falls within the set bounds, otherwise the optimisation will fail. If a value of the current engine design does not lie within the bounds set on that variable, the inputs such as corrected air mass flow for the engine design are updated manually until the resulting engine is able to function as a starting point for the optimisations

Bibliography

[1] Federal Aviation Administration, *Aviation Environmental and Energy Policy Statement*, Tech. Rep. (U.S. Department of Transportation, 2012).

[2] S. Shafiee and E. Topal, *When will fossil fuel reserves be diminished,* Energy Policy **37**, 181 (2009).

[3] U.S. Energy Information Administration, *Annual Energy Outlook 2014 Early Release Overview*, Tech. Rep. (U.S. Department of Energy, 2013).

[4] European Commission *et al.*, *Out of the Box: Ideas about the future of air transport (Part 2)*, edited by T. Truman and A. de Graaf (EUR-OP, 2007).

[5] K. de Cock and R. Nangia, *REsearch on a CRuiser Enabled Air Transport Environment (RECREATE),* in *Applied Vehicle Technology (RTO-MP-AVT-209) Lisbon* (2012).

[6] M. Hepperle, H. Timmermans, G. L. Rocca, J. Early, L. Manfriani, and R. Nangia, *Initial design of cruiser aircraft and feeder aircraft (Deliverable 4.2 of WP 4 of the RECREATE project)*, Tech. Rep. (REsearch on a CRuiser Enabled Air Transport Environment (RECREATE), 2014).

[7] RECREATE, *RECREATE - cruiser-feeder,* (2014), visited on 02-06-2015.

[8] M. Chiozzi, *Conceptual Design of a Nuclear Powered Blended Wing Body Aircraft for the Cruiser/Feeder Concept*, Master's thesis, La Sapienza University of Rome (2012).

[9] Boeing Commercial Airplanes, *Statistical summary of commercial jet airplane accidents,* Online by Aviation Safety (2012).

[10] A. Wrixon, I. Barraclough, M. Clark, A. Diesner-Kuepfer, and B. Blann, *Radiation, people and the environment*, edited by J. Ford (International Atomic Energy Agency, 2004).

[11] M. W. Amos, J. S. Butt, B. L. Campbell, R. G. Diehl, J. W. J. Fanning, G. M. Lacy, R. J. Luczak, J. E. M. Moorman, J. W. Shattuck, and V. K. Wilkinson, *Nuclear Aircraft Feasibility Study (volume 1)*, Master's thesis, Air Force Institue of Technology (1975).

[12] J. C. van der Sluis, *Prospects and Problems of Nuclear Propelled Aircraft*, Master's thesis, TU Delft (1975).

[13] F. E. Rom and C. C. Masser, *Large nuclear-powered subsonic aircraft for transoceanic commerce*, Vol. 2386 (National Aeronautics and Space Administration, 1971).

[14] F. C. Maienschein, F. T. Bly, and T. A. Love, *Gamma Radiation in a Divided Aircraft Shield*, Tech. Rep. (Oak Ridge National Laboratory, 1954).

[15] J. Roskam, *Airplane Design: Parts 1-8* (DARcorporation, 1985).

[16] D. P. Raymer, *Aircraft design: a conceptual approach*, edited by J. S. Przemieniecki (American Institute of Aeronautics and Astronautics, 2006).

[17] J. M. Wild, *Nuclear propulsion for aircraft,* in *AIAA 3rd Propulsion Joint Specialist Conference*, General Dynamics/Convair (American Insitute of Aeronautics and Astronautics, 1967).

[18] C. Collins, F. Davanloo, M. Iosif, R. Dussart, J. Hicks, S. Karamian, C. Ur, I. Popescu, V. Kirischuk, J. Carroll, *et al.*, *Accelerated emission of gamma rays from the 31-yr isomer of ^{178}Hf induced by X-ray irradiation,* Physical review letters **82**, 695 (1999).

[19] C. E. Hamilton, *Design Study of Triggered Isomer Heat Exchanger-Combustion Hybrid Jet Engine for High Altitude Flight*, Master's thesis, AIR FORCE INSTITUTE OF TECHNOLOGY (2002).

[20] F. F. Karpeshin and M. B. Trzhaskovskaya, *Triggering the ^{178m2}Hf isomer and resonance conversion: contemporary problems,* in *2nd International Conference Current Problems in Nuclear Physics and Atomic Energy* (2008) pp. 373–380.

[21] M. Fleischmann and S. Pons, *Electrochemically induced nuclear fusion of deuterium,* Journal of electroanalytical chemistry and interfacial electrochemistry **261**, 301 (1989).

[22] J. Shrair, *Developing an efficient low-temperature nuclear fusion reaction,* Infinite energy magazine **93**, 1 (2010).

[23] E. Adamov and Y. Fuji-Ie, *Developments and tendencies in fission reactor concepts,* in *Handbook of nuclear chemistry* (Springer, 2011) pp. 2663–2729.

[24] A. C. Marshall, *An Assessment of Reactor Types for Thermochemical Hydrogen Production*, Tech. Rep. (Sandia National Laboratories, 2002).

[25] E. P. Loewen and A. T. Tokuhiro, *Status of research and development of the lead-alloy-cooled fast reactor,* Journal of NUCLEAR SCIENCE and TECHNOLOGY **40**, 614 (2003).

[26] V. Tcharnotskaia, C. Ammerman, T. Darling, J. King, N. Li, D. Shaw, L. Snodgrass, and K. Woloshun, *Liquid lead-bismuth materials test loop,* in *Proc. ADTTA/ACCAPP*, Vol. 1 (Citeseer, 2001).

[27] N. Li, *Active control of oxygen in molten lead-bismuth eutectic systems to prevent steel corrosion and coolant contamination,* Journal of Nuclear materials **300**, 73 (2002).

[28] N. Novikova, Y. Pashkin, and V. Chekunov, *Some features of sub-critical blankets cooled with lead-bismuth,* in *International conference on accelerator driven technologies and applications, ADTTA 99.* (1999).

[29] M. P. Short and R. Ballinger, *Design of a functionally graded composite for service in high temperature lead and lead-bismuth cooled nuclear reactors,* Nuclear Technology **177**, 366 (2012).

[30] R. B. Doyle, *Calculated Performance of Nuclear Turbojet Powered Airplane at Flight Mach Number of 0.9*, Research Memorandum E50B23 (National Advisory Committee for Aeronautics, 1950).

[31] S. Comassar, *Comprehensive Technical Report, General Electric Direct-Air-Cycle Aircraft Nuclear Propulsion Program; Aircraft Nuclear Propulsion Application Studies*, Tech. Rep. (General Electric, Nuclear Materials and Propulsion Operation, Flight Propulsion Laboratory Department, 1962).

[32] W. W. Wachtl and F. E. Rom, *Analysis of the Liquid-Metal Turbojet Cycle for Propulsion of Nuclear Powered Aircraft*, Research Memorandum E51D30 (National Advisory Committee for Aeronautics, 1951).

[33] G. Angelino, *Carbon dioxide condensation cycles for power production,* Journal of Engineering for Power **90**, 287 (1968).

[34] V. Dostal, *A supercritical carbon dioxide cycle for next generation nuclear reactors*, Ph.D. thesis, Massachusetts Institute of Technology (2004).

[35] H. Schwartz, *Investigation of a Sodium Vapor Compressor Jet for Nuclear Propulsion of Aircraft*, Tech. Rep. NAA-SR-134 (North American Aviation, 1953).

[36] J. B. Noriega, *Design method for s-CO_2 gas turbine power plants*, Master's thesis, TU Delft (2012).

[37] K. Hsia, *Nuclear Aircraft Propulsion System, conceptual design*, Master's thesis, TU Delft (2013).

[38] R. B. Doyle, *Calculated Performance of a Mercury-compressor-jet-powered Airplane using a Nuclear Reactor as an Energy Source*, Research Memorandum RM-E51F14 (National Advisory Committee for Aeronautics, 1951).

[39] A. Lokhov, *Load-following capabilities of NPPs,* Nuclear Engineering International **57**, 34 (2012).

[40] J. E. Cha, T.-H. Lee, J.-H. Eoh, S.-H. Seong, S.-O. Kim, D.-E. Kim, M.-H. Kim, T.-W. Kim, and K.-Y. Suh, *Development of a supercritical co2 brayton energy conversion system coupled with a sodium cooled fast reactor,* Nuclear Engineering and Technology , 1025 (2009).

[41] R. Poul, P. Ruzicka, D. Hanus, and K. Blahous, *Design of carbon composite driveshaft for ultralight aircraft propulsion system,* Acta Polytechnica **46**, 40 (2006).

[42] R. L. Pierres, D. Southall, and S. Osborne, *Impact of mechanical design issues on printed circuit heat exchangers,* in *Proceedings of SCO2 Power Cycle Symposium 2011* (2011).

[43] P. Colonna and T. van der Stelt, *Fluidprop: A program for the estimation of thermophysical properties of fluids,* Software (2005).

[44] R. A. Jeniski Jr. and R. L. Kennedy, *Development of ATI Allvac 718Plus Alloy and Applications,* in *Second Symposium on Recent Advantages of Nb-Containing Materials in Europe* (2006) pp. 1–10.

[45] J. E. Hesselgreaves, *Compact Heat Exchangers*, edited by J. E. Hesselgreaves (Gulf Professional Publishing, 2001).

[46] D. E. Kim, M. H. Kim, J. E. Cha, and S. O. Kim, *Numerical investigation on thermal-hydraulic performance of new printed circuit heat exchanger model,* Nuclear Engineering and Design **238**, 3269 (2008).

[47] X. Xu, T. Ma, L. Li, M. Zeng, Y. Chen, Y. Huang, and Q. Wang, *Optimization of fin arrangement and channel configuration in an airfoil fin PCHE for supercritical CO2 cycle,* Applied Thermal Engineering **70**, 867 (2014).

[48] K. Nikitin, Y. Kato, and L. Ngo, *Printed circuit heat exchanger thermal-hydraulic performance in supercritical CO2 experimental loop,* International Journal of Refrigeration **29**, 807 (2006).

[49] J. Attinello, *The jet wing,* in *IAS 25th Annual Meeting, IAS Preprint No. 703* (IAS, 1957) pp. 10–11.

[50] D. Kuchemann, *The Aerodynamic Design of Aircraft* (Pergamon Press, 1978) p. 229.

[51] A. Ko, L. T. Leifsson, W. H. Mason, J. Schetz, B. Grossman, and R. T. Haftka, *MDO of a blended-wing-body transport aircraft with distributed propulsion*, Tech. Rep. 6723 (American Institute of Aeronautics and Astronautics, 2003).

[52] AKME-engineering, *SVBR-100,* http://www.akmeengineering.com/svbr100.html (2011).

[53] G. la Rocca, M. Li, and M. Chiozzi, *Feasibility study of a nuclear powered blended wing body aircraft for the cruiser/feeder concept,* in *CEAS 2013: The International Conference of the European Aerospace Societies* (2013).

[54] M. Bunn and A. Wier, *Terrorist nuclear weapon construction: How difficult?* The Annals of the American Academy of Political and Social Science **607**, 133 (2006).

[55] R. L. Puthoff, *A 400 FT/SEC impact test of a two foot diameter model nuclear reactor containment system without fracture*, Tech. Rep. NASA TM X- 52915 (National aeronautics and space administration, 1970).

[56] R. L. Puthoff, *A 640 FT/SEC impact test of a two foot diameter model nuclear reactor containment system without fracture*, Tech. Rep. NASA TM X- 67997 (National aeronautics and space administration, 1971).

[57] R. L. Puthoff, *A 810 FT/SEC soil impact test of a 2-foot diameter model nuclear reactor containment system*, Tech. Rep. NASA TM X-68180 (National aeronautics and space administration, 1972).

[58] R. L. Puthoff, *A 1055 FT/SEC impact test of a two foot diameter model nuclear reactor containment system without fracture*, Tech. Rep. NASA TM X-68103 (National aeronautics and space administration, 1972).

[59] R. L. Puthoff, *High speed impact tests of a model nuclear reactor containment*, Tech. Rep. NASA TM X-67856 (National aeronautics and space administration, 1971).

[60] R. E. Morris, *Permanent impact deformation of spherical shells*, Tech. Rep. NASA TM X-2067 (National aeronautics and space administration, 1970).

[61] R. E. Morris, *Empirical correlation of small hollow sphere impact failure data using dimensional analysis*, Tech. Rep. NASA TM X-52874 (National aeronautics and space administration, 1970).

[62] A. A. Ezra and R. J. Fay, *An assessment of energy absorbing devices for prospective use in aircraft impact situations,* in *Dynamic response of structures*, edited by G. Herrmann and N. Perrone, Stanford University (Pergamon Press Inc., 1971) pp. 225–246.

[63] J. R. McGehee, *Experimental investigation of parameters and materials for fragmenting-tube energy-absorption process*, Tech. Rep. (National Aeronautics and Space Administration, 1966).

[64] R. L. Puthoff and K. H. Gumto, *Parametric study of a frangible-tube energy-absorption system for protection of a nuclear aircraft reactor*, Tech. Rep. (National aeronautics and space administration, 1970).

[65] K. Gumto and R. Puthoff, *Static tests of 4-inch-outside-diameter frangible tube energy absorbers for nuclear aircraft*, Tech. Rep. (National Aeronautics and Space Administration, 1971).

[66] W. F. Scott, *Feasibility Study on Fast-Acting Valves for Airborne Nuclear Containment Systems*, Tech. Rep. (Sandia Laboratories, Albuquerque, New Mexico, 1973).

[67] P. M. Finnegan and F. E. Rom, *Will the nuclear-powered aircraft be safe?* Astronautics and Aeronautics **6**, 32 (1968).

[68] F. Paolacci, M. S. Reza, and O. S. Bursi, *Seismic analysis and component design of refinery piping systems,* in *COMPDYN 2011: III ECCOMAS Thematic Conference on Computational Methods in Structural Dynamics and Earthquake Engineering*, edited by M. Papadrakakis, M. Fragiadakis, and V. Plevris (2011).

[69] D. Ma, *Seismic analysis of a large LMFBR with fluid-structure interactions*, Tech. Rep. (Argonne National Lab., IL (USA), 1985).